

CZECH UNIVERSITY OF LIFE SCIENCES PRAGUE

Faculty of Environmental Sciences  
Department of Applied Geoinformatics and Spatial  
Planning



Integration of Airborne High-Resolution  
Spectral and Vertical Structure  
Information for Environmental Mapping

DOCTORAL THESIS

2019



Author:  
Jiří Prošek

Supervisor:  
doc. Ing. Petra Šímová, Ph.D.

Reviewers:  
prof. Ing. Lena Halounová, CSc.  
Czech Technical University in Prague

Dr. Marta Szostak  
University of Agriculture in Krakow

Dr. Julián Tomašík  
Technical University of Zvolen

## Declaration

I have written the thesis by myself, and have not used sources or means without their declaration in the text. Any thoughts by others or literal quotations are clearly referenced. The thesis was not published elsewhere except for individual studies that had already been published in scientific journals.

## Acknowledgements

I would like to thank my supervisor Petra for showing me what the scientific world is about and taking care of me throughout my doctoral studies. I would like to acknowledge all my co-authors who contributed to this thesis and all my colleagues (in particular Vít'an, even if he doesn't care), who helped and supported me. I would also like to thank Jarek for proofreading and valuable comments.

My greatest thanks go to my family, especially to my mother, who has always been supportive of me in everything I did. Last but definitely not least, thank my Katka for standing by me, and be my mainstay.

# Abstract

Map layers with a high level of spatial, temporal and thematic detail represent a crucial data source for environmental research. Methods of remote sensing have over the last decades become instrumental in acquisition of such data. To fully utilize the potential of remote sensing data, it is necessary to understand the pros and cons of individual platforms and sensors, of individual processing and validation methods and to be able to choose the most suitable of each for the particular research.

The presented dissertation consists of four commented case studies aimed at new ways of utilization of high resolution airborne data in environmental mapping, with integration of spectral and vertical information acquired through airborne imaging being the central topic of the thesis. By applying suitable methods of data acquisition, processing and integration, we managed to acquire detailed information about the horizontal and vertical structure of the studied environment. The photogrammetric processing of imagery from unmanned aerial vehicles (UAVs) led to acquisition of a very accurate terrain model, even in a rugged terrain of succession steppes and forests of spoil heaps. Integration of vertical and spectral data acquired from processing of UAV data further improved the classification accuracy and allowed us to create thematic layers describing vegetation on the level of individual species/genera. The fusion of spectral data with vertical information moreover improved the robustness of the classification. Our results also indicate that improving spatial resolution of the input data for classification cannot act as a surrogate for the additional information represented by vertical data or additional spectral bands. Combination of hyperspectral data and characteristics acquired from airborne laser scanning (LiDAR) improved the accuracy and relevance of classification/identification of water bodies in the post-mining areas. Besides, integration of datasets led to eliminating misclassification of water bodies and shadows.

Besides presenting tangible options for improvement of environmental mapping, the results of individual studies also document the principal influence of the following factors on the accuracy and quality of the obtained products:

(i) The date and time of data acquisition – when mapping vegetation, the full vegetation season is the most suitable time for data acquisition while when aiming at identification of water bodies or creating terrain model, off-leaf season is preferable. Timing data acquisition in a way ensuring homogenous lighting conditions facilitates radiometric calibration and selection of a suitable time of day may help in elimination of shadows.

(ii) Choosing a suitable platform and sensor – a high quality sensor allowing individual settings and selected flight parameters affects the accuracy and quality of the resulting products. Studies also illustrate the typical capabilities and limits of spatial extent for individual platforms, from hectares to hundreds square kilometres.

(iii) The use of suitable processing methods and classification approaches – the differences in classification results have been strongly affected by the used classification methods. Besides, preliminary testing confirmed that pixel-based approaches provide inferior results when performing fusion of high resolution data than object oriented approaches.

## Abstrakt

Mapové vrstvy s vysokým prostorovým, časovým a tematickým detailem jsou zásadním datovým podkladem pro environmentální výzkum. Nezastupitelným zdrojem pro získání takových podkladů se v posledních desetiletích staly metody dálkového průzkumu Země. Využití plného potenciálu dat dálkového průzkumu Země pro environmentální mapování spočívá v pochopení výhod a limitů jednotlivých platforem a sensorů, zvládnutí způsobu zpracování dat a výběru vhodné metody pro vyhodnocení přesnosti a relevance získaných produktů.

Disertační práce tvoří komentovaný soubor čtyř případových studií zaměřených na nové způsoby využití leteckých dat vysokého rozlišení v environmentálním mapování. Tématem studií je integrace spektrálních a vertikálních informací získaných leteckým snímkováním. Vhodnými metodami pořízení, zpracování a integrace dat se podařilo získat podrobné informace o horizontální a vertikální struktuře zkoumaného prostředí. Fotogrammetrické zpracování snímků z bezpilotních letadel umožnilo získat velice přesný model terénu a to i v členitém prostředí stepních a lesních porostů sukcesních výsypek. Integrace výškových a spektrálních informací získaných zpracováním snímků z bezpilotních letadel zvýšila přesnost klasifikace a umožnila vytvořit vrstvy v tematickém detailu druhů/rodů vegetace. Navíc přidání vertikální informace zvýšilo robustnost klasifikačního přístupu a výsledky indikují, že vyšší prostorové rozlišení v klasifikacích nezastoupí chybějící spektrální či vertikální informace. Spojení hyperspektrálních dat a charakteristik z laserového skenování (LiDAR) zvýšilo přesnost a relevanci získaných výsledků klasifikace/identifikace vodních ploch v prostředí post-těžebních lokalit. Navíc se integrací datových sad podařilo odstranit záměny v klasifikaci vodních ploch a stínů.

Krom konkrétních možností pro zlepšení environmentálního mapování dokumentují výsledky studií zásadní vliv následujících faktorů na přesnost a kvalitu získaných produktů:

(i) Termín a čas pořízení dat – V případě mapování vegetace je vhodná plná vegetační sezóna. Naopak pořízení dat mimo vegetační sezonu je vhodné při identifikaci vodních ploch a modelování terénu. Načasování pořízení snímků při homogenních světelných podmínkách usnadňuje radiometrické kalibrace a navíc volbou vhodné denní doby lze eliminovat stíny.



(ii) Volba vhodné platformy a senzoru – Kvalitní sensor s možností individuálního nastavení a zvolené letové parametry ovlivňují přesnost a kvalitu získaných produktů. Navíc studie demonstrují typické možnosti a limity prostorového rozsahu pro pořízení dat pomocí leteckého snímkování v rozsahu hektarů až stovek kilometrů v závislosti na zvolené platformě.

(iii) Použití vhodných metod zpracování a klasifikačních přístupů – Rozdíly ve výsledcích klasifikací se silně odvíjely od použitých klasifikačních metod. Navíc předběžné testování potvrdilo, že „pixel-based“ přístupy poskytují při integraci dat velmi vysokého rozlišení slabší výsledky nežli objektově orientované přístupy.



## Table of Contents

Chapter I – Thesis Preface.....	- 13 -
Chapter II – Objectives.....	- 15 -
Chapter III - Theoretical Background .....	- 17 -
Chapter IV – STUDY 1 .....	- 31 -
Chapter V – STUDY 2.....	- 53 -
Chapter VI – STUDY 3 .....	- 77 -
Chapter VII – STUDY 4.....	- 101 -
Chapter VIII – Discussion and Conclusions.....	- 123 -
References.....	- 139 -
Curriculum vitae .....	- 157 -

# Foreword

---

*Deja-vu*

*or*

*New wave with old content*

---

As fast as the development in the field of remote sensing moves forward, new questions and challenges for further research keep arising, often making it necessary to come back to the basics and start over. In view of new platforms, sensors and data, old paradigms have to be revised, new methods of data acquisition and processing must be tested from the perspective of relevance and applicability. The same spirit can be found in this thesis and in the ideas presented in individual studies included in this thesis. At the beginning, we expected to be able to quickly and directly apply newly acquired data and to easily target so far unanswered questions about many environmental topics. After the very first attempts for data acquisition using an own unmanned aircraft, we sobered up quickly and landed on the ground as we found out that we indeed had to go back to the beginnings, i.e. to case studies, methods of data acquisition and processing, to the very basics of the use and integration of data in environmental mapping.

# Chapter I – Thesis Preface

The last two decades have seen an unprecedented boom of remote sensing (RS), driven by technological developments such as the ever increasing potential and capacity of information and computing infrastructure on the one hand and demand for products of remote sensing and their application on the other. RS thus became an irreplaceable and integral part of many areas of primary and applied research, commercial applications and management/decision support. However, multiple factors including spatial, spectral and temporal sensing abilities of platforms and sensors represent limitations of the use of RS. Over the last decades of the research of traditional remote sensing methods (i.e. ground-based measurements, manned aircraft and satellite observations) many paradigms for acquisition, processing and application of remote sensing datasets have been developed, verified and introduced into everyday practice. A new wave and one of driving forces of the present day RS was brought by the introduction of Unmanned Aerial Vehicle (UAV) platform. UAVs, along with their unique combination of spatial and temporal capability, new sensors and processing, filled the existing gaps in traditional RS platforms and suitably complemented their capabilities. This is one of the reasons why UAVs have become a more or less separate field of RS over the last decade. Traditional manned aircraft in combination with the new unmanned aircraft represent the most detailed sources of RS datasets and due to their mass use, many various datasets with fine spatial-temporal resolution have come into existence.

Remotely sensed datasets (both continuous data and extracted thematic layers) are valuable sources of information for environmental mapping, i.e. for the process of information acquisition and of trying to comprehend the way ecosystems and environment function. A typical example of the use of remotely sensed data in environmental mapping on various scales is acquisition of information about land use and land cover (LULC), which allows the analysis of changes, study of processes affecting landscape structures, or modelling of distribution of individual species and explanation of the processes in ecological communities. Two principal approaches can be observed in environmental mapping – one focusing on global processes with a high degree of generalization and low detail, the other on detailed research with limited spatial extent. With the growing detail, demands for spatial, spectral and temporal resolution of remotely sensed data grow. Integration (fusion approach) of data from multiple platforms, sensors

and/or from multiple time points leads to obtaining additional information and thus a finer detail for subsequent analyses.

This thesis focuses on the field of environmental mapping based on integration of high resolution spectral information with information on vertical structure from manned and unmanned aircraft. Theoretical background provides a brief summary of the state of the art: (i) suitable platforms for fine resolution data acquisition; (ii) high resolution data processing methods and (iii) accuracy assessment in the context of environmental research. Case studies subsequently investigate and verify the usability of new platforms, sensors and processing methods in applied Earth observation and environmental mapping.

The topics of the studies gradually progress from (i) methods of acquisition and processing of vertical data from various types of UAVs for terrain mapping in a mining-affected area; through (ii) two parallel studies aimed at mapping and classification of vegetation down to the level of species or genera, based on integration and classification of multispectral, vertical and thermal information from UAVs; up to (iii) a study dedicated to integration of hyperspectral data and LiDAR variables from an airborne platform for mapping small water bodies in a mining-affected area.

## Chapter II – Objectives

The presented thesis investigates the integration and use of airborne high resolution data in environmental mapping. The main objective is to contribute towards understanding and development of the application of fine resolution remotely sensed datasets in environmental mapping and thus to support the utilization of the full potential of RS for environmental research. In four presented and commented case studies, processing methods are being tested and the accuracy and relevance of products obtained from airborne remotely sensed datasets is being evaluated. The studies are discussed in the context of their potential for environmental applications and ecological modelling with emphasis on the evaluation of possible inaccuracies and impact of such inaccuracies. On the theoretical level, the aim is to formulate recommendations for data processing and to verify its principles in order to maximize the utilization of the potential of high resolution remotely sensed spectral and vertical information. On the level of practical application, the aim is to present specific methods for acquisition and processing of the data leading to creating products (namely thematic land cover maps and digital elevation models) suitable for further use in environmental research.

### The research questions:

A) How can integration of newly available airborne sensed datasets contribute towards mapping of composition and structure of biotopes? Emphasis is laid on the:

(i) Possibility of terrain mapping at post-mining areas and deriving vertical structure of vegetation by UAVs.

(ii) Improvement of classification accuracy and relevance at the detailed level of vegetation by fusion of UAV-acquired spectral data and additional derived vertical information.

(iii) Benefits of integration of airborne hyperspectral data and LiDAR variables in the identification of small water bodies in heterogeneous environment.

B) What are the effects and impacts of (i) date and time of data acquisition; (ii) selection of a suitable sensor; (iii) use of suitable processing methods; and (iv) used evaluation methods on the quality of resulting environmental mapping products?





## Chapter III - Theoretical Background

---

*„Remote sensing can be defined as a collection of information about an object without physical contact with such object. Aircraft and satellites are typical platforms used for RS. The term encompasses methods utilizing electromagnetic energy as a means for measurement of target characteristics.“*

*(Sabins, 1978)*

---

Besides the general principle that the term remote sensing (RS) describes any non-contact technique whereby the object in space can be observed, this definition also implies the principal vectors of that field, i.e. platforms, sensors and data processing methods that can be used to get description and characteristics of the observed/studied object. From the technical perspective, the RS development in the last decades has been driven by the platform and sensor advancements and by continuously increasing information infrastructure and computing power. Hand in hand with the improvement of technology, the scope of possible applications keeps increasing. The definition of the limits and capabilities of RS is growing ever more complex. It is no longer true that RS serves for classical topographic mapping and land cover classification only (Toth and Józków, 2016). Due to this growing complexity and scope of application, this thesis and its theoretical background cannot and will not aim to capture the entire scope and state of the art of RS in a complex manner.

Where RS platforms and sensors are concerned, a combination of three parameters is crucial for their performance - spatial, spectral and temporal sensing abilities (Blaschke et al., 2014; Lillesand et al., 2015; Toth and Józków, 2016). Taking these parameters into account, we will in this thesis disregard the continuous development of the “conventional” satellite and airborne remote sensing platforms and focus on other important vectors of the current RS:

- i) Relatively new Unmanned Aerial Vehicle (UAV) platform (Colomina and Molina, 2014; Manfreda et al., 2018)
- ii) Combination of multiple platforms, sensors or data sources (Pohl and Genderen, 2014; Toth and Józków, 2016)

# Suitable platforms for fine resolution data acquisition

The perception of what is high or low resolution depends on the relationship between the size of the observed object on the one side and on the detail provided by the sensor (e.g. spatial/cell resolution) on the other side. The term low resolution can therefore be used where individual resolution cells are bigger than the observed object and, conversely, the term high resolution describes resolution where resolution cells of the image are smaller than the observed object (Strahler et al., 1986). Specifically, in the context of this thesis, airborne RS (i.e. UAVs and manned aircraft) are perceived as suitable platforms for high resolution data acquisition.

---

*„Let them fly and they will create a new remote sensing market in your country“*

*(Colomina and Molina, 2014)*

---

## AIRBORNE PLATFORMS - MANNED AIRCRAFTS and UAVs

Until recently, most RS datasets originated from ground-based measurements, manned aircraft, satellite observations or combinations thereof. The last decade has however seen a new trend complementing the above mentioned methods - UAVs. UAVs brought significant development to many fields of the theoretical and applied Earth observation. Across the field of environmental studies, their unique combination of spatial and temporal capability fills a gap as they are capable of providing data with fine spatial resolution over relatively large areas combined with capacity for enhanced temporal retrieval in a relatively cost-effective way (Manfreda et al., 2018). Being a relatively new platform, however, UAVs also come with limitations, such as weakness in the state of the art when compared with the traditional RS platforms obviating that UAVs still have a lot to catch up on. Another limitation is represented by legislative regulations of their operation, which may be quite strict in some states. Conceptual regulations on the supranational level are at present in various stages of development (Stöcker

et al., 2017). The requirements for UAV operation are therefore also subject to frequent changes.

In contrast to UAVs, airborne data acquisition by manned aircraft is one of the oldest forms of remote sensing. Even after satellites started to be used for RS, manned aircraft still complemented those data by providing detailed spatiotemporal and spectral resolution. From the technical point of view, manned and unmanned aircraft are similar in principle (e.g. composite airframes; aerodynamics; flying speed, available equipment/sensors, flight planning) (Neininger and Hacker, 2012). On the other hand, differences between UAVs and manned aircraft include usable payload, operational aspects in the sense of spatiotemporal resolution and operating radius/area, potential restrictions on operation, safety and cost-efficiency (Colomina and Molina, 2014). A more detailed analysis of usable equipment will be provided in the next subchapter, a general observation however obviates that manned aircraft can be mounted with more, heavier, bigger and, in effect, better sensors (Toth and Józków, 2016). At present, some UAVs mounted with multiple sensors are commercially available (Nevalainen et al., 2017), the typical process of acquisition of multiple sensor data using a UAV however still involves several flights with a single sensor (Ahmed et al., 2017; Komárek et al., 2018; Sankey et al., 2017a).

The operational radius (and, therefore, the extent of the mapped area) of the airborne manned or unmanned aircraft differs in the: (i) technical capabilities (range/flight time, range of the control unit in the case of UAV) (Neininger and Hacker, 2012), (ii) minimum flight height and speed (Manfreda et al., 2018) and (iii) legislative restrictions (Stöcker et al., 2017). It can be generally said that manned aircraft is capable of mapping substantially larger areas (tens to hundreds of square kilometres in a single flight mission) while UAVs allow mapping of up to tens square kilometres but due to their minimum flight height, they provide a better per pixel resolution.

Other factors that must be taken into consideration when choosing between manned or unmanned aircraft include e.g. portability, flexibility, the demands (including time demands) of processing and, last but not least, cost-effectiveness. UAVs are often referred to as cost-effective instruments for mapping or data acquisition purposes (Anderson and Gaston, 2013; Diaz-Varela et al., 2014; Manfreda et al., 2018). The cost-effectiveness must be however always considered in view of the quality (e.g. per pixel resolution, spectral resolution) and quantity (i.e. spatial extent) of the data. From the perspective of spatial extent, UAVs can be only effective for small areas while for larger areas, the use of manned aircraft

or satellites is much more productive (Matese et al., 2015; Neiningner and Hacker, 2012). This implies that at present, manned aircraft are an irreplaceable platform in the applied Earth observation and environmental research and those two types of platforms complement each other very well.

## SENSORS for AIRBORNE RS

An RS platform consists of a carrier and sensing payload. The basic classification of sensors is according to their principle to active and passive sensors (Gomarasca, 2009). Passive sensors (also called optical sensors) detect electromagnetic energy reflected or radiated by the observed/recorded objects. Depending on the requirements and specifications of the particular application, sensors with various spatial and spectral resolutions (e.g. numbers and spectral width of bands or central wavelengths) have been and are being developed (Lillesand et al., 2015). Active sensors work on the principle of signal emission and subsequent detection of the signal reflected from the studied object(s). The main types of active sensors suitable for airborne RS are the Light Detection and Ranging (LiDAR; in combination with aircraft, a commonly used term is Airborne Laser Scanning, ALS) (see Vosselman and Maas, 2010) and microwave/radar sensors (see Woodhouse, 2017). Colomina and Molina (2014) distinguish the following categories of sensing payloads: (i) Visible-band, near-infrared and multi-spectral cameras; (ii) Hyperspectral cameras; (iii) Thermal imaging; (iv) Laser scanners and (v) Synthetic aperture radar. Those categories cover the full portfolio of sensors used for Earth Observation.

When manned aircraft is used as the platform, the size and weight of the sensing payload is not limiting and full emphasis can be thus put on the sensor quality. The economic side of things thus represents the principal limiting factor when using manned aircraft, which usually leads into a compromise between the technical parameters and the price of equipment and sensors. On the other hand, search for an optimum combination of a UAV carrier and sensing payload is a significant limitation of that platform. The technical capabilities of UAV carriers (load bearing capacity, balancing and preservation of flight parameters, properties and safety) are in conflict with the sensor requirements (spatial, temporal and spectral resolution, sensor overall and optical quality) (Manfreda et al., 2018). However, as soon as 2013, Van Blyenburgh (2013) reported over 400 imaging and ranging instruments suitable or optimized for UAVs including active and passive systems, ranging from visible spectrum through near infrared up to thermal infrared, LiDAR and microwave systems. The number of suitable

instruments and sensors for UAVs is ever increasing and the current broad portfolio of available sensors leads to a gradual closure of the gap between UAVs and other RS platforms.

## High resolution data processing methods

The range of methods for RS data processing is as wide as the use of RS itself. This chapter aims to provide a summary of principles and methods utilized in the individual studies that form a part of this thesis and offers thus a basic insight into the topic of data processing with overreach into environmental mapping. In particular, the algorithms and methods of extraction of vertical information from optical data, classification approaches for creating new thematic layers and maps, and fusion approaches for integration of multiple datasets to add additional information allowing e.g. better classification or modelling, will be discussed in this chapter.

### VERTICAL STRUCTURE from REMOTE SENSING IMAGERY

Photogrammetry in general deals with the description of physical characteristics and dimensions of objects measured in photographs or images ([McGlone, 2013](#)). Photogrammetry techniques also include image-matching algorithms allowing extraction of 3D structure from individual images. Structure from Motion (SfM) and Multi View Stereo (MVS) are among the most widely used and most well known techniques of such extraction. Both techniques use the overlap of the images acquired from various viewpoints. First, the algorithm determines the (i) internal camera/image geometry (lens properties) and the (ii) position and orientation of the camera/sensor. Based on those values, a 3D representation of the recorded object (as a point cloud) is calculated ([Micheletti et al., 2015](#)). Unlike common photogrammetric methods, this does not require any pre-defined or ground control points ([Westoby et al., 2012](#)). Ground control points are usually only used to pinpoint the 3D model into the coordinate system.

SfM and MVS photogrammetric methods support processing of data from low-cost, consumer grade, cameras as well as from expensive, high quality, metric

cameras (Turner et al., 2012). In the context of photogrammetry and remote sensing, these methods are especially used for acquisition of orthomosaics and elevation or surface models (Colomina and Molina, 2014). Such creation of 3D models of course calls for a comparison with methods of direct terrestrial measurement using global navigation satellite system (GNSS) or terrestrial laser scanning (TLS) as well as with methods of airborne laser scanning (ALS). GNSS and laser scanning achieve a better accuracy than SfM, both are however costly and in case of TLS also time demanding. (Gehrke et al., 2008; Nex and Remondino, 2014). SfM, on the other hand, with its relatively low price and easy portability of instrumentation, offers an interesting and flexible alternative to terrestrial or airborne laser scanning for applications such as acquisition of topographic models and data (Wallace et al., 2016; Westoby et al., 2012).

## CLASSIFICATION METHODS – PIXEL vs. OBJECT BASED

---

*“What’s wrong with pixels?”*

*(Blaschke and Hay, 2001)*

---

RS produces a spatially continuous and consistent representation of the Earth surface with good spatial-temporal resolution, which makes it instrumental for creating thematic layers and maps (typically land cover thematic layers but any other layers can be also created). Thematic mapping is usually based on classification of remotely sensed data (Foody, 2002). The principal premise is that different feature types or observed objects on the Earth surface possess different observable properties (e.g. spectral reflectance and emissivity, height, structure, thermal properties), according to which they can be recognized and classified into respective classes. Classification is therefore a process of categorizing the entire dataset into individual classes, during which the continuous (quantitative) representation is transformed into a thematic (qualitative) one (Lillesand et al., 2015).

A typical and frequently used classification is so-called pixel-based approach where classification procedures reflect properties of individual pixels (cells) (Lillesand et al., 2015). However, with an improving resolution of remotely sensed data, single pixels can no longer provide crucial characteristics for classification of the object.

With the increasing variability of characteristics within an individual class, the ability to distinguish between classes using pixel-based classification approaches declines sharply. This leads to a drop in classification accuracy, which is represented e.g. by a so-called „salt-and-pepper problem“, i.e. a problem when individual pixels within a single observed object are classified differently from neighbouring pixels (Yu et al., 2006).

Several methods have been developed to overcome problems associated with pixel-based classification of high resolution data, such as image pre-processing (e.g. low-pass filtering or textural analysis, Genteno and Haerte, 1995; He et al., 2016; Mueller and Hoffer, 1989; Panchal and Thakker, 2017) or post-classification processing (e.g. mode filtering, morphological filtering, or rule-based processing (He et al., 2016; Huang and Lu, 2014; Su, 2016) utilizing neighbourhood relationships between individual pixels. A robust approach for classification high-resolution data is represented by Object-Based Image Analysis (OBIA) where evaluation of neighbourhood relationships is a crucial step of the classification procedure (Blaschke, 2010; Liu et al., 2015). OBIA produces better results in comparison to pixel-based approaches, (Addink et al., 2007; An et al., 2007) and has therefore become one of widely used methods for processing and analysis of high resolution data (Alonzo et al., 2014; Diaz-Varela et al., 2014; Hartfield et al., 2011; Peña et al., 2013; Rampi et al., 2014).

In OBIA approach, the whole image is divided into parts (so-called segments) based on one or more criteria of homogeneity in one or more dimensions. Depending on the segmentation algorithm (e.g. point, edge or region based), the homogeneity criteria may be represented by spectral or spatial properties of pixels forming the segment. The classification algorithm subsequently assigns the individual segments into classes based on (i) spectral characteristics (e.g. mean and standard deviation in individual spectral bands in the segments), (ii) textural characteristics (e.g. contrast variance or entropy within the segment) and (iii) spatial characteristics (e.g. area, length of edge, compactness, convexity or roundness of each segment). It is also possible to (iv) consider relationships among individual segments (e.g. distance, similarity, shape of similar or neighbouring segments), even in multiple layers (Blaschke et al., 2008). The OBIA approach thus significantly reduces problems associated with noise and with edges/mixed pixels (Alonzo et al., 2014; Blaschke et al., 2014) as well as the salt-and-pepper problem Yu et al. (2006).

## FUSION APPROACHES - DEFINITION, HISTORY and TRENDS

---

*„With the availability of multisensor, multitemporal, multiresolution and multifrequency image data from operational Earth observation satellites, the fusion of digital image data has become a valuable tool in remote sensing image evaluation.“*

*(Pohl and Genderen, 1998)*

---

Even though back in 1998, the above quote was mostly related to satellite RS, it still underlines the growing significance of image or data fusion coming with the growing number of available RS platforms, sensors and, therefore, of available data. A general definition of image fusion is given as: *"Image fusion is a combination of two or more different images to form a new image by using a certain algorithm"* (Genderen and Pohl, 1994). The image fusion may be used to improve the spatial, temporal and spectral resolution at the level of pixels; at the level of objects, it may be used for image sharpening, for improving geometric corrections, providing stereoviewing capabilities, enhancing certain features not visible in either of the single data alone, complementing datasets for improved classification, for detection of changes, and/or for substitution of missing or replacement of defective information (Pohl and Genderen, 1998).

Since the beginning of 1990s, many fusion approaches and principles have become commonplace. Pansharpening became a standard method for combining high and low-resolution RS images and was implemented in widely used software (e.g. ENVI, SNAP). Similarly, combining multitemporal images is now a generally accepted method for radiometric calibration (e.g. Google Earth Engine) just like land cover and land use change detection based on multi-temporal datasets (Lunetta et al., 2004, 2006; Zhu and Woodcock, 2014a). Combining datasets from various platforms, sensors or different time points is another method for improving classification (will be discussed in more details in the following chapter). In their review of the image fusion concept, Pohl and Genderen (2014) mention new challenges for image fusion: (i) increasing demand for accuracy and precision of processing due to the ever increasing spatial resolution of available sensors, (ii) integration and use of data from aircraft and UAVs mounted with multispectral and hyperspectral, Light detection and ranging (LiDAR) and radar sensors. In a recent review on RS data fusion, Ghamisi et al. (2018) concluded that



fusion of spectral information and a point cloud (LiDAR or photogrammetry based) is an important and underdeveloped field of RS open for further investigation, both from the theoretical perspective and from the perspective of practical application. As a driver of the development, he mentions the necessity of integration of diverse datasets acquired from satellites, manned and unmanned aircraft.

## FUSION CLASSIFICATION

Fusion classification approaches allow integration of multiple data sources for creating thematic layers or maps and, therefore, represent a method that played a crucial role in this thesis. This subchapter summarizes its potential and possible use in environmental mapping.

Nowadays, there are many methods for composing and matching images from multiple sensors and data sources. [Wenbo et al. \(2008\)](#) demonstrated on widely used approaches for image fusion (namely Smoothing Filter-based Intensity Modulation, High Pass Filter, Modified Brovery, Multiplication, IHS transformation, and Principle component analysis) that when being used for various classifications, fused datasets contain more information than the original data and thus provide better classification results. Many studies using satellite and/or airborne data have suggested that a fusion of spectral imagery and vertical information may represent a suitable technique for improving the classification accuracy (e.g. [Bork and Su, 2007](#); [Hartfield et al., 2011](#); [Holmgren et al., 2008](#); [Luo et al., 2016](#)). Combining optical imagery data with vertical information characterizing e.g. vegetation height or terrain slope is a popular approach, which benefits from the increasing availability of remote sensing data acquired by different sensors for the same area ([Pohl and Genderen, 1998](#)). Most often, such information is derived from LiDAR in case of manned or unmanned aircraft and radar in case of satellites. It is increasingly common to have both LiDAR and spectral data available for the same area ([Asner et al., 2015, 2007](#); [Hanuš et al., 2016](#)). LiDAR data provide information complementary to optical images that is not affected by shadows. For example, [Degerickx et al. \(2019\)](#) used airborne LiDAR as an additional data source for spectral unmixing of urban land cover. [Alonzo et al. \(2014\)](#) fused high-spatial resolution hyperspectral data with LiDAR datasets at scale of the individual tree crowns to map tree species in a urban area. [Gilvear et al. \(2004\)](#) combined hyperspectral and LiDAR data for mapping estuary and river hydromorphology. [Dalponte et al. \(2012\)](#) and [Naidoo et al. \(2012\)](#) integrated such data for mapping tree species in Alps

and African savanna, respectively. First studies are also available on such a fusion using UAV-acquired data and benefits of such approach is being discussed (Husson et al., 2017; Komárek et al., 2018; Prošek and Šimová, 2019; Sankey et al., 2017a). All the mentioned studies suggest that the fusion of spectral (RGB, multispectral or hyperspectral) and vertical (LiDAR or SfM) information also leads to an overall improvement of accuracy.

## Accuracy assessment – types, reasons and impact of error in environmental mapping

---

*“There are many reasons for performing accuracy assessment. Perhaps the simplest reason is curiosity – the desire to know how good a map you have made”*

*(Congalton and Green, 2002)*

---

### POTENTIAL REASONS for ERROR

More and more detailed classification results can be achieved and the demand for such detailed results grows. Classification of remotely sensed datasets has shown the possibility of classification to the level of genera or even species (Ahmed et al., 2017; Colomina and Molina, 2014; Husson et al., 2017; Sankey et al., 2017a). Where temporal resolution is concerned, we are able to analyse changes in the magnitude of days or even hours (Fensholt et al., 2011; He et al., 2013; Sapiano and Arkin, 2009; Streets et al., 2013). However, despite the ultra-fine spatial and temporal resolution of data acquired from the state of the art RS platforms and the most advanced processing techniques, results of data analyses are still burdened by uncertainties (Olofsson et al., 2014). Such errors are in particular caused by: (i) semantic differences in the definitions of classes; (ii) misregistration of pixels or object boundaries and (iii) misclassifications,

i.e. errors caused by the classification process (Oort, 2007); as a fourth reason, we may add errors caused by incorrect accuracy assessment (Congalton and Green, 2002).

## ACCURACY ASSESSMENT

A transparent design and statistically robust approach for accuracy assessment is essential for maintaining integrity when evaluating RS methods (Olofsson et al., 2014). A deterministic evaluation of (in)accuracies would require analysis at the level of each individual object or even pixel when considering raster representation. While this could be interesting, it is in view of the extent of studied areas practically impossible. Therefore, in real life, only a part of classified objects can be validated against reality and the results must be extrapolated on the full extent (Foody, 2002).

Olofsson et al. (2014) stated the following general good practices for accuracy assessment: (i) implementation of a probability sampling design ensuring accuracy and area estimation in the best possible way (with respect to practical considerations such as costs or availability of reference data); (ii) usage of reference (true) samples with a better accuracy than evaluated (validated) samples (so-called response design protocol); (iii) usage of analyses that are compatible with sampling design and response design protocol; (iv) where thematic assessment is concerned, an error matrix with estimates of overall accuracy, user's accuracy and producer's accuracy should be provided; (v) quantification of uncertainties and evaluation of the variability and potential error in the reference data; (iv) proper description of utilized methods of accuracy assessment with emphasis on potential deviations from standard methods.

The chosen methods and design accuracy assessment is, in accordance with the above recommendations, described and discussed in detail in the individual case studies. Here, we will however continue by description of basic types of error, typical methods of accuracy assessment and examples of their impact in the research field of environmental classification.

## POSITIONAL ACCURACY ASSESSMENT

Positional accuracy or error is a parameter used for evaluation of inconsistency between the map/image feature's coordinates or elevation and their „true“ position on the Earth surface – in this sense, we can consider horizontal (planimetric) or vertical (elevation) accuracy. The accuracy assessment of positional error aims to estimate statistical parameters of the error distribution as mean, standard deviation and standard error. Root-mean-square error (RMSE) is a widely used estimation method, indicating an average deviation of the evaluated product from the true state (Congalton and Green, 2002).

The positional accuracy of the (ground) true samples used for calibration and validation of mapping results (e.g. classification) must be better than the size of classified objects (Olofsson et al., 2014). The opposite would lead to incorrect calibration of the classification algorithm and subsequent misclassifications (Lillesand et al., 2015) or false results of accuracy assessment (Gu et al., 2015).

Another problem resulting from the positional error in classifications and/or raster sampling is represented by so-called mixed or edge pixels. The problem occurs when a single image cell/pixel contains multiple categories (Foody, 2004). This inevitably leads to classification errors, to overestimation of common classes and underestimation of minority classes (Blanco et al., 2013). Fusion approach to classification is in addition faced with another problem - misalignment of fused datasets. The proper integration of multitemporal or multisensor datasets thus requires minimization of misalignment (Pohl and Genderen, 2016). This is especially problematic when data originate from different platforms. A perfect alignment of the data would require several integration steps, from mounting the instruments on board of the same aircraft, to a precise time registration of each measurement and final data fusion method (Asner et al., 2012). However, mounting the instruments on board of the same aircraft is often not feasible (typically in the case of UAVs due to low load bearing capacity) and is of course not applicable where individual datasets were acquired at different times. Remaining crucial steps include precise (geo)referencing of datasets and a proper use of the fusion method.

Finally, from the perspective of the use of the products of integration in environmental research, positional accuracy is one of principal characteristics affecting the usability and relevance of the results. When trying to identify land cover changes from data burdened with positional error, false changes are detected in the misalignment areas (Dai and Khorram, 1998; Foody, 2009a, 2009b). When modelling distribution of a particular species by species distribution models,

positional error is one of the principal sources of uncertainty. Positional error causes incorrect characterization of conditions suitable for occurrence of the species in question, which leads to reduction of the model performance (e.g. overestimation of the species habitat areas; see more in a review by [Moudrý and Šimová, 2012](#)).

## THEMATIC ACCURACY ASSESSMENT

Thematic accuracy is a parameter characterizing how well the predicted or classified value fits the reality. So-called confusion (error) matrices are among the most common ways of presenting thematic accuracy. The following metrics/characteristics are included in confusion matrix: overall accuracy (ratio of correctly predicted values to the total number of true samples), producer's accuracy (the likelihood that the object will be classified correctly) and user's accuracy (also called reliability - the likelihood that the class shown on the map will match the reality) ([Congalton and Green, 2002](#)). Characterization from the opposite perspective, i.e. from the perspective of error, is also widely used (Overall Error; Omission Error as a complement to producer's accuracy; Commission Error as a complement to user's accuracy).

When evaluating the quality of classification results, it is necessary to consider the producer's accuracy/omission error as well as user's accuracy/commission error because even if the overall accuracy may be high, a closer look may reveal a low producer's or user's accuracy of an individual class and the respective class is therefore represented incorrectly. Such a problem would limit the usability of the resulting species occurrence maps for subsequent research or management purposes. This is especially true when some of the classes possess very distinct characteristics (spectral properties, LiDAR or vertical characteristics, etc.) while others do not. Land cover classification containing artificial surfaces (such as tarmac or gravel roads), which are almost 100% distinguishable from vegetation, may serve as an example of such result. The extremely high "success rate" in the classification of such surfaces then artificially increases the overall accuracy. Hence, interpretation of the model accuracy only on the basis of the overall accuracy and subsequent usage of thus derived maps or data for ecological research may lead to biased results ([Chignell et al., 2018](#); [Fisher et al., 2018](#); [Moudrý and Šimová, 2012](#); [Schmidt et al., 2017](#); [Šimová et al., 2019](#)). For example, if the presence of a particular shrub species is important for the occurrence of an endangered bird species due to its feeding habits, the failure to correctly identify that particular shrub species (despite a high overall accuracy) provides

incorrect input data for the analysis of the particular bird occurrence. The results of such an application would therefore be invalid; if they are however perceived as reliable due to the high overall accuracy of the map, it could lead in effect to incorrect management decisions (Prošek and Šimová, 2019). Hence, the producer's and user's accuracy have to be considered in addition to the overall accuracy as integral characteristics that should always be reported by product creators and taken into account by product users (Congalton et al., 2014).

## Chapter IV – STUDY 1

### Title:

Comparison of a Commercial and Home-Assembled Fixed-Wing UAV for Terrain Mapping of a Post-Mining Site under Leaf-Off Conditions

### Authors:

Vítězslav Moudrý, Rudolf Urban, Martin Štroner, Jan Komárek, Josef Brouček and **Jiří Prošek**

### Author's contribution: 10%

Investigation and field work; Consultation and co-writing of the original draft, review – with regard to photogrammetric (SfM) procedure, camera and UAVs parameters and settings

### Journal:

*International Journal of Remote Sensing*, IF (2018) 2.493 – 14 of 30 (Q2) rank in WOS category Remote Sensing; AIS (2018) 0.531 – Q2 rank

### Full citation:

Moudrý, V., Urban, R., Štroner, M., Komárek, J., Brouček, J., & Prošek, J. (2019). Comparison of a commercial and home-assembled fixed-wing UAV for terrain mapping of a post-mining site under leaf-off conditions. *International Journal of Remote Sensing*, 40(2), 555-572.

### Cited:

7 times cited on WOS (2019 August), with the statute of a highly cited paper in field.

## ABSTRACT

Unmanned aerial vehicle (UAV) platforms are rapidly becoming popular in many research and industry sectors. Due to their relatively low purchase price and the fact they can be used to monitor areas that are difficult or even unsafe to access, they have been increasingly used in land surveying and mapping of smaller areas. Numerous UAV platforms equipped with various cameras are increasingly available on the market, differing in their suitability for environmental mapping. Surveyors therefore face a question whether to buy or assemble their own UAV. The objective of this study is to assess the performance of two fixed-wing UAV systems for land survey and mapping applications. In particular, we: (1) compared a commercial eBee platform equipped with a Sony Cybershot DSC-WX220 camera with zoom lens and a home assembled EasyStar II equipped with Nikon Coolpix A with a lens of fixed focal length to find out if a home-assembled solution can compete with specialized commercial platform; (2) investigated the utilization of UAV images acquired under leaf-off conditions for digital terrain model (DTM) generation with respect to vegetation cover (steppes and forests); (3) assessed whether an increase in the image quantity can compensate for a lower quality of images; and (4) compared the DTM derived from UAV imagery with the official Czech Republic airborne laser scanning (ALS) derived DTM. One flight with Easystar II and two perpendicular flights with eBee were performed. From these three flights, four point clouds were derived (one from each flight, and one resulting from a combination of two eBee flights), supplemented with four ground filtered point clouds. The accuracy of point clouds and DTM was assessed through a comparison with a conventional GNSS survey. We successfully identified the bare ground during the leaf-off period in the deciduous forest using images from both platforms. Point densities of point clouds acquired with Easystar II exceeded the densities of those acquired with eBee even after combining images from two eBee flights. Root mean square error of all derived point clouds ranged between 0.11 and 0.19 m, exceeding the accuracy of a nationwide ALS-derived DTM in both forest and open steppe areas. The most accurate point cloud was acquired using Easystar II. This is likely due to a combined effect of the quality of onboard cameras, camera settings and environmental conditions during the flight. For users who prefer to have greater control over their options rather than being dependent on the commercially available kit solution, home-assembled kits utilizing drones capable of carrying any camera available on the market may be an advantage.



## KEYWORDS

digital elevation models; stereo imagery; LiDAR; accuracy; area; calibration; reclamation; topography; quality

## Introduction

Mining has a significant effect on the environment and has caused extensive transformations of landscapes throughout Europe. Surface lignite mining and associated disturbances affect large areas. Original ecosystems are removed, excavated overburden is deposited on spoil banks, biodiversity is significantly reduced, aesthetic value is also degraded, and landscapes are affected by operation facilities and coal processing plants (Hendrychová and Kabrna, 2016; Svobodova et al., 2012). While rehabilitation of such areas plays an integral part already at the mine planning stage, the effect of rehabilitation methods on landscape restoration success is still subject to extensive research (Vymazal and Sklenicka, 2012). Studies devoted to mining and post-mining areas have been carried out at the landscape scale as well as at the scales of individual mines or quarries. Data for such studies are increasingly acquired by means of satellite (Bodlák et al., 2012), airborne (Wężyk et al., 2015) or terrestrial (Pukanska et al., 2014; Tong et al., 2015) remote sensing. However, satellite remote sensing provides limited information in terms of spatial resolution while terrestrial measurements are labour-intensive and time-consuming. In this context, Unmanned Aerial Vehicle (UAV) platforms show a great potential to fill the existing gap between satellite remote sensing and field measurements.

UAV platforms are increasingly being used as an important source of data for monitoring, surveillance, and 3D modelling of areas affected by mining activities. Due to their advantages such as the capability to monitor areas that are difficult or even unsafe to access, they have been used to monitor, for example, rock slides (Fraštia et al., 2014), spoil heaps (Koska et al., 2017), surface mines (Kršák et al., 2016; Tong et al., 2015) or artificial rock outcrops (Blistan et al., 2016). They are usually used in combination with digital cameras and acquired images are processed using a combination of Structure from Motion (SfM) and Multi View Stereo (MVS) approaches allowing extraction of 3D point clouds similar to those produced by laser altimetry (Nex and Remondino, 2014).

Laser altimetry, commonly referred to as Light detection and ranging (LiDAR) or airborne laser scanning (ALS), is an active remote sensing technology that has enabled terrain measurement with great extent and high accuracy (Wehr and Lohr, 1999). LiDAR pulses can penetrate through gaps in vegetation canopies and register multiple returns representing both canopy and terrain. LiDAR point clouds can be classified using a specialized software to distinguish between ground and vegetation returns. Ground returns are then used to generate digital terrain model (DTM), while returns representing vegetation canopy can be used to derive various forest metrics (Hawrylo et al., 2017; Mikita et al., 2013). Airborne laser scanning data are increasingly available and provided free of charge through government agencies in Europe (e.g. Fogl and Moudrý, 2016). However, due to the high acquisition costs, coverage is still lacking in many areas.

Digital photogrammetry methods are based on images from passive sensors. The character of photogrammetrically generated point clouds is therefore inherently different, and their utilization for terrain surveys is mostly limited to bare-ground surfaces due to constraints presented by vegetation canopies (Meng et al., 2010). Dense vegetation constitutes a particularly challenging environment for bare ground detection as it is strongly affected by a number of systematic errors caused by the fact that only the uppermost layer is usually detected with digital photogrammetry methods. Indeed, the inability to acquire an accurate DTM under vegetation canopies is a frequently mentioned limitation preventing a wider uptake of digital photogrammetry in forestry applications (Jensen and Mathews, 2016; Tomaščík et al., 2017). In the case of deciduous forest stands, however, it is possible to acquire data during the leaf-off period, which is also a common approach for ALS data acquisition (e.g. Hodgson et al., 2005). However, the usability of images acquired under leaf-off conditions for modelling terrain underlying deciduous forest stands has been scarcely tested. Ni et al. (2015) and more recently DeWitt et al. (2017) have shown that it is indeed possible using satellite images, Dandois and Ellis (2013) reported similar success with UAV images. However, a deeper understanding of the possibilities and limitations of image data acquired from UAV platforms under leaf-off conditions is still lacking.

Numerous UAV platforms equipped with various cameras are increasingly available on the market, differing in their suitability for environmental mapping (Boon et al., 2017; Thoeni et al., 2014; Torresan et al., 2017). Surveyors then often face a question whether to buy or assemble their own UAV. Some of the commercially available drones may be equipped only with vendor provided cameras. While home assembled drones are easily altered and upgraded anytime

(e.g. with a new camera), it may take some time until new equipment is available from the vendor in the case of a commercial drone.

Consumer grade cameras have not been designed for photogrammetric applications (in contrast to metric cameras) and, as a result, they exhibit greater distortion and interior orientation instability (Fraser, 2013). The accuracy of point clouds or derived products such as DTM are also affected by other camera specifications (e.g. lens focal length or maximum aperture). Although cameras with zoom lens are used, cameras with a fixed focal length are considered superior for photogrammetry applications (Fraser, 2013; Shortis et al., 2006). Furthermore, the products' resulting accuracies are affected by camera calibration and image orientation. While these tasks are solved separately for photogrammetric applications, in many applications they have to be computed at the same time using self-calibration procedures. However, it has been shown that self-calibration procedures used as a part of the bundle adjustment process may lead to errors in derived DTMs (Harwin et al., 2015; James et al., 2017; James and Robson, 2014). In addition, collection of UAV imagery can be affected by environmental factors such as complex shadowing effects (e.g. Milas et al., 2017) and/or leaf and/or twig movements caused by the wind (e.g. Jensen and Mathews, 2016), which may consequently complicate the image matching algorithm. Besides, adjacent image overlaps can vary due to interference of external factors such as gusts of wind with the UAV stability (Jensen and Mathews, 2016).

The general aim of this study is to compare the suitability of two fixed-wing UAV systems equipped with different cameras to survey a complex terrain of a non-reclaimed spoil heap. In particular, we: (1) compared a commercial eBee platform equipped with a Sony Cybershot DSC-WX220 camera with zoom lens and a home assembled EasyStar equipped with Nikon Coolpix A with a lens of fixed focal length to find out if a home-assembled solution can compete with specialized commercial platform; (2) investigated the utilization of UAV images acquired under leaf-off conditions for DTM generation with respect to vegetation cover (steppes and forests); (3) assessed whether an increase in the image quantity can compensate for a lower quality of images; and (4) compared the DTM derived from UAV imagery with the official Czech Republic LiDAR DTM.

# Materials and methods

## STUDY AREA

Our study area is located in north-west Bohemia, Czech Republic, in the Most mining district (50°34' N, 13°34' E). The present study was conducted on an area of 68 ha located in the southern part of Hornojřetínská spoil heap (Figure 1). Due to existing plans to mine the underlying coal seam in the future, this part of the Hornojřetínská spoil heap has never been technically reclaimed. The terrain morphology has remained rugged as a result of heaping that has formed a typical undulated terrain (e.g. [Doležalová et al., 2012](#)). It has been observed that rough terrain and dense vegetation negatively affect the accuracy of point clouds (e.g. [Meng et al., 2010](#)). Therefore, such a challenging environment provides an ideal location for exploring the quality of point clouds and DTMs. The vegetation is in a late succession stage 35–50 years after heaping and consists of aquatic vegetation in terrain depressions (e.g. common reed *Phragmites australis* and common cattail *Typha latifolia*), steppes (low vegetation, especially bush grass *Calamagrostis epigejos* and tall oat grass *Arrhenatherum elatius* with scattered shrubs and trees such as elder *Sambucus*, rosehip *Rosa*, birch *Betula*, hawthorn *Crataegus*), and forests. Forests occupy approximately 20% of the study area and tree height is up to 30 m (Figure 1). The forest type and structure vary significantly throughout the study area. In order to take into account the effect of the forest type and structure on point clouds accuracy, we distinguished three forest areas: (1) afforested plantations of European ash (*Fraxinus excelsior*); (2) spontaneously grown forest dominated by Birch (*Betula pendula*); and (3) mature forest of Willow (*Salix* spp.) and Alder (*Alnus* spp.) (Table 1, Figure 1). The size of the study area is larger than the area where control points are located, which allowed us to verify the stability of the UAV-derived photogrammetric model.

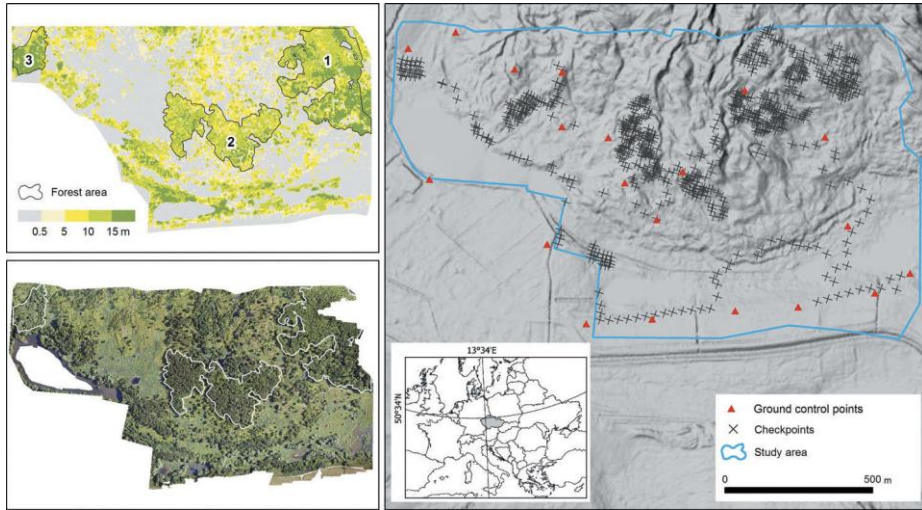


Figure 1. Location of the study area in the southern part of Hornojřetínská spoil heap (right); Canopy height model and location of three forest areas (top left); Orthophoto during leaf-on period (bottom left).

## LiDAR DATASETS

Two LiDAR datasets were available for the study area. The first one was collected over the study area in the leaf-on period (May 2017) using a remote sensing platform called the Flying Laboratory of Imaging Spectroscopy equipped with a Riegl LMS-Q780 LiDAR (Hanuš et al., 2016). Data collection flights were conducted at 1030 m above ground with a velocity of 110 knots (ground speed) and with a 55% flight line side overlap. This provided an average density of 7.7 points per m<sup>2</sup>. We used this dataset to calculate vegetation structure characteristics of forests (Table 1).

The other LiDAR dataset was collected during the leaf-off period and was thus used as a reference surface for validation (hereinafter, DTM<sup>LiDAR</sup>). It was procured from the State Administration of Land Surveying and Cadastre. The model is based on ALS data gathered between 2010 and 2013. Minimum initial density of the raw acquisition data was 1 point per m<sup>2</sup> while the final product was delivered in the form of terrain heights of discrete points forming a Triangulated Irregular Network (TIN). The declared Root Mean Square Error (RMSE) of heights is 0.18 m in a terrain without continuous vegetation and 0.30 m in terrain with dense vegetation (i.e. forests). The accuracy has been evaluated by several studies (e.g. Hubacek et al., 2016; Šilhavý and Čada, 2015) and the model was previously

used, for example, in studies of yield prediction (Kumhálová and Moudrý, 2014; Moravec et al., 2017). Both LiDAR datasets were provided in the Datum of Uniform Trigonometric Cadastral Network (S-JTSK; EPSG: 5514) and Baltic Vertical Datum – after adjustment (Bpv; EPSG: 5705).

*Table 1. General characteristics of forests structure. Maximum, average, and standard deviation of height are calculated from a Canopy Height Model. Other characteristics are calculated directly from a classified point cloud. Canopy cover is calculated as the number of first returns above breast height (1.37 m) divided by the number of all first returns. Density of (D) ground, shrubs, and trees represents the number of returns in each height interval divided by total number of returns.*

Forest	Area (ha)	Max. height (m)	Avg. height (m)	SD of height (m)	Canopy cover (%)	D. ground (%)	D. shrubs (%)	D. low trees (%)	D. high trees (%)
Plantations of European ash	6.8	29.4	12.4	5.0	58.0	42.3	4.8	40.8	12.0
Spontaneously grown forest of Birch	5.0	21.3	10.6	4.1	60.0	40.6	3.0	52.8	3.6
Mature forest of Willow and Ader	1.2	23.4	15.3	4.4	75.0	27.7	2.0	28.8	41.5

## GROUND CONTROL POINTS and VALIDATION CHECKPOINTS

Prior to the UAV flights, twenty ground control points (GCPs) were established within and in the vicinity of the study area (Figure 1). GCPs were made of white wooden boards (dimensions 0.40 m by 0.40 m) with a black circle dia 0.15 m in the centre. GCPs coordinates were surveyed using Trimble GeoXR 6000 handheld differential global navigation satellite system (GNSS) receiver with Zephyr 2 external antenna mounted on a pole in dual-frequency differential real-time kinematic (RTK) mode with a 15 s observation time. It was connected to the Czech positioning system (CZEPOS) permanent GNSS network.

Another RTK GNSS survey was conducted over the study area on 28 March 2017 (leafoff period) to locate checkpoints for point clouds evaluation using a dual-frequency Leica GPS1200 receivers. RTK mode with a 5 s observation time connected to the CZEPOS permanent GNSS network was used. As collecting GNSS data under tall canopies even during the leaf-off period was a challenging task, a conventional total station survey (with the total station position determined using GNSS) was also used in forested areas. In total, 721 checkpoints were collected for this study (Figure 1). In order to assess quantitatively the effects of vegetation canopies on point clouds accuracy, the information on vegetation

canopy (i.e. forest or steppe) was recorded during the survey for each checkpoint. 422 points were obtained in forests and 299 points in steppes. All GCPs and checkpoints were transformed into the S-JTSK and Bpv coordinate system and provided 2–4 cm horizontal and vertical relative accuracies (Štroner et al., 2013).

## UAV SYSTEMS

Two UAV systems were used for the collection of images (Table 2). A commercial eBee system produced by SenseFly is a ready-to-deploy fixed-wing aircraft with removable wings and a push propeller. EBee was equipped with a Sony Cybershot DSC-WX220 camera with a resolution of 18.2 MPix and a zoom lens of equivalent focal length of 25 to 250 mm. Easystar is a home-assembled drone that consists of a commercially available motor glider Easystar II and 3DR Pixhawk autopilot allowing a fully autonomous flight. Easystar was equipped with Nikon Coolpix A camera with a 16.2 megapixel resolution and a fixed lens with an equivalent focal length of 28 mm.

*Table 2. Comparison of the two UAVs. The prices are listed for the year of purchase (2015).*

Item	eBee	Easy Star
UAV type	fixed-wing	fixed-wing
Motor	Electric pusher propeller, 160 W	Electric pusher propeller, 235 W
Aircraft weight with camera	Approx. 0.7 kg	Approx. 1.0 kg
Payload	only vendor provided cameras	any camera
Wingspan	96 cm	136.6 cm
Flight time	40 minutes	40 minutes
Flight speed	11–25 m/s	10–24 m/s
Autopilot	integrated	Pixhawk
Batteries	3S LiPo, 2150 mAh	3S LiPo, 2200 mAh
Cost (with equipment)	Approx. \$20,000	Approx. \$5,000

## UAV SURVEYS

The UAV images were collected on different days during March 2017 (Table 3). The days may have slightly differed in environmental conditions (e.g. light, wind speed), both days, however, met the conditions required for a successful survey. One flight with Easystar and two flights with eBee were performed to assess the effect of image quantity on accuracy and a density of a point cloud. The eBee flights were mutually perpendicular and differed in flight trajectories (Figure 2). Hereinafter, we refer to these flights as Easystar, eBee<sup>1</sup> and eBee<sup>2</sup>. For both systems, an overlap of 85%, sidelap of 65% and a ground sampling distance

of about 30 mm per pixel was set. Height and speed of the UAV flight were set in both systems by the ground control software, depending on the required resolution. For both systems, the flight height was about 100 m above the ground level. The camera settings were manually set to ISO 400 and shutter speed priority (1/1250 s) for Easystar while eBee camera used default, manufacturer recommended settings (User Manual – WX Camera; Table 3).

*Table 3. Camera settings, parameters, photos acquired and camera interior orientation parameters. eBee Easystar Camera Sony Cybershot DSC-WX220 Nikon Coolpix A. (\*physical focal length \*\*Equivalent Focal Length for 35 mm film )*

Camera	eBee Sony Cybershot DSC-WX220	Easystar Nikon Coolpix A
<i>Specifications and settings</i>		
Sensor (Resolution (Mpix)/Crop)	18.2/2.3	16.2/1.5
Focal length (real*/ekv.**)(mm)	4.45/25	18.05.2028
Aperture	3.3	2.8 – 4.5
ISO	100 – 125	400
Shutter speed (s)	1/250 – 1/640	1/1250
Date of flight	28-03-2017	11-03-2017
Number of photos (eBee <sup>1</sup> /eBee <sup>2</sup> )	1004/903	940
Number of aligned photos (eBee <sup>1</sup> /eBee <sup>2</sup> )	941/869	938
<i>Interior orientation parameters</i>		
Focal length (F)	4.5539	18.5764
Principal point (Cx/Cy)	2437.82/1848.56	2458.75/1659.73
Radial distortion parameters (K1/K2/K3)	-0.0033/-0.0338/0.0290	-0.0742/0.0901/-0.0467
Tangential distortion parameters (P1/P2)	0.0025/-0.0012	-0.0003/0.00002

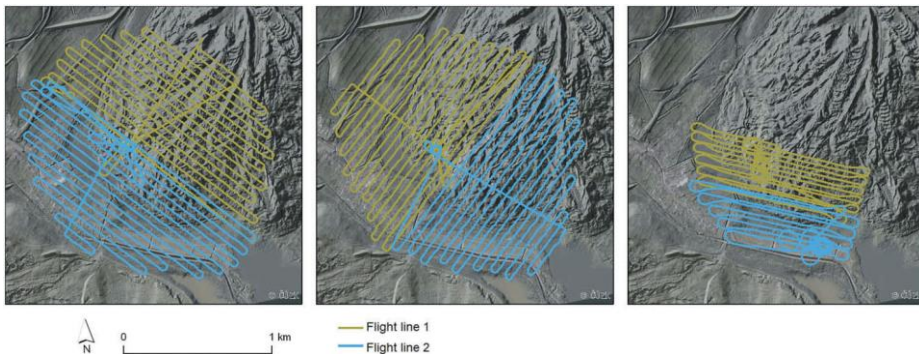


*Figure 2. Flight line trajectories (left to right eBee<sup>1</sup>, eBee<sup>2</sup> and Easystar).*



## IMAGE PROCESSING and 3D POINT CLOUD GENERATION

To generate 3D point clouds, acquired images were processed in the Agisoft's PhotoScan Professional version 1.2.6. Processing was done separately for each individual flight (Easystar, eBee<sup>1</sup>, eBee<sup>2</sup>) and the two eBee flights were also combined (hereinafter, we refer to this as eBee<sup>1,2</sup>) to test the improvement in terrain representation. The procedure consisted of the alignment process, iteratively refining external and internal camera orientations and camera locations through a least squares method, generating a sparse point cloud, followed by the dense multi-view 3D reconstruction algorithm. The images, along with positional data estimated by the onboard GPS during the flight, were loaded into PhotoScan software. The alignment was subsequently completed using accuracy parameter set to 'high' and pair pre-selection to 'disabled'. Accuracy set to 'high' ensured the use of the original image resolution while 'disabled' pair pre-selection ensured the best image matching. The limit for key points (indicating the maximum number of points sampled within each image) was set to 20,000 and for tie points (the number of points used for image matching) to 5,000. The GCPs were loaded and identified in the images, their assumed accuracy was set to 2 cm. Six points were completely removed from the evaluation due to their displacement or complete destruction by animals. This devaluation was caused by a time gap between the measurement of the ground control points and the flights, which was in turn caused by the necessity to wait for the appropriate weather conditions (no snow cover, low wind speed, etc.). Dense point clouds were built with a high reconstruction quality and mild depth filtering. The point clouds were transformed into the S-JTSK and Bpv coordinate systems and exported to the LAS format. To determine the accuracy of the photogrammetric model, the total coordinate error E was calculated for each point cloud as follows:

$$E = \sqrt{\frac{\sum_{i=1}^N (\sqrt{X_{err}^2 + Y_{err}^2 + Z_{err}^2})_i}{N}}$$

where  $X_{err}$ ,  $Y_{err}$  and  $Z_{err}$  are coordinate differences of GCPs, and N is the number of control points. For all point clouds (Easystar, eBee<sup>1</sup>, eBee<sup>2</sup>, eBee<sup>1,2</sup>), points representing ground surface were identified using LAS Ground tool of the ArcGIS software and exported as new ground filtered point clouds (hereinafter, we refer to those as Easystar<sup>Ground</sup>, eBee<sup>1,Ground</sup>, eBee<sup>2,Ground</sup>, eBee<sup>1,2,Ground</sup>).

## POINT CLOUDS and DMR5G ACCURACY ASSESSMENT

We compared cameras calibration (i.e. focal length, principal point coordinates, radial and tangential distortion coefficients) and residual errors. Besides, we compared point clouds in terms of their density and calculated height differences between point clouds and checkpoints. The GNSS surveyed checkpoints have the greatest accuracy and were thus used as the reference dataset (true elevation) to evaluate the point clouds. To quantitatively evaluate the impact of vegetation on point cloud accuracy, we performed the evaluation separately for steppes and three forest types (Table 1). We evaluated the accuracy of all point clouds (Easystar, eBee<sup>1</sup>, eBee<sup>2</sup>, eBee<sup>1,2</sup>, Easystar<sup>Ground</sup>, eBee<sup>1, Ground</sup>, eBee<sup>2, Ground</sup>, eBee<sup>1,2,Ground</sup>) and DTM<sup>LiDAR</sup>. We also show a profile to visually compare the photogrammetric point clouds (Easystar, eBee<sup>1,2</sup>) with LiDAR. In addition, we performed pairwise combinations between the two ground filtered point clouds and DTM<sup>LiDAR</sup>. Water areas were manually vectorised over orthophoto and removed from the analysis. All analyses were performed in ArcGIS 10.4.1 and Cloud Compare 2.9.1.

Due to the presumed presence of outliers, we used a robust L1 norm method (Koch, 1999). This method, being a function of the probability distribution, directly uses Laplace distribution, which is more suitable for dealing with outlying measurements than normal distribution. For nonhomogeneous measurements (measurements with varying standard deviations), a robust weight change is given by the function,

$$w_i = 1/|v_i|$$

where  $w$  represents weights,  $v$  residuals and iteration step. The calculation is done iteratively, residuals acquired from one calculation are used to calculate robust weights' changes in the next calculation. The outliers are determined by residuals exceeding the limit value (2.5 times the standard deviation calculated from residuals). After finding the first set of outliers, new value of mean and standard deviation is determined, followed by a new robust analysis of outliers. As a maximum, ten iterations were used and the number of outliers did not exceed 10%.

Subsequently, we calculated vertical differences between 721 checkpoints and the individual point clouds. The point cloud heights at the positions of checkpoints were derived using 2.5D Delaunay triangulation from six nearest points. Mean error  $\bar{x}$ , standard deviation  $s$  and RMSE were calculated for vertical differences. Both the systematic and random error of the differences contribute

towards RMSE while only the random error component is included in the standard deviation.

$$\bar{x} = \frac{\sum_{i=1}^N (x_i - x_{\text{Ref}})}{N}$$

$$s = \sqrt{\frac{\sum_{i=1}^N (x_i - \bar{x})^2}{N - 1}}$$

$$\text{RMSE} = \sqrt{\frac{\sum_{i=1}^N (x_i - x_{\text{Ref}})^2}{N}}$$

where  $x_i$  is the  $i$ th elevation from point cloud,  $x_{\text{REF}}$  is the corresponding ‘true’ measured elevation,  $\bar{x}$  is mean error, and  $N$  is the number of checkpoints.

## Results and discussion

### CHARACTERISTICS of CAMERAS and GEOREFERENCING

Calibration results of both cameras including estimates of focal length, principal point coordinates, radial and tangential distortion coefficients, and residual errors are shown in Figure 3 and Table 3. The Nikon Coolpix A camera (Easystar) achieved very small residual errors after calibration (max. approx. 0.2 pixels) due to the overall quality of the prime lens (fixed focal length). The calibration model eliminated the radial distortion in the centre of the camera very well. In contrast, the DSC-WX220 (eBee) residual error after calibration was higher (max. approx. 0.7 pixels). This is likely due to the naturally inferior quality of the zoom lens when compared with a prime lens, and therefore different distortion values during shooting. According to the radial and tangential distortion parameters (Table 3), the Coolpix A lens has a bigger radial distortion than the DSCWX220. However, Coolpix A calibration successfully eliminated the distortion while the DSC-

WX220 indicate a radial distortion that increases in the direction of the perspective centre (Figure 3).

The total coordinate errors associated with the georeferencing of the point clouds in Agisoft’s Photoscan are shown in Table 4. The higher total coordinate error for eBee point clouds is likely caused by the lower quality of images. We noticed many GCPs were blurred with the central black circle difficult or even impossible to discern. Such a blur in these images is likely to occur due to a combination of abrupt changes in UAV speed or position in strong gusts of wind (Jensen and Mathews, 2016) and the slower shutter speed of the camera. Posterior comparison revealed that the default camera settings used on the eBee platform used a different compensation method to achieve uniform luminosity than the shutter speed priority used on the Easystar UAV (Table 3).

Table 4. Summary of point cloud characteristics. Point density is shown as Mean  $\pm$  Standard deviation. Void fraction is a percentage of  $1m^2$  resolution cells that did not contain any ground point.

Flight	Total coordinate error (m)	Total points	Point density (points/m <sup>2</sup> )	Ground points	Ground point density (points/m <sup>2</sup> )	Percentage ground (%)	Void fraction (%)
Easystar	0.041	205,311k	330 $\pm$ 54	169,507k	277 $\pm$ 84	82.6	1.3
eBee <sup>1</sup>	0.081	163,290k	274 $\pm$ 84	113,525k	197 $\pm$ 93	69.5	7.2
eBee <sup>2</sup>	0.053	129,003k	208 $\pm$ 37	105,960k	173 $\pm$ 53	82.1	1.3
eBee <sup>1,2</sup>	0.050	145,129k	241 $\pm$ 76	111,088k	188 $\pm$ 79	76.5	5

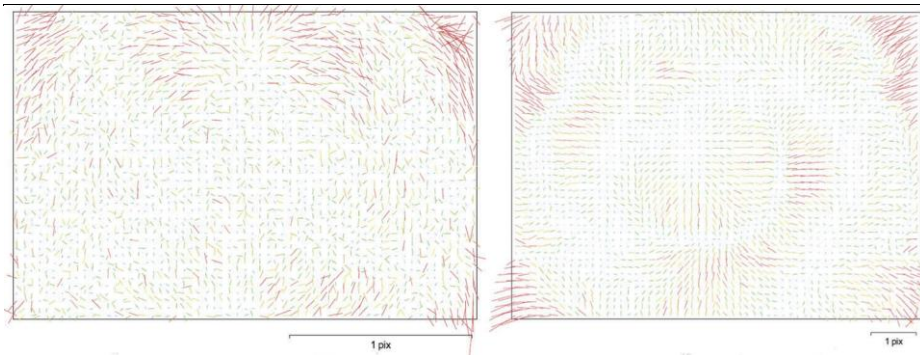


Figure 3. Visualisation of distortion characteristics of lens mounted on the two platforms/ (left – EasyStar, right – eBee).

While the Easystar mounted Nikon Coolpix A camera with its larger sensor, which is less prone to noise generation, allowed a higher ISO setting and therefore higher shutter speed (1/ 1250s), Sony DSC-WX220 camera mounted on eBee in the manufacturer-recommended auto mode used low ISO and compensated for changing lighting conditions predominantly by changing shutter speed.

## DENSITY and ACCURACY of PHOTOGRAMMETRICALLY DERIVED POINT CLOUDS

Point cloud characteristics for the acquired datasets varied significantly (Table 4). The most dense point cloud was acquired with Easystar. Its average density was 330 points per m<sup>2</sup>, while the average density of all eBee derived point clouds was below 280 points per m<sup>2</sup>. When overlaid with a grid at 1 × 1 m resolution, Easystar and eBee<sup>2</sup> provided a similar number of cells containing at least one ground point (a low value of void fraction). It is evident that the images acquired with Easystar were of very high quality allowing proper image matching and thus a greater number of points. Moreover, ground points were successfully generated even in the forest areas. In contrast, eBee<sup>1</sup> contained a number of void areas in forests. The point density was significantly lower for eBee<sup>1,2</sup> and eBee<sup>2</sup> than for Easystar but it still achieved relatively good results in terms of ground coverage, especially in problematic forested areas (Figure 4; see below). Furthermore, we found that the proportion of ground points was not dependent on the total number of points in the point cloud as eBee<sup>1</sup> showed a lower proportion of ground points despite having a higher point density.

The accuracy of point clouds was relatively consistent throughout the three forest types under study and the results shown represent evaluation throughout all forested areas (Table 5). Easystar point cloud achieved the best accuracy in both the forests (Table 5) and steppes (Table 6) with the RMSEs of 0.11 m and 0.12 m, respectively. A combined processing of two individual flights eBee<sup>1,2</sup> resulted in a lower RMSE than individual eBee point clouds, both the RMSE (due to a greater systematic error) and the number of excluded measurements were however still worse than Easystar results. The eBee<sup>2</sup> point cloud, despite displaying a higher RMSE and number of outlying values than Easystar, still yielded a very good overall accuracy of the data. The eBee<sup>1</sup> flight achieved the worst results in the forest areas.

The high number of outliers for eBee<sup>1,2</sup> and especially for eBee<sup>1</sup> point cloud was caused by gaps in forested areas where no points were identified by the software.

Contrary to our expectations, a higher number of images did neither lead to a better coverage, nor higher point densities or lower void fraction (Table 4). On the contrary, the results were inferior to those acquired from a single eBee<sup>2</sup> flight. Triangulation between distant points in these gap areas (without a single point identified) created a terrain significantly different from reality, and points were evaluated as outlying. We did not notice these gaps in steppes and indeed the number of outliers is much lower in that environment (Table 6). Although Clapuyt et al. (2016) have shown that topography derived from repeated surveys differed in the magnitude of centimetres which is in accordance with our results, they have performed their study in an area covered by pasture and arable fields without crops. As we detected relatively large gaps where no points were identified for eBee<sup>1</sup> point cloud, it is apparent that under suboptimal conditions (e.g deciduous forest during leaf-off period), the repeatability of a survey is problematic.

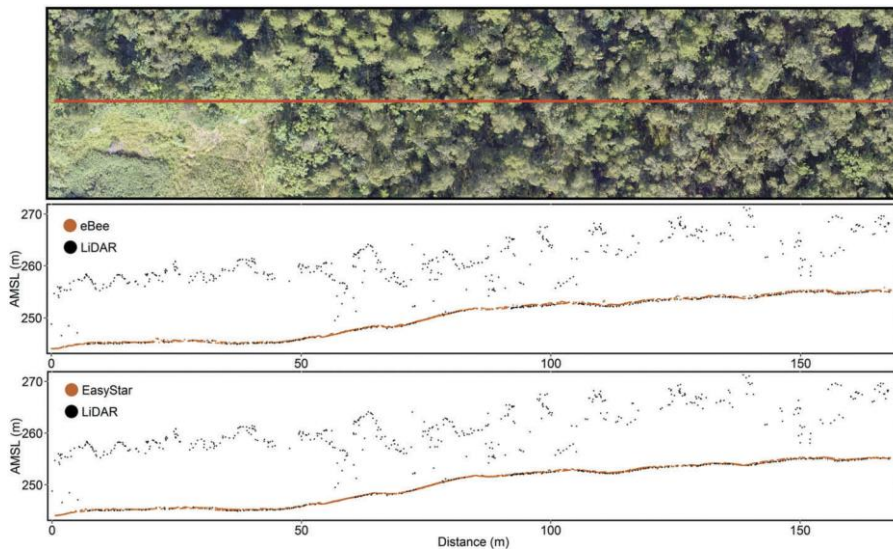


Figure 4. Orthophoto and location of a profile (top) and structure of photogrammetric point clouds under forest stands derived from eBee<sup>1,2</sup> (middle) and EasyStar (bottom) in comparison with LiDAR point cloud acquired during leaf-on period (May 2017). Note that both photogrammetric point clouds show a great potential for detecting ground in forest during the leaf-off period. The profile is 1 m wide.

Table 5. UAV and GNSS differences (422 points in forest).

Flights	Mean difference (m)	RMSE(m)	SD (m)	No. of outliers
Easystar	0.04	0.11	0.10	3 (1%)
eBee <sup>1</sup>	0.08	0.17	0.15	31 (7%)
eBee <sup>2</sup>	0.10	0.15	0.11	10 (2%)
eBee <sup>1,2</sup>	0.08	0.13	0.10	13 (3%)
Easystar <sup>Ground</sup>	0.05	0.11	0.10	1 (0%)
eBee <sup>1,Ground</sup>	0.07	0.19	0.17	47 (11%)
eBee <sup>2,Ground</sup>	0.10	0.15	0.11	16 (4%)
eBee <sup>1,2,Ground</sup>	0.08	0.13	0.11	15 (4%)
DTM <sup>LiDAR</sup>	0.21	0.24	0.13	21 (5%)

Table 6. UAV and GNSS differences (299 points in steppes).

Flights	Meandifference(m)	RMSE(m)	SD(m)	No.ofoutliers
Easystar	0.05	0.12	0.11	3(1%)
eBee <sup>1</sup>	0.15	0.19	0.11	1(0%)
eBee <sup>2</sup>	0.16	0.19	0.09	4(1%)
eBee <sup>1,2</sup>	0.14	0.16	0.07	3(1%)
Easystar <sup>Ground</sup>	0.04	0.11	0.10	3(1%)
eBee <sup>1,Ground</sup>	0.16	0.19	0.11	5(2%)
eBee <sup>2,Ground</sup>	0.16	0.19	0.10	7(2%)
eBee <sup>1,2,Ground</sup>	0.15	0.17	0.08	12(4%)
DTM <sup>LiDAR</sup>	0.27	0.31	0.14	22(7%)

We can only hypothesize what caused the differences between two eBee flights. The most likely explanation lies in differences in the weather conditions between the flights, especially wind speed. The combination of a possible higher wind speed, causing movement of the thin twigs, and slower shutter speed used by the camera in the manufacturer recommended default settings might have caused a greater blur in the forest areas in the eBee<sup>1</sup> flight, which might have subsequently complicated the image matching algorithm.

## The EFFECT of the VEGETATION

The low difference between the RMSE and the standard deviation indicates a minimal systematic error in the forest areas. The obtained standard deviations for the height component are approaching the generally accepted limit of accuracy of the GNSS RTK method of about 0.05–0.1 m, indicating the suitability of UAV photogrammetry for ground detection even in the deciduous forests during the leaf-off period. In the steppes, however, point clouds are affected by a slightly higher systematic shift (Table 6). This slight increase in RMSE for all point clouds is likely caused by the presence of low vegetation and shrubs. The passive photogrammetric methods measure the highest visible terrain points, e.g. grass or small dense shrubs. The systematic shift is caused by the difference between the height of the low vegetation and the terrain.

While the presence of low vegetation is problematic even in winter and the risk that the vegetation is identified as the ground is almost inevitable (Meng et al., 2010), high vegetation (i.e. tree trunks, branches, and twigs) was only residually present in generated point clouds (Figure 4). That is in contrast with Dandois and Ellis (2013; see Figures 2 and 7 in their paper). The different character of acquired point clouds is likely due to the differences in the structure of the forests. The canopy on the three deciduous forest plots (250 × 250 m) in their study was higher (mean canopy height between 20 m and 37 m; maximum height up to 42 m) and the species composition was different (mainly American beech *Fagus grandifolia*, oak *Quercus* spp., hickory *Carya* spp., and tulip-poplar *Liriodendron tulipifera*). Besides, they used a hexacopter and flew only 40 m above the peak canopy height (our flying altitude was almost double that above the canopy).

## ACCURACY of LiDAR DTM

DTM<sup>LiDAR</sup> contains a higher systematic error (shift) and a higher number of outliers compared to the photogrammetrically derived point clouds in both forests and steppes (Table 5, 6). The RMSE of 0.24 m is within the declared accuracy of 0.30 m in forests; in the steppes, however, the RMSE of 0.31 exceeds the declared accuracy; the vertical (in) accuracy of GNSS survey (0.05–0.1 m) used as a true elevation must be however taken into account and hence, the DTM<sup>LiDAR</sup> accuracy may well be maintained even in these areas. The reasons are likely similar to those discussed for photogrammetric point clouds as the vegetation is often dense in these areas, which, in conjunction with the low density of ALS data, may have prevented an accurate recording of the ground surface (see Brazdil, 2012). Furthermore, Hubacek et al. (2016) reported problems in areas where a micro-



relief objects were present. It is likely that it might have been difficult to accurately represent the undulated terrain with low density of points.

There is a systematic shift of  $DTM^{LiDAR}$  compared to the acquired photogrammetric point clouds (Table 7), which corresponds to their higher accuracies (Tables 5 and 6). Height differences range from  $-0.20$  m to  $0.56$  m and from  $-0.28$  m to  $0.58$  m for ground filtered Easystar and eBee<sup>1,2</sup> point clouds, respectively, prior to the L1 norm application, and therefore containing the outliers (Figure 5). Outside the area with ground control points, the point clouds acquired by the individual UAVs (after ground filtering) are affected by the stability and rigidity of the model. In the area between the ground control points (central part), the differences are very close to zero for both Easystar and eBee; nevertheless, the accuracy drops outside the area with the ground control points. Note that the areas of lower accuracy slightly differ between the point clouds (Figure 5). UAV platforms are less costly to deploy in comparison to ALS surveys and able to provide data at higher spatial resolutions that are more appropriate for microtopographic studies (Lucieer et al., 2014). On the other hand, they are highly limited by weather conditions (snow, wind, cold and the movement of the sun) that are often, especially during the winter season, not very inviting for a survey.

*Table 7. Image-derived point clouds comparison with LiDAR DTM (147,111 points).*

Point clouds	Mean difference (m)	RMSE (m)	SD (m)	No. of outliers
EasystarGround	0.15	0.21	0.14	3805 (3%)
eBee <sup>1,Ground</sup>	0.13	0.22	0.17	6772 (5%)
eBee <sup>2,Ground</sup>	0.11	0.18	0.14	5576 (4%)
eBee <sup>1,2,Ground</sup>	0.12	0.18	0.13	6569 (4%)

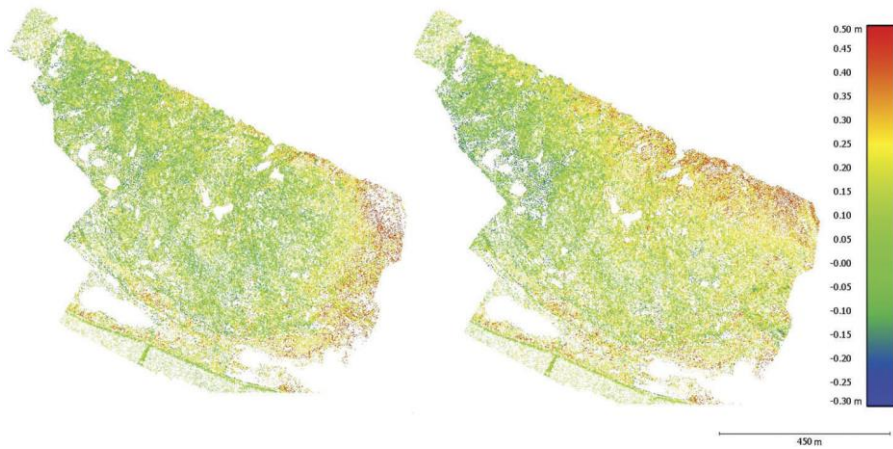


Figure 5. Comparison of point clouds  $eBee^{1,2,Ground}$  (left) and  $Easystar^{Ground}$  (right) with LiDAR DTM expressed as vertical difference (LiDAR – Point Cloud). Red colour indicates areas of overestimation and blue color areas of underestimation of LiDAR DTM compared to point clouds. Note that high overestimation occurs mainly in areas outside the ground control points, which indicates decreasing accuracy of point clouds outside the area defined by GCPs.

## Conclusions

We compared the suitability of two UAV systems (a commercial eBee system by SenseFly and a home assembled Easystar II motor glider with 3DR Pixhawk autopilot) for mapping of undulated terrain of post-mining site (spoil heap) during a leaf-off period. We want to emphasize that our goal was to compare the overall performance (i.e. drone + camera) of a commercially available ready-to-use platform with a cheap customizable home-assembled kit and it was not our intention to evaluate suitability of particular cameras (as various cameras can be mounted on Easystar), nor to evaluate the automated vs manual setting of parameters, although they are likely the main cause of the differences.

The acquired point clouds were evaluated in two environments – forests and steppes. Easystar achieved better results than eBee in both point density and accuracy, which is most likely due to the use of a better camera (lens with fixed focal length and bigger sensor allowing higher ISO setting and therefore faster shutter speed). A better accuracy after ground filtering of the point clouds was acquired for the forest environment with RMSEs of 0.11 and 0.13 for Easystar

and eBee, respectively. Accuracies acquired in the steppe environment were slightly inferior with RMSE 0.11 and 0.17 for Easystar and eBee, respectively. A combination of images from two mutually perpendicular flights led to a higher accuracy but failed to increase the density of the point cloud. Despite differences between the acquired point clouds, both systems were able to accurately detect terrain in open steppes and under forest canopy under leaf-off conditions with a higher accuracy than a nationwide LiDAR-derived DTM. Hence, we can report that photogrammetric methods can be used successfully in steppes and deciduous forest stands under leaf-off conditions to generate accurate DTM. Further research is however needed to quantitatively assess the quality of models acquired under leaf-off conditions in deciduous forest stands of different characteristics (e.g. tree species, structural, and site characteristics).

Both solutions (Easystar and eBee) have pros and cons and they pose different requirements on the user. It is well known that cameras with fixed focal length are more appropriate for photogrammetry and it is fair to note that senseFly have recently made another camera available for their eBee system, the 20 MPix senseFly S.O.D.A. However, for users who prefer to have greater control over their options rather than being at the vendor's mercy, home-assembled kits utilizing drones capable of carrying any camera available on the market may be an advantage.

## ACKNOWLEDGMENTS

We are grateful to two anonymous reviewers and Jaroslav Janošek for their comments that improved the quality of the manuscript. This work was supported by the Grant Agency of the Czech Technical University in Prague under Grant No. SGS17/067/OHK1/1T/11; the Internal Grant Agency of the Faculty of Environmental Sciences, CULS Prague under Grant number 20164242, and the Czech Science Foundation under Grant No. 17-17156Y.

## FUNDING

This work was supported by the Czech Science Foundation [Grant No. 17-17156Y]; Grant Agency of the Czech Technical University in Prague [Grant No. SGS17/067/OHK1/1T/11]; Internal Grant Agency of the Faculty of Environmental Sciences, CULS Prague [Grant number 20164242]



## Chapter V – STUDY 2

### Title:

The Potential of Unmanned Aerial Systems: A Tool towards Precision Classification of Hard-To-Distinguish Vegetation Types?

### Authors:

Jan Komárek, Tomáš Klouček, **Jiří Prošek**

### Author's contribution: 15<sup>0</sup>%

Preliminary testing and field work; co-writing of the original draft, cooperation and consultation of UAV data processing, classification approach and results interpretation.

### Journal:

*International Journal of Applied Earth Observation and Geoinformation*, IF (2018) 4.846 – 5 of 30 (Q1) rank in WOS category Remote Sensing; AIS (2018) 1.098 – Q1 rank

### Full citation:

Komárek, J., Klouček, T., & Prošek, J. (2018). The potential of Unmanned Aerial Systems: A tool towards precision classification of hard-to-distinguish vegetation types? *International Journal of Applied Earth Observation and Geoinformation*, 71, 9-19.

### Cited:

6 times cited on WOS (2019 August).

## ABSTRACT

Detailed plant species classification using very high spatial resolution data is a challenging task. Exploring the potential of imagery acquired by Unmanned Aerial Vehicle (UAV) to identify individual species of plants and assessing values of additional inputs such as height and thermal information into classification process are hot research topics. Our study uses a fusion of visible, multispectral and thermal imagery acquired through the low altitude aerial survey for detail classification of land cover and vegetation types. The study area is located in the central part of the Czech Republic and situated in an environmentally specific area – an arboretum of 2.45 ha. Visible (i.e. RGB), multispectral, and thermal sensors were mounted on a flying fixed-wing Unmanned Aerial System. The imagery was acquired at a very detailed scale with Ground Sampling Distance of 3–18 cm. Besides three mosaics (one from each sensor), normalized Digital Surface Models were built from visible and multispectral sensors. Eight classification models were created – each mosaic (visible/multispectral) was enriched with height data, thermal data, and combined height and thermal information. A classification into a three level system was performed through Geographic Object-based Image Analysis using Support Vector Machine algorithm. In general, Overall Accuracy grew with the amount of information entering the classification process. Accuracy reached 77 – 91% depending on the level of generalization for the best model based on multispectral data and 67 – 80% for data from the visible sensor. Both thermal data and height information improved the accuracy; however, the statistical evaluation did not reveal any significant difference between the contribution of height and thermal data. Results also indicate that increasing spectral resolution leads to a significantly better performance of the models than higher spatial resolution. UAVs equipped with a proper sensor provide a convenient technology for detail land cover classification even in areas with many similar plant species.

## KEYWORDS

Low altitude aerial survey, Classification accuracy, Fine spatial resolution, Normalized digital surface model (nDSM), Geographic object-based image analysis (GEOBIA), Multispectral and thermal imagery fusion, Image processing, Structure from motion (SfM)

# Introduction

Nowadays, it is relatively easy to acquire one's own image data with a detailed spatial, sufficient spectral and variable temporal resolution. Unmanned Aerial Vehicles (UAVs) and their use are among the most dynamically developing fields of remote sensing (RS), being a suitable source of data for environmental analyses focused e.g. on classification of vegetation (Gini et al., 2014; Husson et al., 2017; Laliberte et al., 2011; Lisein et al., 2015; Michez et al., 2016; Weil et al., 2017) invasive plant detection (Müllerová et al., 2017), pests (Näsi et al., 2015), plant diseases and water stress detection (Baluja et al., 2012; Berni et al., 2009; Calderón et al., 2013; Nishar et al., 2016; Zarco-Tejada et al., 2012), modelling of individual treetops (Díaz-Varela et al., 2015), in agriculture (Moravec et al., 2017; Pérez-Ortiz et al., 2015), or for monitoring animal species (Chrétien et al., 2016).

One of the major UAV challenges lies in a detail classification of the land cover (Ahmed et al., 2017), which may support decision-making mechanisms and operations. Besides low altitude UAV surveys, other technologies are used for precision classification, e.g. for species classification of trees (Ali et al., 2004; Holmgren et al., 2008), of vegetation specific for various environment types (Alonzo et al., 2014; Bork and Su, 2007; Feng et al., 2015; Hartfield et al., 2011; Husson et al., 2017; Rampi et al., 2014; Reese et al., 2015; Sankey et al., 2017b), or a complex land cover classification (Kuria et al., 2014; Szostak et al., 2014; Teo and Huang, 2016; Zhou and Qiu, 2015).

Classification accuracy can be affected by the properties and quality of both the spectral information and height data from (a) digital terrain models (DTMs); (b) digital surface models (DSMs) or (c) normalized digital surface models (nDSM). For land cover classification, a fusion approach combines multi(hyper)-spectral satellite data (Reese et al., 2015; Zhou and Qiu, 2015), airborne (Alonzo et al., 2014; Bork and Su, 2007; Teo and Huang, 2016) and UAV-borne (Sankey et al., 2017a) with Airborne Laser Scanning (Alonzo et al., 2014; Bork and Su, 2007; Holmgren et al., 2008; Zhou and Qiu, 2015) or with airborne images processed through photogrammetric image matching (Reese et al., 2015). The height data (point clouds) can be also derived from UAV-borne imagery by a photogrammetric Structure from Motion (SfM) method. However, the height data are frequently inappropriately neglected during classification utilizing UAV imagery (Feng et al., 2015) despite the fact that they can be instrumental in achieving better results (Husson et al., 2017).

The accuracy of resulting classification is also affected by the classification approach. If processing very high resolution data (e.g. UAV-borne data), classifications based on Geographic Object-based Image Analysis approach (GEOBIA; Blaschke, 2010; Liu et al., 2015) tend to provide better results than the traditional pixel-based approach (Yu et al., 2006). The benefit of GEOBIA has been repeatedly shown in multiple studies utilizing predominantly satellite or airborne high spatial resolution data (Addink et al., 2007; Alonzo et al., 2014; An et al., 2007; Diaz-Varela et al., 2014; Hartfield et al., 2011; Peña et al., 2013).

UAV sensors are typically RGB cameras recording images in visible (Feng et al., 2015; Gini et al., 2014; Husson et al., 2017; Müllerová et al., 2017) or in near infrared spectrum (Ahmed et al., 2017; Weil et al., 2017). RGB cameras are used on a mass scale due to their availability, their classification accuracy is however substantially lower (Ahmed et al., 2017). On the other hand, the higher spatial resolution may act as a substitution for additional spectral bands in specific RS studies. Other sensors, e.g. hyper-spectral cameras or UAV LiDAR (Sankey et al., 2017a) are also available, however, their costs are high.

Due to current restrictions and regulations, use of UAV is limited by country-specific legislation. Applicability is also limited by a higher price of miniaturized sensors or a relatively high UAV susceptibility to failures (Freeman and Balas, 2014; Zuiiev et al., 2015). UAV is still a novel technology, therefore use is still facing challenges and problems that need to be identified and overcome than the traditional remote sensing methods (Ahmed et al., 2017). The analysis of imagery obtained through other (non-UAV) methods have led to the development of many more or less standardized approaches over the years. It is likely, although not properly verified yet, that for various environment-related analyses, these approaches will be also applicable very high resolution data (magnitude of a few cm). Recent general reviews of UAV applications have been published (Marris, 2013; Pajares, 2015), more studies using different types of UAV imaging sensors are however needed to increase the potential of the utilization of such new platforms in vegetation inventorying and other environmental applications. Despite the fact that UAVs have been a hot research topic in the recent years, only a few studies focused on their usability for precise classification using a set of sensors have been published.

The aim of our study is to evaluate the potential of UAV acquired data (namely of images acquired using visible, multispectral and thermal sensors, and height models – nDSMs – derived from such data) for classification of land cover, particularly on the level of individual plant species. Following research questions



are presented: (i) Is it possible to classify individual plant species with a sufficient accuracy based on UAV imagery? (ii) Is it possible to substitute additional spectral data by an RGB sensor with a higher spatial resolution for classification of plant species? (iii) Do the height data contribute to improving the classification more than thermal data? (iv) Do the thermal data constitute an important source of information for detailed land cover classification?

## Materials and methods

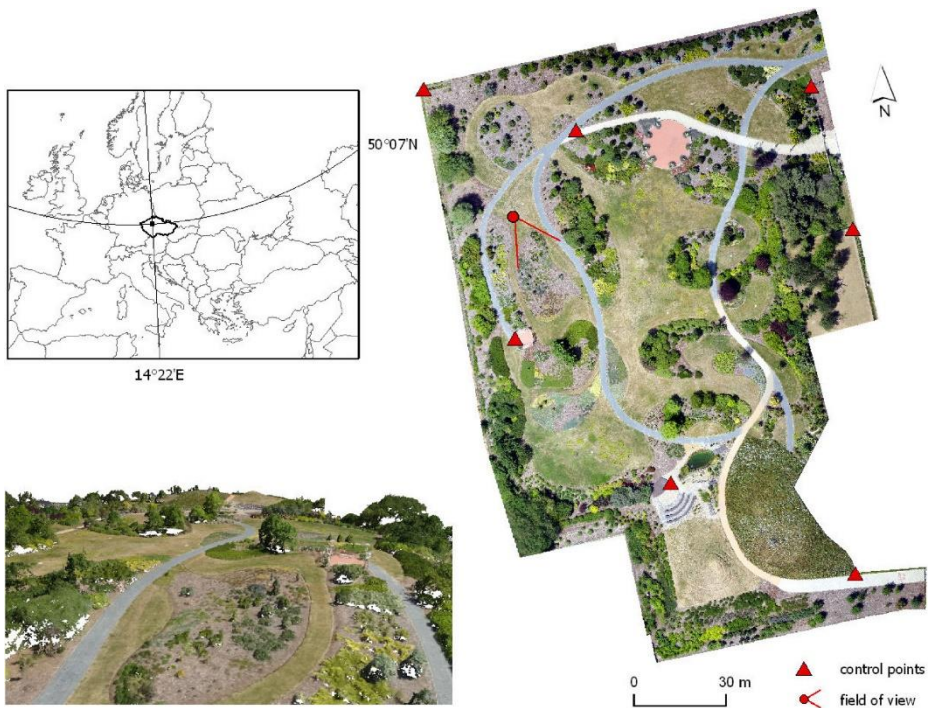


Figure 1. (Above left) Location of the study area. (Right) The study area, a part of the Libosad arboretum (2.45 ha). Seven ground control points were used to facilitate further data processing. (Bottom left) Oblique view of the coloured densified Point Cloud from the point indicated on the orthophotomap. The map corresponds to ETRS 1898 LAEA projection (EPSG 3035).

## STUDY AREA

The area of interest is an arboretum (called Libosad) on site of the campus of the Czech University of Life Sciences in Prague, Czech Republic (Figure 1). The arboretum, founded in 2007, takes up 2.67 ha and includes approximately 900 plant species, divided into 22 thematic units. The relief of the area of interest is topographically homogeneous (elevation ranges 280–289 amsl).

## IMAGE DATA COLLECTION

UAV imagery was acquired during the full vegetation period between 20th and 22nd June 2017, always between 12:00 -13:00 (proper sun angle, minimizing the effect of shadows). The eBee aerial platform (senseFly, Switzerland), a miniature fixed-wing vehicle with a maximum take-off weight approximately 0.8 kg and the wingspan of 0.96 m, was used for image acquisition. The following cameras were used for individual flights: (a) DSC-WX220 (Sony, Japan, Figure 2 A) – a consumer grade digital compact camera; (b) MultiSPEC 4 C (Airinov, France, Figure 2 B) – a 4-channel multispectral camera and (c) ThermoMAP (senseFly, Switzerland, Figure 2 C) – an eBee-ready thermal camera based on FLIR Tau sensor. Detail characteristics of the cameras are available from the manufacturer's websites, parameters important for the study are collected in Tables 1 and 2.

Flight missions were performed using eMotion 2 ground station software. The flight plan was conducted using perpendicular flight lines with 80% overlaps and sidelaps to acquire high quality data. Conditions for UAV flight mission were convenient, ceiling and visibility were fine, the weather was sunny without clouds, the temperature of 30–31 °C, and a light breeze of 2–5 m.s<sup>-1</sup>. Only vendor-provided sensors, one at a time, can be mounted on the eBee platform. Therefore, three separate specific flights with the UAV equipped with (a) visible (i.e. camera records in a visible part of the spectrum) camera; (b) multispectral camera and (c) thermal camera were conducted; flight details are shown in Table 2. A grayscale calibration target with known reflectance values was captured for further image calibration. For data post-processing, a total number of seven Ground Control Points (GCP), designed as 0.5 m white numbered boards with a centre hole for survey rod, was surveyed using GPS Leica 1200 (Leica, Germany) through real-time kinematic connected to the CZEPOS network of permanent GNSS stations.

## IMAGE PROCESSING and ORTHOMOSAIC BUILDING

All acquired imagery was processed using a photogrammetric software Pix4Dmapper 3.1.2 (Pix4D S.A., Switzerland). Firstly, point clouds (densified) were created for all data types using stereo-photogrammetry based photo-reconstruction method (Structure from Motion). Orthomosaics were built and accurately georeferenced using Ground Control Points, the Root Mean Square Error (RMSE; mean of X, Y, and Z) was 0.038 m for RGB mosaic and 0.054 m for MSC mosaic. RMSE, which indicates how was the model fitted to the GCPs, was lower than a double value of Ground Sampling Distance (GSD). As the last step, the Surface Reflectance values were calculated from the multispectral mosaic using values from onboard irradiance sensor (Sun irradiance and Sun angle) and the calibration target. The values were subsequently verified in the terrain using the GreenSeeker (Trimble, US) crop sensing system. Similarly, thermal sensor values were corrected using object emissivity values estimated from NDVI vegetation index.

## CREATING NORMALIZED DIGITAL SURFACE MODELS

Digital surface models were created through the Inverse Distance Weighing and using an algorithm implemented in Pix4Dmapper, the digital terrain model with a resolution of 5 x GSD was derived (software limitation due to robustness, see Pix4D User Manual). A normalized digital surface model was subsequently created in ArcGIS for Desktop 10.4 (ESRI, US) by subtracting DTM raster from DSM raster for both RGB and MSC mosaics, resulting in two distinct models, namely (a)  $nDSM_{RGB}$  and (b)  $nDSM_{MSC}$ .

Table 1. Selected characteristics of utilized UAV sensors; abbreviations: B (Blue), G (Green), R (Red), RE (Red Edge), NIR (Near Infrared), LWIR (Long Wavelength Infrared), GSD (Ground Sampling Distance), FWHM (Full Width at Half Maximum).

Sensor (abbreviation)	Image resolution	GSD at 100 m (cm/px)	FWHM (nm)	Band Peak (nm)	Weight (g)
DSC-WX220 (RGB)	17.98 MPx (4896x3672)	2.75	B:410-490 G:460-600 R:580-660	B: 460 G: 530 R: 660	113
MultiSPEC 4C (MSC)	4 x 1.23 MPx (1280x960)	10	G:530-570 R:640-680 RE:730-740 NIR:770-810	G: 550 R: 660 RE: 735 NIR: 790	160
ThermoMAP (TMP)	0.33 MPx (640x512)	18.5	LWIR:7.5k- 13.5k	LWIR 10k	134

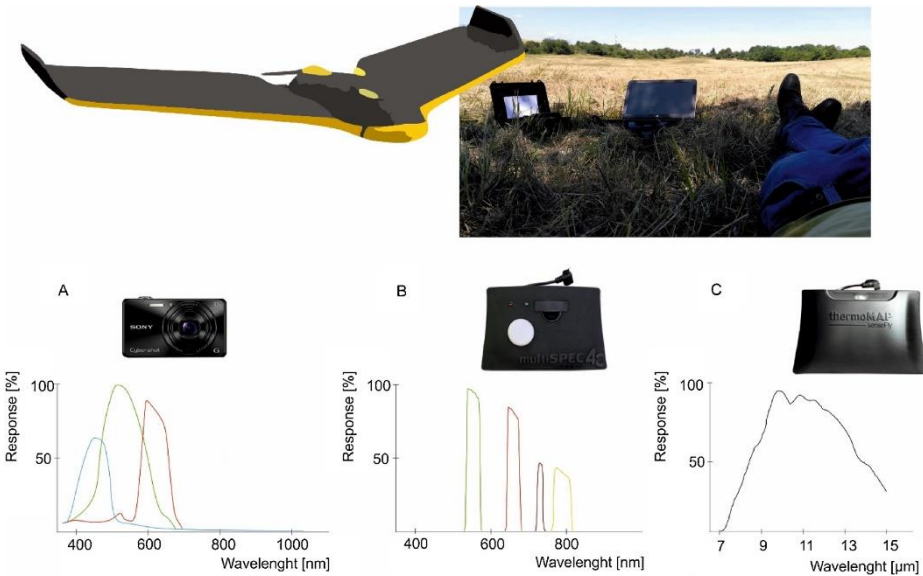


Figure 2. Used devices: Unmanned Aerial Vehicle eBee was equipped with a visible (A), multispectral (B), and thermal camera (C).

Table 2. Basic parameters of the flight missions and data processing parameters. Flight height, a high number of gained images and points density for ThermoMAP is a subject of technical specification of the sensor; AGL (Above Ground Level).

Sensor	Date of Acquisition	Fly Area (ha)/ Fly Time (min)	Fly Height AGL (m)	No. of gained images	No. of aligned images	Avg. points density per m <sup>2</sup>
DSC-WX220	June 22	15.0/21	70	218	217	274.5
MultiSPEC 4C	June 20	13.8/27	60	28	408	18.8
ThermoMAP	June 20	10.1/27	100	4794	386	1.6

## CLASSIFICATION MODELS

Image to image registration was conducted due to different spatial resolutions of built mosaics and models (Table 3). Thermal mosaic and nDSM data were resampled (Nearest Neighbour) to the same pixel size as RGB and MSC mosaics. Input datasets were cropped to fit the study area using ArcGIS and classification models were subsequently created in ENVI 5.4 (Exelis VIS, US). Selected combinations of obtained image mosaics and nDSMs were layered into a single image using the Layer Stacking tool. In total, eight classification models were created from various combinations of input data, see Table 4.

Table 3. Input datasets. Description of the created mosaics (RGB, MSC and TMP) and normalized digital surface models (nDSM).

Inputdataset	Bands	Ground Sampling Distance (cm/px)	Description
RGB mosaic	Blue, Green, Red	2.2	Image mosaic built from imagery taken by DSC-WX220 sensor.
MSC mosaic	Green, Red, RE, NIR	5.7	Image mosaic built from imagery taken by MultiSPEC 4 C sensor.
TMP mosaic	LWIR	20.1	Image mosaic built from imagery taken by ThermoMAP sensor.
nDSM <sub>RGB</sub>	Normalized height	10.8	Normalized height created by subtraction of DTM <sub>RGB</sub> from DSM <sub>RGB</sub> .
nDSM <sub>MSC</sub>	Normalized height	28.4	Normalized height of objects created subtraction DTM <sub>MSC</sub> from DSM <sub>MSC</sub> .

## DELINEATION of LAND COVER and VEGETATION TYPES

The land cover structure was created using pre-existing inventory records and maps from 2015, accurately describing the occurrence of plant species in the area of interest. Species represented by less than 10 individuals were not included. This step was necessary for the study as the area of interest was an arboretum

containing a high number of species and cultivars with a small number of individuals, which could have possibly complicated the interpretation of the results. The structure contained 24 classes, consisting of 17 elements of living and 7 of inanimate nature on the most detailed level (see Table 5).

*Table 4. Classification models. An overview of the eight classification models derived from combinations of selected input datasets.*

Classification model	Input dataset
MSC	MSC mosaic
MSC-TMP	MSC mosaic, TMP mosaic
MSC-nDSM	MSC mosaic, nDSM <sub>MSC</sub>
MSC-nDSM-TMP	MSC mosaic, nDSM <sub>MSC</sub> , TMP mosaic
RGB	RGB mosaic
RGB-TMP	RGB mosaic, TMP mosaic
RGB-nDSM	RGB mosaic, nDSM <sub>RGB</sub>
RGB-nDSM-TMP	RGB mosaic, nDSM <sub>RGB</sub> , TMP mosaic

## GROUND DATA COLLECTION

The field survey was performed at the same time as the UAV flights by recording exact positions of objects into a detail orthomosaic built within pre-analysis. The data collection process was conducted using a Collector for ArcGIS (ESRI, US) application to verify the inventory records. In total, 436 reference polygons (each containing a single taxonomic individual) covering approx. 7% of the area of interest were classified into 24 land cover types. For each class, 10 polygons were randomly selected for analysis and each of those sets was, again randomly, divided into training data (5 polygons) and validation data (remaining 5).

## CLASSIFICATION PROCESS

Verification of suitability of UAV input data acquired using various sensors for classification was performed through object classification (Blaschke, 2010; Blaschke et al., 2014) using Feature Extraction method in ENVI, see Figure 4 for classification workflow. Individual classification models and training data were used as input data (Table 4). In all, therefore, eight individual classifications using identical training data and classification parameters were performed (see Figure 3). Image segmentation was performed using the following parameters: (a) Scale level: 30, Scale Algorithm: Edge, and Segment bands: MSC/ RGB bands only; (b) Merge

level: 98, Merge Algorithm: Full Lambda Schedule and Merge Bands: MSC/RGB bands only, and (c) Texture Kernel Size: 9. As the software manufacturer recommendation is not to use data with variable value range as Segment bands data, neither nDSM nor thermal data were used for segmentation (ENVI Help). The optimum setting of segmentation parameters was found experimentally using ENVI Preview. In the second step, the classification itself, we used the Support Vector Machine (SVM) classifier in default settings (Radial Basis kernel type) with selected classification attributes (chosen by logic/experimental) as follows: (a) Spectral (Mean, Standard Deviation), (b) Texture (Range, Mean, Variance, Entropy), (c) Spatial (Compactness, Elongation, Hole Area/Solid Area).

*Table 5. A class structure used in the study, consisting of 24 classes divided into a 3-level system.*

Level 1	Level 2	Level 3
Coniferous plants	Tall	Fir (Abies), Pine (Pinus)
	Low (under 3 m)	Juniper (Juniperus), Golden Juniper (Juniperus), Pine (Pinus), Spruce (Picea), Yew (Taxus), Golden Yew (Taxus)
Broadleaf plants	Tall	Maple (Acer), Willow (Salix)
	Low (under 3 m)	Cotoneaster (Cotoneaster), Lavender (Lavandula), Cinquefoil (Potentilla), Rose (Rosa), Spiraea (Spiraea)
Herbaceous (Grasses)	Lawns	Lawns
	Meadows	Meadows
Non-vegetation	Artificial surfaces Shadows	Pavement, gravel, crushed stones, bark-dust, wooden elements, metallic elements

## VALIDATION ASSESSMENT

The accuracy of individual models was assessed through comparison with validation samples. Stratified random sampling design utilizing supervised object-based classification suggested by Zhen et al. (2013) was used. The number of validation samples was set to 600 (Cochran, 1977). In each of the validation polygons of each class, five simple random samples were created. The relative accuracy of the classifications acquired through comparison with validation samples via Confusion Matrix (Foody and Boyd, 2013; Olofsson et al., 2014; Stehman, 2013), together with 95% Confidence Interval for accuracies in order to cover classification errors. The differences among individual models were tested

through a test for homogeneity with a binomial distribution using Holm's p-value adjustment method to compensate for multiple comparisons (used for example by Klouček et al., 2015), see Figure 5. All statistical analyses were done at three hierarchical levels: (a) Level 1 (4 classes); (b) Level 2 (8 classes); (c) Level 3 (24 classes).

## Results and discussion

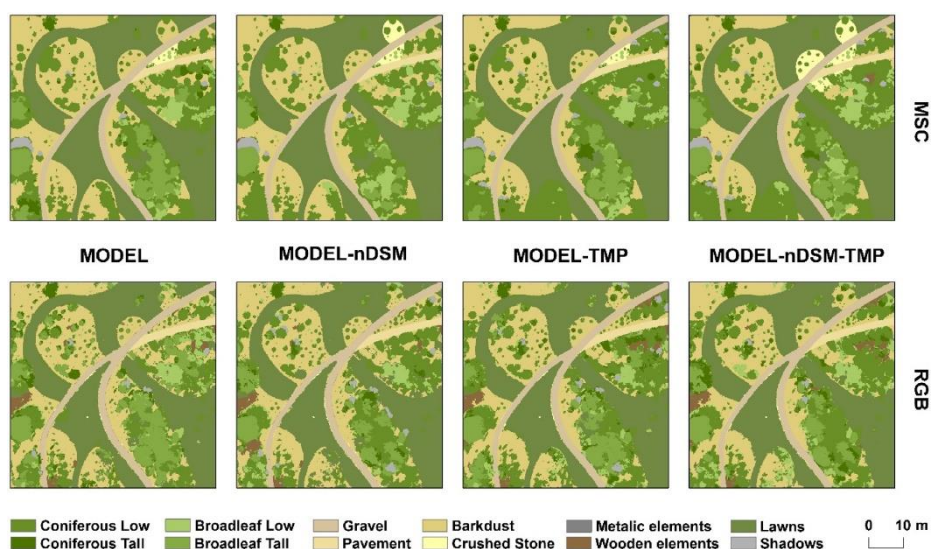


Figure 3. An example of all created classification models. For clarity, data on artificial surfaces are presented at Level 3 while vegetation classes depicted at Level 2.

The Overall Accuracy of models in general increases with the amount of information entering the classification process and with decreasing level of detail. The results imply that models based on multispectral data are of significantly better quality than those based solely on data from the visible sensor. The highest Overall Accuracy on the individual levels (Level 1, 2 or 3) was acquired through models combining all input data both for multispectral data (model MSC-nDSM-TMP 77.33 – 90.50%) and for visible data (model RGB-nDSM-TMP 66.83 – 79.33%). Conversely, one-input models were the least accurate on any given levels (model MSC 64.00 – 85.00% and RGB 59.00 – 71.17%). Addition of a second input did yield a significant improvement of the



relative accuracies besides one-input models (MSC-nDSM 73.00 – 86.50%; MSC-TMP 70.67 – 90.00%; or RGB-nDSM 64.33 – 75.83%; RGB-TMP 63.17 – 77.50%); however no significant differences between the two-input models of both individual sensors were detected with respect to the Overall Accuracy, see Table 6.

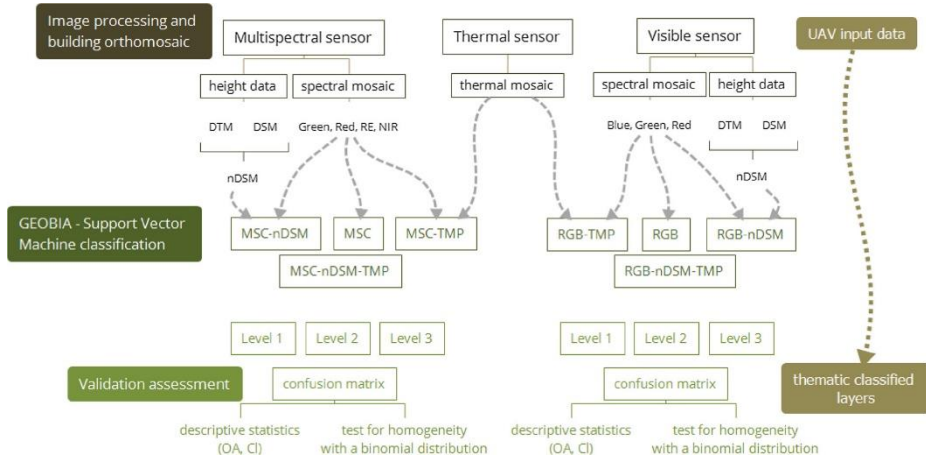


Figure 4. A scheme depicting the principles of the methodology used in the study.

## ASSESSMENT in INDIVIDUAL CLASSES

### Plant species at level 3

The overall classification accuracy of individual plant species at the most detailed level grew in the case of MSC based models with the increasing number of input data (51.47 – 69.33%). For species recognition, the role of height data (63.20%) appears to be greater than that of the thermal data (57.33%). However, both inputs have a significant positive impact on the quality of models (see Table 7). MSC-only model was more accurate for recognition of a single species class (e.g. Fir). On the other hand, a two-input model combining the spectral model with thermal data provided significantly better results in four classes, with nDSM data in five classes and models using all inputs were better in eight out of fifteen classes. Regardless of the number of inputs, the worst distinguishable classes were Fir and Cotoneaster. The use of multiple inputs did not yield any significant improvement from using a single MSC input for classes Juniper, Yew, Golden Yew, Willow, Cinquefoil and Rose. The accuracy of recognition of remaining classes was however improved by additional inputs. In all MSC-based models, some classes were significantly overestimated (e.g. Low Pines) while other underestimated

(e.g. Cotoneaster), see Figure 6 for illustration. The misclassification occurred most often between these extremes and the under- and overestimation was decreasing with increasing number of inputs, see Appendix A for details.

*Table 6. A comparison of the accuracies of models derived from the multispectral and visible sensors using Support Vector Machine algorithm within object classification; OA = Overall Accuracy (%); 95% CI = 95% Confidence Interval.*

Classification model	Level 1		Level 2		Level 3	
	OA	95% CI	OA	95% CI	OA	95% CI
MSC	85.00	82.14 – 87.86	75.33	71.88 – 78.78	64.00	60.16 – 67.84
MSC-TMP	90.00	87.60 – 92.40	82.17	79.10 – 85.23	70.67	67.02 – 74.31
MSC-nDSM	86.50	83.77 – 89.23	82.00	78.93 – 85.07	73.00	69.45 – 76.55
MSC-nDSM-TMP	90.50	88.15 – 92.85	85.83	83.04 – 88.62	77.33	73.98 – 80.68
RGB	71.17	67.54 – 74.79	64.33	60.50 – 68.17	59.00	55.06 – 62.94
RGB-TMP	77.50	74.16 – 80.84	69.00	65.30 – 72.70	63.17	59.31 – 67.03
RGB-nDSM	75.83	72.41 – 79.26	72.17	68.58 – 75.75	64.33	60.50 – 68.17
RGB-nDSM-TMP	79.33	76.09 – 82.57	75.17	71.71 – 78.62	66.83	63.07 – 70.60

*Table 7. A comparison of overall percentage accuracies of models derived from the multispectral and visible sensors for individual models. Level 1a represents the accuracy of analysis focused on differentiation of Coniferous vs Broadleaf plants; Level 1b on Tall vs Low vegetation; Level 2 differentiation between Tall Coniferous, Low Coniferous, Tall Broadleaf, and Low Broadleaf plants; Level 3 presents accuracy of detail plant species classification. Values of Overall Accuracy are derived from the confusion matrix in Appendix A.*

Classification model	Level 1a	Level 1b	Level 2	Level 3
MSC	81.07	78.67	65.60	51.47
MSC-TMP	86.93	82.13	74.40	57.33
MSC-nDSM	83.47	89.07	76.27	63.20
MSC-nDSM-TMP	87.73	86.93	80.27	69.33
RGB	60.53	65.87	49.60	42.67
RGB-TMP	71.47	71.73	57.87	50.13
RGB-nDSM	65.07	78.67	59.20	48.27
RGB-nDSM-TMP	74.13	86.13	67.47	55.73

RGB-based models reveal a similar pattern as the MSC-based ones. The contribution of additional inputs, however, unlike for MSC-based models, differed for individual classes and, in most cases, was lower than for corresponding MSC-

derived models. The overall classification accuracy of plant species acquired through RGB-based models was in all instances lower than that of MSC-based models. The least accurate model was RGB only (42.67%) while the most accurate model is RGB-nDSM-TMP (55.73%). Slightly higher Overall Accuracy was achieved using thermal (50.13%) than height data (48.27%), see Table 7. The over- and underestimation of classified individual classes is smaller than in the case of MSC models, see Figures 6 and 7 for comparison. Conversely, when compared to the one-input RGB model, including TMP into the model provided a significant improvement of accuracy of five classes, including nDSM of six classes and a model containing all input data led to improvement in eight classes. RGB data appear to be ineffectual (throughout all models) for distinguishing classes low Pine, low Spruce and Cinquefoil. Using additional inputs has no effect on the accuracy of classes Golden Juniper and Golden Yew. Conversely, enhancing the models by at least one input leads to a significant improvement of the accuracy of remaining classes, see Appendix A.

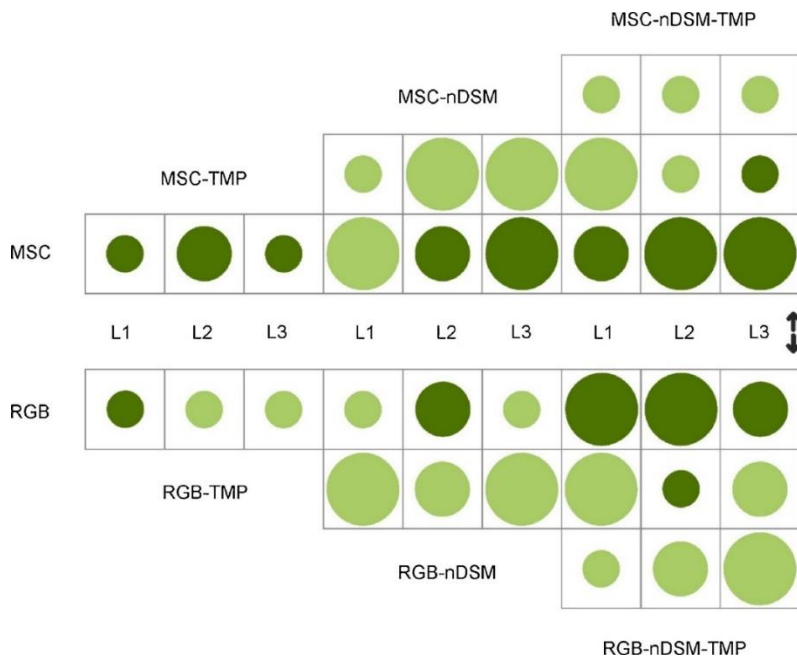


Figure 5. Test for homogeneity with a binomial distribution of models generated from visible and multispectral sensors. The figure illustrates (dis)similarity of individual models at all levels. Dark represents the statistically significant difference between models (95% level of significance); light represents models that cannot be distinguished at the particular level. The size of the circle illustrates the strength of the relationship (high, moderate, or low).

## Plant species at level 2

At Level 2, MSC-based models show a better Overall Accuracy than RGB-derived models in distinguishing Tall Coniferous, Low Coniferous, Tall Broadleaf, and Low Broadleaf plants (65.60 – 80.27% for MSC and 49.60 – 67.47% for RGB) and the accuracy for both grew with the number of inputs, see Table 7. The only class classified more accurately through RGB-based models is Tall Coniferous plants. Conversely, the best accuracy was achieved in both instances for Low Coniferous plants, see results of Level 2 in Appendix A.

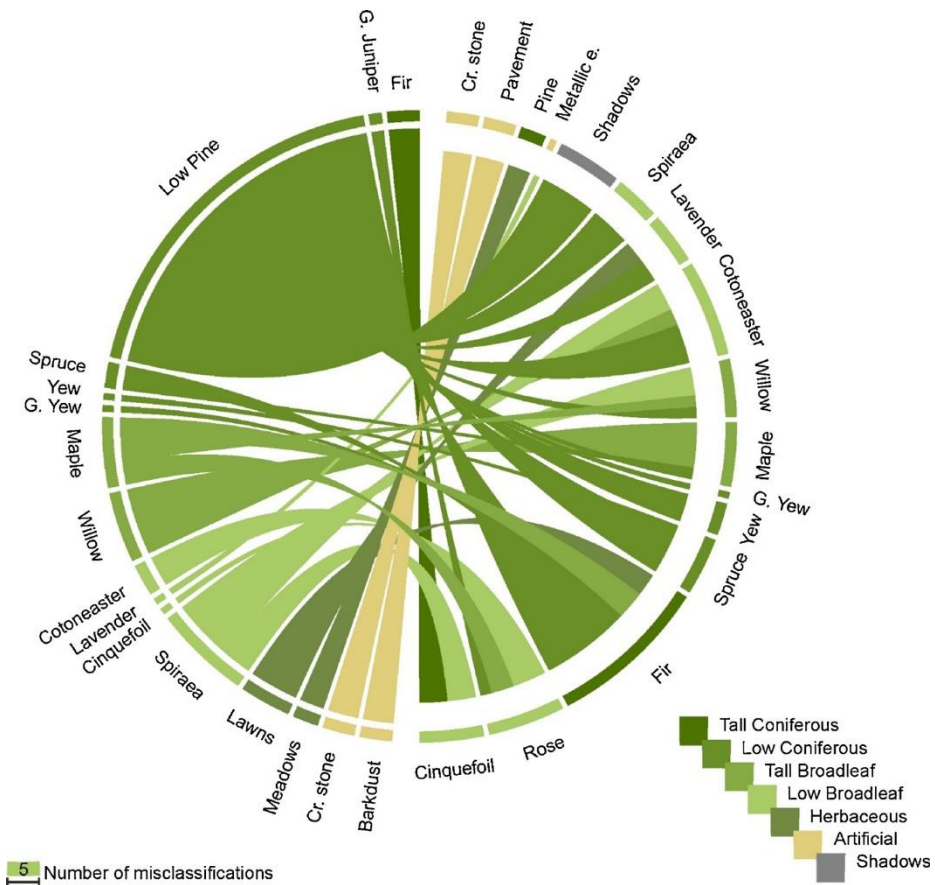


Figure 6. Visualization of the confusion matrix. The circular plot of the MSC-nDSM-TMP model at Level 3 represents the misclassifications (lines connect misclassified classes, hence the larger section, the more incorrectly classified polygons in the class).

### Plant species at level 1

Distinguishing Broadleaf and Coniferous plants were also better when using MSC-based models (Overall Accuracy of 81.07 – 87.73% for MSC vs 60.53 – 74.14% for RGB; depends on model, Table 7). The difference from the previous levels lies in a significantly higher accuracy of thermal-based two-input models than the height. For both sensors, the classification of Coniferous plants was more accurate than that of the Broadleaf plants (with the exception of the RGB-only model). When enhancing the models with additional inputs, however, the accuracy of the classification of Broadleaf plants grew, significantly more so for MSC-based models (65.14 – 81.14%) than for RGB-derived models (61.71 – 65.14%), see Level 1 accuracies in Appendix A. Conversely, when detecting differences in the vegetation height, both RGB and MSC models achieved very high accuracy (78.67 – 89.07% for MSC vs 65.87 – 86.13% for RGB), see Table 7. MSC-based models were more accurate where low vegetation was concerned, while RGB-based models provided very similar results for both Low and Tall vegetation.

The accuracy of the MSC and RGB models inside individual classes was increasing with decreasing level of detail, i.e. the incorrect classification occurred more frequently at more detailed levels. Results from all levels and both data types indicate that during classification, the misclassification of Coniferous and Broadleaf plants for Artificial surfaces or Herbaceous plants is negligible while the misclassification for Shadows occurs substantially more often.

### Non-vegetation and Herbaceous classes at all levels

The accuracy of models derived from both sensors for Artificial surfaces is high. Additional inputs improve the MSC models classification (89.33 – 96.00%) while they do not elicit any significant improvement in RGB model (92.00 – 95.33%) at Level 3. One of the lowest accuracies were recorded in one-input MSC model in the classification of Gravel, Crushed stone and Metallic elements, which were misclassified for Barkdust. Increasing land cover generalization corresponds with classification accuracy for all sensors and models. At Levels 1 and 2; the accuracy for both MSC and RGB-based models is very high and comparable, see Appendix A.

A similar pattern can be observed in the Herbaceous class where both MSC-and RGB-based models reveal almost similar, highly accurate, results. The Overall Accuracy for Herbaceous is 94.00 – 100% for MSC and 92.00 – 98.00% for RGB. Classification of Lawns was performed with lower accuracy than that of Meadows. For example, one-input RGB model lies in negligible misclassification (overestimation) of meadows for classes of low broadleaf plants. The accuracy

of Lawns classification is increasing in both sensors with the addition of thermal data while the addition of height information surprisingly does not improve accuracy. Conversely, meadows achieve the same accuracy independently of sensors/models, see Appendix A.

The least accurate results were recorded for the class of Shadows, which was frequently mistaken for Coniferous plants classes (Figures 6 and 7) and where the Overall Accuracy for either of the sensors did not exceed 60%. Even here, however, the observation that additional inputs increase the performance was confirmed.

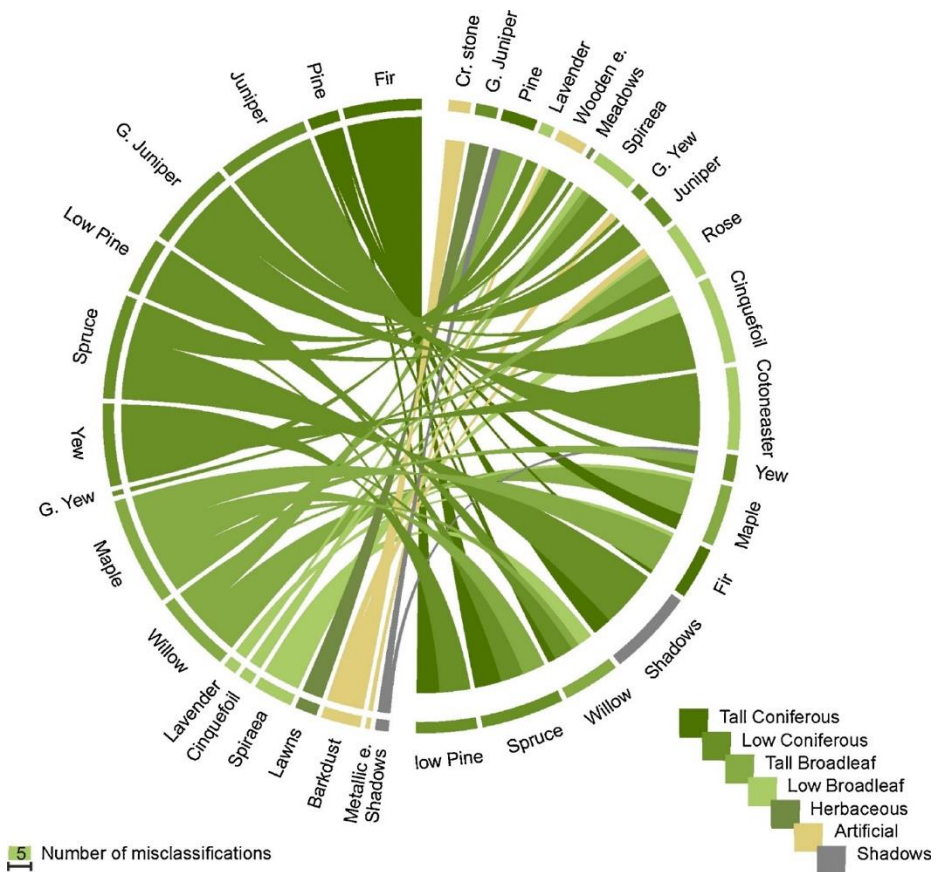


Figure 7. Visualization of the confusion matrix. The circular plot of the RGB-nDSM-TMP model at Level 3 represents the misclassifications (lines connect misclassified classes, hence the larger section, the more incorrectly classified polygons in the class).

## OVERALL ACCURACY ASSESSMENT

The study results are in the general sense similar for both multispectral and visible sensors. It is obvious that multiple-input based information increases the accuracy of the classification and, therefore, models based on more information provide better results. Besides, models based on multispectral sensor perform better than RGB-derived models. To achieve a detailed classification of the vegetation types, it is therefore not feasible to substitute higher spectral resolution (multispectral sensors) with higher spatial resolution (visible sensor, see RQ ii). In both sensors, it is necessary to use both height and thermal data to achieve the best results at a detailed scale. This requirement, however, increases both the economic and temporal demands on the analysis as well as demands on the personnel performing the analysis and computational capacity. Based on the resulting accuracies, we therefore recommend using a combination of data acquired through a multispectral sensor with nDSM. However, for some classes (e.g. Lawns) or lower detail levels, thermal data are a more significant predictor than nDSM and enhancing the models with thermal data is, therefore, a welcome contribution. Our results also indicate that the land cover and vegetation types can be classified with a sufficient accuracy (almost 81%) using UAV at the level of individual plant species (RQ i) even in an environmentally very specific area. When analyzing the usability of individual models, it is necessary to take into account, besides Overall Accuracy, their potential for individual classes of the vegetation types as well. For some classes, the accuracy may be inconsistent with the Overall Accuracy due to a lower or, contrary, higher accuracy of other classes.

## CLASS-SPECIFIC ASSESSMENT

Based on the results of the individual plant species (Level 3), multispectral data are necessary for achieving a sufficient accuracy. The RGB spectral resolution is insufficient for distinguishing between these classes as their reflectance values in this bandwidth are very similar and even the addition of height or thermal data cannot make up for this lack of spectral information. The accuracy of most classes is in accordance with the trend of the Overall Accuracy and the assumption that including more inputs into the analysis improves the plant species classification accuracy was confirmed for both thermal and nDSM data.

The Fir class was frequently misclassified for low Pine and Spruce in MSC-based models. A possible explanation for this fact lies in the absence of the blue band in the multispectral data, which may be significant for distinguishing a large number of garden varieties of coniferous plants. The situation was altogether

different for Pines that were classified with a sufficient accuracy; pines are present in the non-intervention zone of the arboretum and only one cultivar was present. This simple comparison can lead us to an assumption that in natural or near-natural areas, the classification can be more accurate than in an artificial landscape such as arboretum. The assumption of the blue band significance is further backed by results at Level 1 where RGB models detected Coniferous plants with a greater accuracy than MSC models. To achieve the best Overall Accuracy of classification of both Coniferous and Broadleaf plants (Level 1–3), however, it is necessary to use MSC based models. For classification of Herbaceous and Artificial surfaces, RGB and MSC data are interchangeable and thermal data do not play any significant role as the addition of nDSM data into the model is sufficient to improve the model accuracy. Conversely, additional data are needed for the class of Shadows as neither MSC, not RGB sensors provide good enough results and their supplementing by nDSM (for RGB sensor) and/or TMP (MSC sensor) improves the results. The need for different additional data is caused by the different spectral characteristics acquired by the different sensors.

## UNCERTAINTIES ASSESSMENT

The accuracy of the performed classifications may be affected, besides the input data, by (a) the selection of the classification system (pixel-based or object-based) and, subsequently, classifier. It is customary in the remote sensing community to use object classification for high resolution data as that type of classification brings multiple benefits. In this case, an SVM non-parametric classifier was selected due to its robustness as it was shown that SVM can be used without compromising accuracy even if the reference polygons are not ideally distributed (Lu and Weng, 2007); (b) the used classification and processing software. The most commonly used classification software in the literature for GEOBIA is the eCognition Developer (Trimble, US) (Husson et al., 2017; Müllerová et al., 2017; Weil et al., 2017) or ENVI software (Ahmed et al., 2017). No study focused on the global comparison of these programs is however available and, therefore, it is hard to make a clear decision on the suitability of one or the other for a particular application. Where photogrammetry is concerned, either Pix4Dmapper or Agisoft PhotoScan (Agisoft LLC, Russia) are the most commonly used. The limitation of Pix4Dmapper is its inability to build a DTM with better spatial resolution than 5 x GSD; (c) the time of UAV image acquisition. Choosing the right season for image acquisition greatly affects the resulting accuracy (Müllerová et al., 2017; Weil et al., 2017). Husson et al. (2017) and Zhen et al. (2013) acquired images in August, Ahmed et al. (2017) in July. Late spring to early summer appeared to



be the most suitable month for image acquisition under the conditions of Czech Republic (tempered zone, Northern hemisphere). Images used in our study were acquired in accordance with the literature in full vegetation (Sankey et al., 2017a; Weil et al., 2017); (d) used accuracy assessment, based on randomly selected spatially independent validation data (different from the training data) (Zhen et al., 2013). The stratified random sampling design was used for the reference polygons to make sure land cover classes with low spatial extent were not omitted. The accuracy assessment was performed in accordance with the good practice as summarized e.g. by Olofsson et al. (2014). Accuracy assessment using reference polygons may lead to its overestimation by up to 10%, as reported by Zhen et al. (2013), we minimized that effect by maintaining the percentage representation of individual classes of land cover in the reference polygons (training and validation data) proportional to reality. As accuracy assessment by Confusion Matrix is highly dependent on the area of interest (Olofsson et al., 2014), we have added 95% Confidence Intervals allowing a more general application of results. Another approach used in some studies lies in multiple selections of validation and training data (Weil et al., 2017).

## COMPARISON WITH OTHER UAV STUDIES

Our results are in accordance with findings from previous studies, however, to our best knowledge no study published so far took thermal data in detail scale into consideration, much the less combining it with visible, multispectral or height data. Ahmed et al. (2017) achieved 79% accuracy of hierarchical classification of the land cover on a detailed scale (10 categories) when using the visible camera and 82% when using multispectral imagery; height data (DSM, it was not stated if the model was normalized) was used. When taking into account Level 2 in our study with a similar number of categories (8), 72% accuracy was achieved for RGB and 82% for MSC when including height data (nDSM); further enhancement of the model with thermal data led to an increase of accuracy to 75% and 86%, respectively. Weil et al. (2017) reported an average accuracy of their classification of nine categories to be 85% (predominantly forest and herbaceous vegetation in the East Mediterranean). A combination of SVM and object classification was used by Müllerová et al. (2017) who achieved 65 – 86% accuracy of their binary detection of invasive plant species in the Czech Republic by the visible camera. One of the few studies systematically utilizing nDSM for UAV-based vegetation classification is the study by Husson et al. (2017) using object based classification and Random Forest classifier. The accuracy of recognition of individual water plant species in their study ranged from 52 to 75%. In our study, the accuracy on

a similar detail based on visible data was 60 – 68%, increasing to 63 – 71% when including thermal data into the model and even to 74 – 81% where visible data were replaced with multispectral. Their results are in agreement with ours also in the conclusion that the accuracy decreases with the increasing complexity of the vegetation/land cover. The contribution of the height data for classification of (semi)arid species was also confirmed by [Sankey et al. \(2017a\)](#) who combined data from UAV-mounted hyper-spectral sensor and LiDAR for six categories (one of which were shadows as well) to achieve an 84 – 89% Overall Accuracy and 72 – 76% accuracy where only hyper-spectral data were involved. Similarly to our study, Shadows belonged to the most problematic categories in their study, particularly so when using hyperspectral data only.

The study results do not confirm the usability of visible sensor for a detailed classification of land cover at the level of species, which is in accordance with the findings of the above mentioned studies related to aquatic plants ([Husson et al., 2017](#)), park greenery ([Gini et al., 2014](#)) or detection of invasive plant species ([Müllerová et al., 2017](#)). It is obvious that not even higher spatial resolution can for this purpose act as a surrogate for the missing spectral channels, not even in models utilizing nDSM data where the more detailed height information could have increased the RGB model performance. The visible sensor can be however successfully used for detailed classification of Artificial surfaces and for basic classification of Herbaceous plants. Thanks to the presence of the blue channel, RGB can be used for satisfactory species classification of Coniferous plants. However, the multispectral sensor provides general better results despite the missing blue band.

We could possibly increase the accuracy by substituting the multispectral sensor with hyperspectral ([Sankey et al., 2017a](#)). The question of the degree of improvement when using such an expensive high-grade technology, however, remains unanswered. We can also assume that using multispectral cameras with a higher spectral resolution, such as Micasense Rededge ([Weil et al., 2017](#)), Parrot Sequoia ([Ahmed et al., 2017](#)) or Tetracam Multi-Camera Array ([Laliberte et al., 2011](#)) could further improve the accuracy of the classification and increase the difference between the performance of the multispectral and visible sensors, a comparison is however also missing at present. On the other hand, the accuracy of SfM-derived point clouds is comparable to that of LiDAR-derived point clouds ([Koska et al., 2017](#)) and, therefore, if the vertical structure of the vegetation at each point is not of concern and only the information about the vegetation surface is sufficient, investment into this expensive sensor is not necessary for classification of vegetation.

## GENERAL ASSESSMENT

For a general purpose in any classification analysis based on UAV-borne data, we recommend the combination of a multispectral sensor and nDSM as the most efficient method requiring only a single flight (as the height information can be easily extracted during UAV imagery processing). A statistical evaluation has not revealed if nDSM or TMP data are more valuable for the classification (RQ iii); however, adding any one of these two into the MSC-based model significantly improved the accuracy (RQ iv). When searching for the best compromise between the number of sensors used (costs) and a sufficient classification accuracy, the answer can differ with the level of detail. As it is not possible to generalize the results, a test for homogeneity with binomial distribution was performed for every pair of models. Results indicate that models based on multiple inputs can be utilized for classification of individual plant species; however, distinguishing among individual multi-input models is more difficult (Figure 5). Our study area contains multiple cultivars with not entirely natural height, which potentially affect the result of classification. It can be therefore assumed that in a more natural environment with a smaller number of species, it is possible to achieve even better results and accuracies. We also assume that in such environments, even various models based on two inputs could give results that will be distinguishable both mutually and from all-input models. However, further studies are needed to verify these hypotheses.

## Conclusion

The study proves the contribution of UAV-borne thermal and height data for classification of land cover and vegetation types. Thermal data and normalized height (nDSM) inputs increase classification accuracy when compared to spectral data only, even in a very specific environment of an arboretum. The best Overall Accuracy was achieved by combining all acquired input datasets on the multispectral sensor. The results confirmed our hypotheses that (RQ i) it is possible to classify individual plant species with a sufficient accuracy using UAV-borne data; (RQ ii) RGB sensor with a better spatial resolution cannot fully substitute additional spectral information acquired using MSC sensors; and that (RQ iv) thermal data are an important source of information distinguishing some classes. On the other hand, the hypothesis (RQ iii) that the height data contribute

to the accuracy more than thermal data was not confirmed. Nevertheless, it is clear that UAV technology is, providing suitable parameters and input data, a powerful tool for a detailed and accurate classification of the land cover and recognition of plant species.

## FUNDING

This study was supported by the Czech University of Life Sciences Prague, project No. CIGA 20184206.

## ACKNOWLEDGEMENTS

We acknowledge the anonymous referees for their constructive comments. Also, many thanks for the helpful comments to our colleagues from the Department of Applied Geoinformatics and Spatial Planning at the Czech University of Life Sciences Prague (CULS). We would also like to thank Michal Fogl and Magda Ejemová for help with ground data collection, Ondřej Lagner for help with the acquisition of UAV imagery and Vojtěch Barták for help with R.

## Chapter VI – STUDY 3

### Title:

UAV for Mapping Shrubland Vegetation: Does Fusion of Spectral and Vertical Information Derived from a Single Sensor Increase the Classification Accuracy?

### Authors:

Jiří Prošek, Petra Šimová

### Author's contribution: 50%

Conceptualization of the study, field work and data acquisition, data processing and validation, co-writing of the original draft, review and editing with respect to technical issues.

### Journal:

*International Journal of Applied Earth Observation and Geoinformation*, IF (2018) 4.846 – 5 of 30 (Q1) rank in WOS category Remote Sensing; AIS (2018) 1.098 – Q1 rank

### Full citation:

Prošek, J., & Šimová, P. (2019). UAV for mapping shrubland vegetation: Does fusion of spectral and vertical information derived from a single sensor increase the classification accuracy? *International Journal of Applied Earth Observation and Geoinformation*, 75, 151-162.

### Cited:

2 times cited on WOS (2019 August).

## ABSTRACT

High quality data on plant species occurrence count among the essential data sources for ecological research and conservation purposes. Ecologically valuable small grain mosaics of heterogeneous shrub and herbaceous formations however pose a challenging environment for creating such species occurrence maps. Remote sensing can be useful for such purposes, it however faces several challenges, especially the need of ultra high spatial resolution (centimeters) data and distinguishing between plant species or genera. Unmanned aerial vehicles (UAVs) are capable of producing data with sufficient resolution; their use for identification of plant species is however still largely unexplored. A fusion of spectral data with LiDAR-derived vertical information can improve the classification accuracy, such a solution is however costly. A cheaper alternative of vertical data acquisition can be represented by the use of the structure-from-motion photogrammetry (SfM) utilizing the images taken for (multi/hyper) spectral analysis. We investigated the use of such a fusion of UAV-borne multispectral and SfM-derived vertical information acquired from a single sensor for classification of shrubland vegetation at species level and compared its accuracy with that derived from multispectral information only. Multispectral images were acquired using Tetracam Micro-MCA6 camera in the west of Czechia in a shrubland landscape protected within the NATURA 2000 network. Using (i) multispectral imagery only and (ii) multispectral-SfM fusion, we classified the vegetation into six classes representing four woody plant species and two meadow types. Our results prove that the multispectral-SfM fusion performs significantly better than multispectral only (88.2% overall accuracy, 85.2% mean producer's accuracy and 85.7% mean user's accuracy for fusion instead of 73.3%, 75.1% and 63.7%, respectively, for multispectral). We concluded that the fusion of multispectral and SfM information acquired from a single UAV sensor is a viable method for shrub species mapping.

## KEYWORDS

Fine spatial resolution, Species classification, Multispectral, Normalized digital surface model (nDSM), Structure from motion (SfM), Unmanned aerial systems, Tetracam Micro-MCA6

# Introduction

High quality data on vegetation, ideally up to the level of individual species, count among the essential data sources for ecological research and conservation purposes (Bazzichetto et al., 2018; Chignell et al., 2018; Husson et al., 2017; Mairota et al., 2015; Rapinel et al., 2015; Sankey et al., 2017a). However, the acquisition of species maps with a sufficient spatial and thematic accuracy may present a major challenge. This is especially true in small grain landscapes such as areas with mosaic pattern of heterogeneous shrub and herbaceous formations (Lu and He, 2017; Sankey et al., 2017b; Wang et al., 2018). Such sites with impenetrable thickets consisting of various shrub species make mapping using ground techniques extremely difficult. An attractive alternative for shrub species mapping lies in the use of remote sensing (RS). The classification of RS data to the level of individual species (or genera) however requires a detailed spatial resolution of the imagery, allowing the researcher to distinguish between individual shrubs and (clusters of) herbs. Such requirements however in turn rule out the use of most satellite imagery and suitable airborne data are rarely available for the studied location. A possible solution for an inexpensive acquisition of such data on a local scale may lie in the use of unmanned aerial vehicles (UAVs) that are capable to provide images with pixel size in the order of centimeters (Colomina and Molina, 2014; Husson et al., 2017; Komárek et al., 2018; Sankey et al., 2017b, 2017a).

Even if such detailed data are acquired, the extremely detailed classification (to the level of species/genera) can lead to a low classification accuracy and reliability. It is of course much easier to achieve a high classification accuracy if only generalized classes (e. g. forests, shrubs, meadows) are to be distinguished (Ahmed et al., 2017; Komárek et al., 2018). With greater thematic detail, however, such a decline in accuracy is not only apparent in the overall accuracy but even more so in the producer's accuracy (hereinafter accuracy, i.e., the likelihood that the species will be classified correctly) and/or user's accuracy (i.e., reliability, the likelihood that the class shown on the map will match the reality) of the identification of individual classes. Thus, despite a high overall classification accuracy, a closer look at the accuracy or reliability of individual species can reveal a very low rate of correct identification or representation of some species on the map (see e.g. Komárek et al., 2018). Such a problem would limit the usability of the resulting species occurrence maps for subsequent research or management purposes. This is especially likely to happen if the classification includes non-vegetation surfaces (e.g. tarmac or gravel roads), which are almost 100% distinguishable from

vegetation and, therefore, artificially improving the overall classification success rate. For example, an 80% overall accuracy may look good at the first glance but a closer look revealing a 55% producer's accuracy for a particular species in the analysis tells us that almost half of the real occurrence of the particular species was omitted. A 55% reliability then indicates that almost half of the pixels identified as a particular species are actually a different species in the real world. Using such a map as a basis for subsequent ecological research may lead to biased results (Chignell et al., 2018; Fisher et al., 2018; Moudrý and Šimová, 2012; Schmidt et al., 2017; Šimová et al., 2019). For example, if the presence of a particular shrub species is important for the occurrence of an endangered bird species due to its feeding habits, the failure to correctly identify that particular shrub species (despite a high overall accuracy) provides incorrect input data for the analysis of the particular bird occurrence. The results of such a study would therefore be invalid; if they are however perceived as reliable due to the high overall accuracy of the map, it could lead in effect to incorrect management decisions. It is therefore not sufficient to rely on the overall accuracy, the producer's accuracy and reliability for individual classes must be studied and reported with every such map and, of course, every effort should be made to maximize those values.

Some studies using satellite and/or airborne data have suggested that a fusion of spectral imagery and vertical information (particularly airborne LiDAR data) may represent a suitable technique for improving the classification accuracy in a detailed thematic resolution (Alonzo et al., 2014; Bork and Su, 2007; Hartfield et al., 2011; Holmgren et al., 2008). Very few studies are however available on such a fusion of UAV-acquired data and its benefits (Husson et al., 2017; Komárek et al., 2018; Sankey et al., 2017b, 2017a). All those studies suggest that although the fusion of spectral (RGB, multispectral or hyperspectral) and vertical (LiDAR or structure from motion photogrammetry, SfM) information leads to an overall improvement of accuracy, this may not be the case for some individual classes. From the dates of publication of all those studies, it is obvious that the fusion of UAV-acquired spectral and vertical data is a very novel approach and further research on the classification accuracy in various landscapes is needed.

All the UAV-based studies on the fusion of spectral and vertical data published so far use either UAV LiDAR sensor or SfM as a source of the vertical data. LiDAR is generally considered to provide more accurate vertical information (Dandois and Ellis, 2013; Fonstad et al., 2013; Mancini et al., 2013; Sankey et al., 2017a; Wallace et al., 2016). The price of the LiDAR UAV solution (sensor itself plus a suitable carrier) however remains high. SfM, on the other hand, requires no extra sensor; the vertical data can be extracted from RGB or multispectral images (only



a single flight mission is therefore needed for acquisition of both spectral and vertical data). As indicated in several studies, the use of UAV SfM can produce ultra-fine canopy height models (CHMs) comparable with LiDAR-derived CHMs and have a great potential for use in ecology (Anderson and Gaston, 2013; Cunliffe et al., 2016; Kalacska et al., 2017). The trade-off between the total data acquisition costs (costs of the carrier and sensor, of imaging and data processing) and the accuracy of the vertical information intended for fusion with the spectral data must therefore be considered when choosing the suitable method of UAV data acquisition.

In this study, we classified shrubland vegetation into six classes, namely four shrubs species/genera and two meadow types, based on data acquired using a multispectral sensor during a single flight mission. Our principal aim was to find out if the fusion of the multispectral information and vertical data acquired through SfM from the same imagery can significantly improve the classification accuracy of shrubland vegetation when compared to the use of solely multispectral information. We hypothesized that the addition of the vertical information can, besides improving the accuracy of distinguishing the shrubs from herbs, improve the producer's and user's accuracy of differentiation between individual shrubs species and meadow types.

## Methods

### STUDY AREA

The study was carried out in the west of Czechia (Central Europe), in Doupovské hory (50°18' N, 13°8' E; Figure 1). The predominant vegetation type is shrubland consisting of a mosaic of herbaceous and shrub vegetation. Two sites (8.7 ha and 6.4 ha, 0.7 km apart) were studied. One site is flat; the other covers a mild south-oriented slope. The predominant shrub species on these sites are blackthorn (*Prunus spinosa*), hawthorn (*Crataegus* sp.), elder (*Sambucus nigra*) and willow (*Salix* sp.). The entire area of Doupovské hory is protected under the Directive 2009/147/EC of the European Parliament and of the Council on the Conservation of Wild Birds (The Birds Directive).

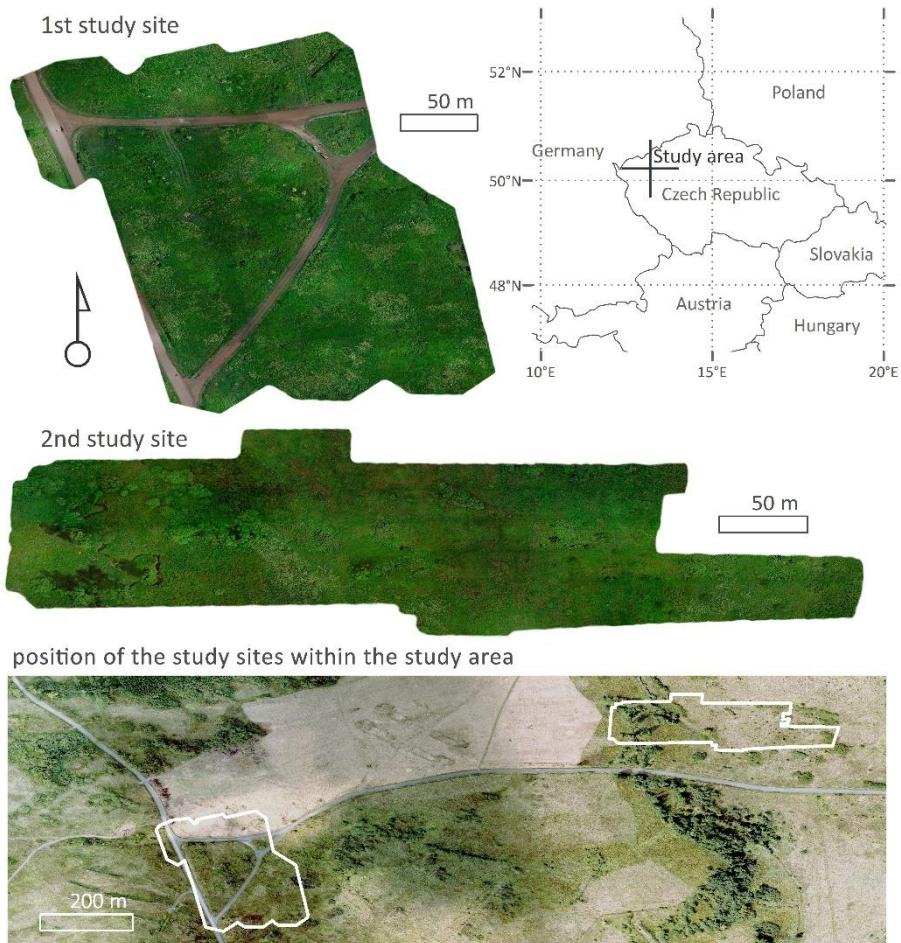


*Figure 1. Study area and study sites.*

## EQUIPMENT and DATA COLLECTION

### UAV, sensor and flight parameters

A multispectral Tetracam Micro-MCA6 camera (1.3 Mpix resolution; 6 spectral bands - B, G, R, RE, 2x NIR, focal length 9.6 mm, equivalent focal length 50 mm) was used for the acquisition of the multispectral data (for detailed information on bands, see Table 1). The camera is equipped with a dedicated lens and sensor (resolution of 1280x1024 pixels) for each spectral band. The images are recorded in a native 10-bit .RAW or 8-bit .RAW.

The multispectral camera was mounted on a UAV using a three-axis gimbal stabilizer for maintaining the nadir position of the camera. The operational time of the used UAV – namely a hexacopter Robodrone Kingfisher (total weight of 7.5 kg including a battery and used sensor; see Figure 2) is approximately 20 minutes. The flights were performed with a direct pilot supervision using an autopilot controlled by the Mission Planner software (V1.3) combined with a Pixhawk control unit. The exact position of the UAV was recorded using GNSS sensor, atmospheric barometer and compass. The UAV flight altitude was 50 m above ground. The flight parameters were designed to ensure a lateral overlap of at least 60%. The flight speed of 2 m/s and the automatic sequence recording of one photo per 2 s ensured the longitudinal overlap of the photos >80%. These parameters resulted in a spatial resolution of <2.5 cm/pix.

*Table 1. Spectral bands of the used multispectral sensor and exposure time proportions.*

Channel/band	$\lambda$ (nm)	Bandwidth (nm)	Proportion of exposure time (%)
1	800	10	30
2	490	10	30
3	550	10	70
4	680	10	30
5	720	10	100
6	900	20	140



*Figure 2. UAV Robodrone Kingfisher with a mounted multispectral camera Tetracam Micro-MCA6.*

Study sites of 8.7 and 6.4 ha, respectively, were scanned on 20. 6. 2016, which represents, in the longitude of Czechia, the foliated period with marked spectral differences among certain species in the late spring phenophase. The flights took place within two hours of the solar midday on a day with minimum cloud cover to minimize the effect of shadows and ensure constant lighting conditions.

### Ground truth data mapping

For the purposes of classification and subsequent accuracy evaluation, ground truth data were collected through a field survey. Two meadow types were distinguished – one with the predominance of grass communities (hereinafter Meadows) and the other with a significant representation of species from Apiaceae family (hereinafter ApiMeadows). In addition, four species (genera) of shrubs were distinguished: elder (*Sambucus nigra*), hawthorn (*Crataegus* sp.), blackthorn (*Prunus spinosa*) and willow (*Salix* sp.), see Figure 3. Originally, polygons of other classes were collected with the intention to include them in the study, such as poplar (*Populus* sp.), common alder (*Alnus glutinosa*), common ash (*Fraxinus excelsior*), meadows with significant representation of other types of high herbaceous plants such as stinging nettle (*Urtica dioica*), low grass vegetation, or bare soil. However, their number, area or spatial distribution were insufficient for the classification and validation and these classes were therefore not included in the results. The distribution, areas and numbers of polygons are summarized in Table 2.

The vegetation was mapped using smart devices (tablets and phones) equipped with the Collector for ArcGIS app combined with a Garmin GLO GPS receiver (GPS external module for smart devices providing improved accuracy of 2 to 5 m). The Collector app allows mobile field data collection combining a custom basemap layer (we used an orthophoto with 5 cm/pix resolution) with the GPS position of the field worker. The operators identified the individual classes in the field, immediately entering the data directly into the Collector and drawing polygons of individual classes. Where the borders between classes were not sufficiently clear from the orthophoto (e.g. borders between different meadow classes or lower shrubs) and the operator therefore needed a more accurate localization for drawing the class-specific polygons, RTK GNSS receivers Leica 1200 with a sub-decimeter accuracy was used instead of Garmin GLO. Altogether, 185 polygons divided into 6 classes were recorded through Collector for ArcGIS, covering a majority of shrubs and trees in the areas of interest. Additional 93 polygons were created using RTK GNSS receivers, predominantly meadows and lower shrubs. This combination of data collection methods allowed us to acquire 278 single class polygons as ground truth data. See Figure 4 for an example of the distribution of the ground truth data.

Table 2. *Vegetation classes and mapped ground truth data - number of polygons and their areas.*

Class	Number of polygons	$\Sigma$ Area (m <sup>2</sup> )
Meadows	59	228
ApiMeadows	56	456
Elder	29	25
Hawthorn	31	69
Blackthorn	20	184
Willow	43	140
$\Sigma$ of others (not used)	60	469
$\Sigma$ Meadows	115	684
$\Sigma$ Shrubs	123	418
Total	278	1471

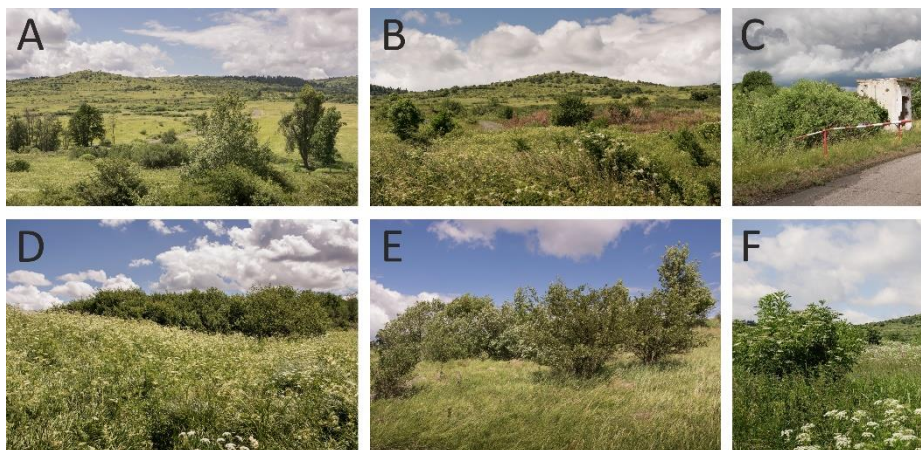


Figure 3. *Study area. A broader view of the study areas (A, B), Willow shrubs (C), ApiMeadows with Blackthorn (D), Meadows with Hawthorn (E). Elder (background), Meadow (central part) and ApiMeadow (foreground).*

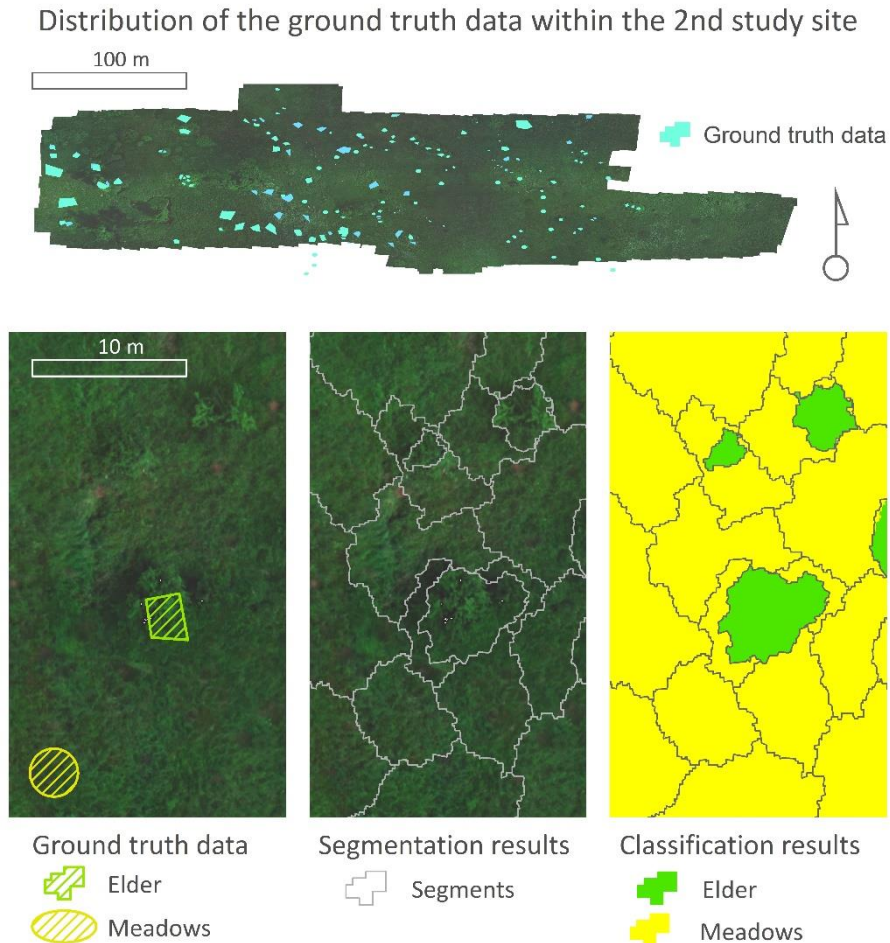


Figure 4. Distribution of the ground truth data (top) and stages of the data processing: ground truth data recorded on the orthophoto (left), results of the segmentation (middle) and of the classification (right).

## PHOTOGRAMMETRY (SfM) DATA PROCESSING

During pre-processing, raw images were converted into multi-band TIFF images with resolution of 7.8 MPix (6x1.3 Mpix) in PixelWrench2 software. 3D point clouds and multispectral mosaics were created in Agisoft PhotoScan V1.3, a software utilizing an SfM algorithm (photogrammetric range imaging technique). Depending on user settings, following steps are performed during batch processing: Alignment of photos (detection of identical points), building a dense point cloud (creating a densified point cloud and an automatic noise points

filtering using a “Depth filtering” function), building digital elevation model (DEM) or Mesh texture, and building orthomosaic. The processing parameters used in our study for both areas of interest are summarized in Table 3. The resulting mosaic and 3D point cloud were georeferenced using 12 ground control points (GCPs). The acquired average positioning accuracy was < 0.3 m and maximum error < 0.6 m. As the data were subsequently utilized for a uni-temporal analysis and the flights were performed under identical weather condition, no radiometric calibration of the scene was necessary. We used a mosaic algorithm for correction of colour and brightness of the entire scene (see more in Agisoft User Guide, 2017).

*Table 3. Photogrammetry procedure – user settings and input data.*

Procedure	Property	Study sites	
Align photos	Accuracy	Highest	
	Generic/reference preselection	Yes	
	Key and Tie point limit	as many as possible/all	
Build Dense cloud	Quality	Ultra High	
	Depth filtering	Aggressive (recommended for aerial data processing)	
Building DEM	Source data	Dense cloud	
	Interpolation	Enabled	
Build Orthomosaic	Surface	DEM/DSM	
	Blending mode	Mosaic	

Accuracy	Property	Study site 1	Study site 2
Images	Number (acquired/used)	225/225	180/169
Spatial resolution of orthomosaic and DEM/DSM	(cm/pix)	2.22	2.33
Tie Points	(points)	5 483 416	1 384 978
Dense point cloud	(points)	84 056 416	54 705 998

## VERTICAL DATA (DSM, DTM, nDSM)

Normalized digital surface model (nDSM) describes relative heights of objects over the bare earth, which in our study means the vegetation canopy height. nDSM was computed by subtracting the digital terrain model (DTM) from the digital surface model (DSM) created from the dense point clouds (see Figure 5 as an example). A crucial step in creating DTM and DSM is the identification of ground points (GP) and non-ground points (NGP) inside the dense point

cloud, which was performed in the Agisoft PhotoScan software. The tool allows to distinguish between categories of GP, NGP, and noise points (outlying points that failed to be removed during depth filtering procedure, see more in Agisoft User Guide, 2017). After several trials, we used the following parameters: Max angle 10°; Max distance 0.2 m; Cell size 5 m. This combination of parameters allowed classification of all taller vegetation as NGPs while the GP category contained enough points for a DTM interpolation. DSM was subsequently created from all categories apart from the noise points while the DTM was computed solely from points identified as GP (see Figure 6 for an example of a resulting profile).

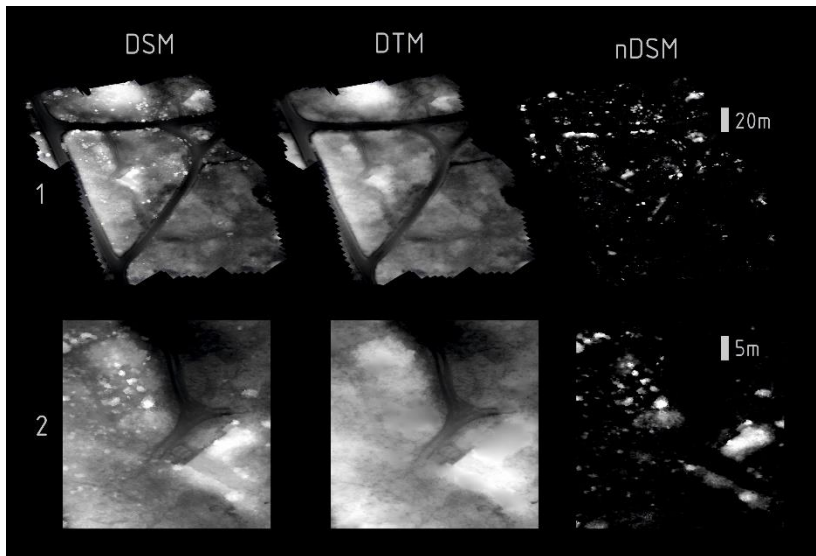


Figure 5. A preview of digital elevation models (DSM, DTM, nDSM) created on the basis of SfM point cloud for the entire area (1) and a detail (2).

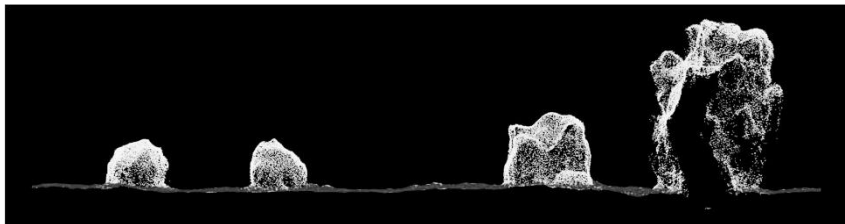


Figure 6. An example of a point cloud profile with classified categories ground points (yellow) and non-ground points (grey).



## SEGMENTATION and SUPERVISED CLASSIFICATION

If processing and analysing very high resolution (VHR) data such as UAV-acquired data, Geographic Object-Based Image Analysis (GEOBIA) method has been shown to provide better results than pixel-based approaches (Alonzo et al., 2014; Blaschke, 2010; Hartfield et al., 2011; Liu et al., 2015). For this reason, we used GEOBIA approach in our study. GEOBIA process, consisting of image segmentation and subsequent classification of the segments, was performed in eCognition software. A multiresolutional segmentation algorithm divided the images into principal segments based on similar spectral, shape and, in our study, height characteristics. The principal user settings are pixel value vs shape. It is also possible to alter the weight of individual channels in the pixel value while the shape of the segments is derived from compactness and smoothness parameters (see eCognition user guide for more information). To acquire optimum results, input parameters were initially tested on several small sample patches – shape parameter in steps by 10 units (from 10 to 200), compactness and smoothness by 0.1 units (in the full range, from 0.1 to 1). After each step, we performed a visual inspection using high resolution orthophotos and nDSM datasets as a reference. Following values resulting from the tests were set based on these preliminary results: Shape 40; pixel value 1:1 for all used bands; compactness 0.4; smoothness 0.6 (see detail in Figure 4 as an example).

A supervised classification method based on the nearest neighbor (NN) algorithm was used for classification of the segments into 6 classes (see Table 1). To evaluate the contribution of SfM based vertical information, we performed independent classifications of a) spectral data only (hereinafter Multispectral approach) and b) a combination of the spectral data with nDSM (hereinafter Fusion approach). In the NN classifications, we used common layer characteristics (mean value, standard deviation and range of pixels in each segment), texture characteristics (contrast, homogeneity and entropy) and shape characteristic (length/width, asymmetry, shape index, compactness, density and roundness). The choice of those characteristics was based on the Space Optimization Tool results (a feature of eCognition software - a tool for automatic identification of significant characteristics for NN classification). For the classification of the fusion data, nDSM was used as an additional band considered in the nearest neighbor algorithm. The entire process is depicted in Figure 7.

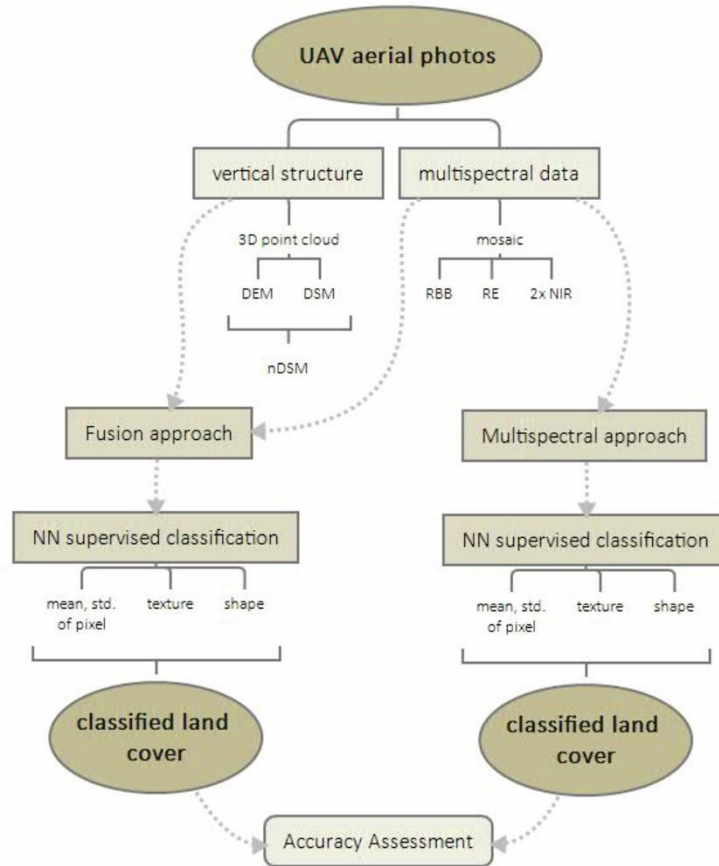


Figure 7. The classification process.

## ACCURACY ASSESSMENT

The nearest neighbor classification is sensitive to the data allocation into calibration and validation datasets and to their spatial distribution (Blaschke et al., 2008). To minimize that effect, we performed a ten-fold random allocation of the acquired ground truth data into the calibration (60%) and validation (40%) datasets and repeated the entire process of calibration and validation ten times. For classification, therefore, 60% of randomly selected ground truth polygons of each of the six distinguished classes were selected. Calculations of producer's accuracy (accuracy, ACC), user/consumer accuracy (reliability, REL) and Cohen's Kappa were based on the overall extent of correctly and incorrectly classified pixels.

This way, we acquired 10 ACC and REL values for each class and for each of the classification approaches (Multispectral and Fusion). The hypothesis that supplementing the spectral data with vertical information improves the classification accuracy (ACC, REL) was tested through one-tailed paired Wilcoxon test (null hypothesis: median ACC (Fusion)  $\leq$  median ACC (Multispectral); REL tested accordingly). The difference in classification was tested in this way for individual classes as well as for the overall accuracy. Based on the results of the Wilcoxon test and interquartile range of ACC and REL values acquired through individual classification approaches, we also assessed if the addition of the vertical information can reduce the classification sensitivity to the changes in the allocation of the calibration and validation data.

## Results

Our results show an improvement of the classification of shrubland vegetation through fusion with SfM-derived vertical data (compared to results of multispectral-only approach). Using the Fusion approach for ten repeated classifications into six classes representing four woody plants species and two meadow types, we achieved an overall accuracy of 88.2%, mean ACC (producer's accuracy) of 85.2%, mean REL (user's accuracy) of 85.7% and Kappa coefficient of 0.84. Classification based solely on multispectral data yielded overall accuracy of 73.3%, ACC of 75.1%, REL of 63.7% and Kappa coefficient of 0.60. The differences between both classification approaches are detailed in Table 4.

Detailed results are also presented in confusion matrices (Table 5). Where vertical information was not utilized (Multispectral approach), Meadows were frequently misclassified for some shrub classes, especially Hawthorn, which led to very low ACC and REL values of both classes (Meadows: ACC 48.7%, REL 61.0%; Hawthorn: ACC 64.1%, REL 49.7%). Adding vertical information improved ACC of meadows with major representation of tall herbaceous plants from the Apiaceae family (ApiMeadows); there was no effect on REL, which was nevertheless high in both classification approaches (the highest of all classes, 94.2% and 95.1%, respectively). In the Elder class, the supplementary vertical information did not increase ACC (even reduced it somewhat, from 86.2% to 84.3%), it however helped to significantly improve REL (86.2% vs 39.3%). For this species, therefore, the high ACC of multispectral classification was only

achieved at the expense of a significant REL reduction, i.e., overestimation of the overall area of the class in question and decreasing the classification reliability (more than 60% of areas denoted as Elder using multispectral data only were in fact ApiMeadows). Principally similar results were obtained for the Blackthorn class. For Willow, Hawthorn and Meadows classes, the use of vertical information yielded significantly better results according to both ACC and REL.

The regression analysis utilizing all ten repeated classifications revealed a strong negative relationship between the improvement in accuracy caused by adding the height data to the model and the accuracy of the original classification using multispectral data only. This correlation is somewhat stronger for REL ( $R=-0.87$ ,  $p<0.001$ ) than for ACC ( $R=-0.84$ ,  $p<0.001$ ). As apparent from Figure 8, both REL and ACC were greatly improved by the fusion where multispectral approach yielded low accuracies. From approx. 80% ACC and 90% REL, respectively, the improvement was however close to zero and equally likely to lead to minor improvement or deterioration.

Results of the statistical analyses furthermore indicate that the allocation and spatial distribution of the validation and calibration data also affect the classification accuracy (both ACC and REL; Table 4 and Figure 9). On the basis of ranges (max-min) comparison, we can say that the effect of allocation of the ground truth data into the classification and validation datasets is in most cases smaller where classification is based on a combination of height and spectral data (Fusion) than when it is built solely on the spectral data (Multispectral).

*Table 4. Results of one-tailed paired Wilcoxon test for each class and overall classification. Asterisks indicate significant improvement of the classification by addition of vertical information (significantly better accuracy of Fusion approach when compared to Multispectral approach). Significance levels: \*\*\* <0.001; \*\*<0.01; - insignificant.*

Class	ACC	REL
Meadows	***	***
ApiMeadows	**	-
Elder	-	***
Hawthorn	***	***
Blackthorn	-	***
Willow	**	***
All classes	***	***

Table 5. Confusion matrices for Fusion and Multispectral approach. Values represent means from 10 repetitions of classifications and validations.

	Meadows	ApiMeadows	Elder	Hawthorn	Blackthorn	Willow	
<b>Fusion</b>							
Meadows	84.0	7.2	0.0	0.0	0.0	0.0	
ApiMeadows	11.4	169.4	1.4	0.0	0.2	0.2	
Elder	0.25	0.6	8.4	0.0	0.0	0.7	
Hawthorn	0.53	0.27	0.0	20.8	2.12	3.9	
Blackthorn	4.3	2.1	0.0	5.1	54.0	8.1	
Willow	1.1	0.3	0.0	1.0	1.7	52.0	<b>Mean</b>
ACC	<b>0.921</b>	<b>0.929</b>	<b>0.843</b>	<b>0.753</b>	<b>0.734</b>	<b>0.929</b>	<b>0.852</b>
REL	<b>0.828</b>	<b>0.942</b>	<b>0.862</b>	<b>0.775</b>	<b>0.930</b>	<b>0.802</b>	<b>0.857</b>
<b>Overall accuracy</b>		<b>0.882</b>		<b>Kappa</b>	<b>0.840</b>		
<b>Multispectral</b>							
Meadows	44.4	6.2	0.0	12.4	9.6	18.6	
ApiMeadows	14.1	144.5	14.1	0.9	3.6	5.3	
Elder	0.2	0.6	9.1	0.0	0.0	0.1	
Hawthorn	2.4	0.1	0.0	17.7	3.6	3.7	
Blackthorn	7.8	0.1	0.0	4.0	58.5	3.3	
Willow	3.8	0.4	0.0	0.7	2.1	49.1	<b>Mean</b>
ACC	<b>0.487</b>	<b>0.792</b>	<b>0.914</b>	<b>0.641</b>	<b>0.795</b>	<b>0.876</b>	<b>0.751</b>
REL	<b>0.610</b>	<b>0.951</b>	<b>0.393</b>	<b>0.497</b>	<b>0.756</b>	<b>0.614</b>	<b>0.637</b>
<b>Overall accuracy</b>		<b>0.733</b>		<b>Kappa</b>	<b>0.596</b>		

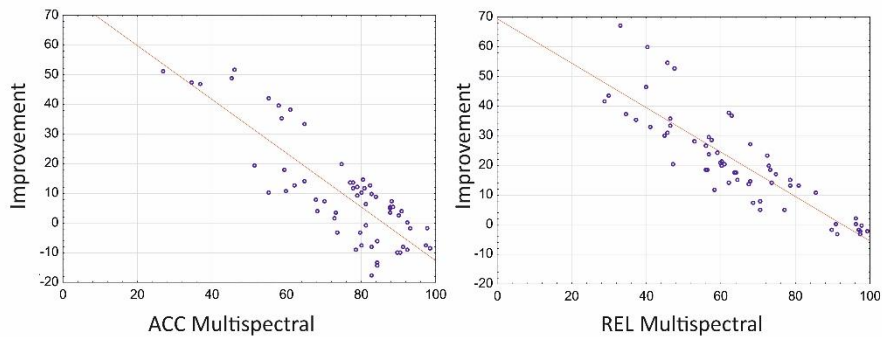


Figure 8. Accuracy improvement due to including height data in the model (Fusion) as a function of the accuracy of the original multispectral classification.



Figure 9. Resulting (A) producer's accuracy ACC and (B) user's accuracy REL for individual classes in ten repeated classifications with a random allocation of ground truth data into calibration and validation datasets. Boxplot: median, quartiles, range.

## Discussion

The novelty of our approach for detail vegetation mapping lies in the fusion of spectral and vertical information acquired during a single flight mission from a single multispectral UAV sensor. In our study, the addition of the vertical information significantly improved both producer's accuracy ACC and user's accuracy (reliability) REL of the entire classification. At least one of the accuracy indicators (either ACC or REL) was increased in each of the six individual classes (four shrub species, two types of meadows). For three classes (Meadows, Hawthorn, Willow), we registered improvement of both ACC and REL.

In the study that is the most similar to our approach, [Sankey et al. \(2017a\)](#) classified five species and bare ground in a forest-grassland ecotone using a UAV-borne hyperspectral sensor and LiDAR. A close comparison of the studies reveals that both producer and user accuracies were (as expected) greater when using the hyperspectral than multispectral sensor (average ACC hyperspectral 86% vs our multispectral 73%; average REL hyperspectral 91% vs multispectral 64%). After supplementing the spectral information with the vertical, however, the differences in results are much smaller (average ACC hyperspectral+LiDAR 89% vs multispectral+SfM 85%; average REL hyperspectral+LiDAR 90% vs multispectral+SfM 86%). It is true that we cannot exclude the possibility that combining our multispectral data with LiDAR would lead to a further classification improvement. This, however, should be an object of further studies, along with a practical question if such a possible improvement of vegetation classification is of a degree justifying the substantial difference in costs of obtaining SfM and LiDAR information, especially in the field of ecological research.

The SfM-based vertical models are generally considered to be less accurate than those based on LiDAR data ([Dandois and Ellis, 2013](#); [Fonstad et al., 2013](#); [Niethammer et al., 2012](#); [Sankey et al., 2017a](#)). As indicated by our results, however, their use for fusion with multispectral data and thus for the improvement of classification of multispectral-based models can represent a cost-effective and viable alternative to the use of LiDAR-based models.

Another study similar to ours in concept, though not in the vegetation type, was that of ([Husson et al., 2017](#)) who combined multispectral data with a vertical information acquired through structure from motion (SfM) photogrammetry for classification of non-submerged aquatic vegetation. The addition of vertical information also improved the classification accuracy by up to 30%, particularly

so for more detailed thematic resolution (7 classes according to the dominant taxa) and for sites with the most complex vegetation.

We have also revealed a strong negative relationship between the improvement of ACC and REL resulting from the addition of the vertical information and the accuracies of the original (multispectral only) classification. In our study, the addition of the vertical information did not improve the (relatively high) reliability of the multispectral classification for ApiMeadows, i.e. meadows with high representation of tall vegetation from Apiaceae family (92.9%), and producer's accuracy of the multispectral classification of Elder (91.4%). In these classes, however, the addition of the vertical information significantly improved the producer's accuracy for ApiMeadows (79.2 to 92.9) and especially the originally very low reliability of Elder (39.3% improved to 86.2 %). The low reliability for Elder in the multispectral approach was caused by numerous misclassifications for ApiMeadows, probably due to a similar spectral response of white umbellate inflorescences of Apiaceae plants and elders *Sambucus nigra*. Another exception from the general trend was the producer's accuracy for Blackthorn, which decreased with the addition of the vertical information from 79.5% to 73.4%. A possible explanation may lie in the notable height variability of the species throughout the sites (20 cm to 3 m).

The relationship between the contribution of vertical information to the accuracy and the original, spectral-only, accuracy deserves in our opinion further research, the results of which could for example help in decisions whether or not to perform a fusion of spectral and vertical data and if so, which sensors should be utilized. Our results indicate that where the spectral-only approach yields high ACC and REL (in our study at least approx. 80% ACC and 90% REL, respectively), any addition of the vertical information is unlikely to further improve the results and, quite on the contrary, can lead to worsening the results.

For some species, the improvement of the classification accuracy through vertical information can be substantial, the result can however still be insufficient for use in ecological modelling. For example, the user's accuracy of Hawthorn improved from 49.7% to 77.5%. Such a result is not explicitly bad; from the perspective of further application, however, we must keep in mind that almost a quarter of pixels classified as Hawthorn were still classified incorrectly (in our study, predominantly as Blackthorn).

The choice of the date of mapping is another very important factor that has to be considered while planning the study (Laba et al., 2005; Müllerová et al., 2017). The mapping date for this study (June 20th, within 2 hours of the solar midday) can be



in our opinion considered as suitable in the latitude and altitude of our study, which is supported by the achieved accuracy results for most classified species. An advantage of the UAV over airborne and satellite missions is, among other things, a flexibility in repetition of the flight missions and, therefore, the possibility of flexible temporal resolution (e.g. [Anderson and Gaston, 2013](#)). Multitemporal image acquisition of the study area in different phenological stages could improve the classification accuracy of species for which the mapping in a single phenological stage has not yielded results of a sufficient accuracy (in our study, Hawthorn). On the other hand, a disadvantage of UAVs when compared to satellite and airborne datasets may lie in a more time-consuming image acquisition. While airborne or satellite sensors can record large areas in a matter of minutes, UAV image recording takes much longer and a single flight mission can only encompass a few hectares. Thus, mapping of a large area using UAVs could be affected by changes of weather conditions, daytime effects (sun position and shadows) and, in extreme cases (e.g. when adverse weather conditions persist), even by a change of the phenological stages. For these reasons, we selected two distinct study sites, a few hectares in size each, to be able to perform image acquisition over the course of a single day under ideal weather conditions. Such an approach is common in other recent studies utilizing new rotary wing UAVs for acquisition of ultra-high resolution images, e.g. for vegetation type classification ([Husson et al., 2017](#); [Komárek et al., 2018](#); [Sankey et al., 2017a, 2017b](#)), for study of vegetation structure of rocky habitats ([Díaz-Varela et al., 2018](#)), for description of dryland vegetation structure ([Cunliffe et al., 2016](#)) or for detection of individual trees ([Nevalainen et al., 2017](#)).

Our study also confirms the assumption that the allocation of calibration and validation data affects the quality and accuracy of the classification. For example, [Olofsson et al. \(2014\)](#) reported the differences in accuracy assessment of up to  $\pm 10\%$ . We have eliminated the problem to a major degree by performing a 10-fold random allocation of the ground truth polygons into calibration and validation datasets and a 10-fold repeated classification and validation. The results (Figure 9) indicate significant differences in the obtained accuracies, in some species up to  $\pm 20$  per cent from the medians. The results also indicate that supplementing the multispectral data with vertical information has a positive effect on reducing this sensitivity for most classes.

Other factors possibly limiting the accuracy of vegetation classification include the segmentation and classification algorithms and the validation method ([Blaschke et al., 2014](#); [Liu et al., 2015](#); [Olofsson et al., 2014](#)). To minimize those effects, we performed a pre-assessment, testing both pixel based classification and GEOBIA

approaches. Pixel based classification led to significantly worse results and, in accordance with those pre-assessment results and with recent publications (Alonzo et al., 2014; Diaz-Varela et al., 2014; Hartfield et al., 2011; Peña et al., 2013; Rampi et al., 2014) we used GEOBIA that is considered to be more suitable for classification of VHR images. Because we had to deal with non-normal distribution of the input data, we chose a non-parametric (nearest neighbor) classification algorithm, in line with Lu and Weng (2007). The non-normal distribution of the data is most obvious for the nDSM data across all classes, it was however also present in several multispectral bands (see Figure 10). Although we used a robust, non-parametric algorithm, the results show that the classification results strongly depend on the selection of ground truth data (see the ranges of accuracy and reliability in Figure 9), which further underlines the importance of our approach using 10-fold repetition.

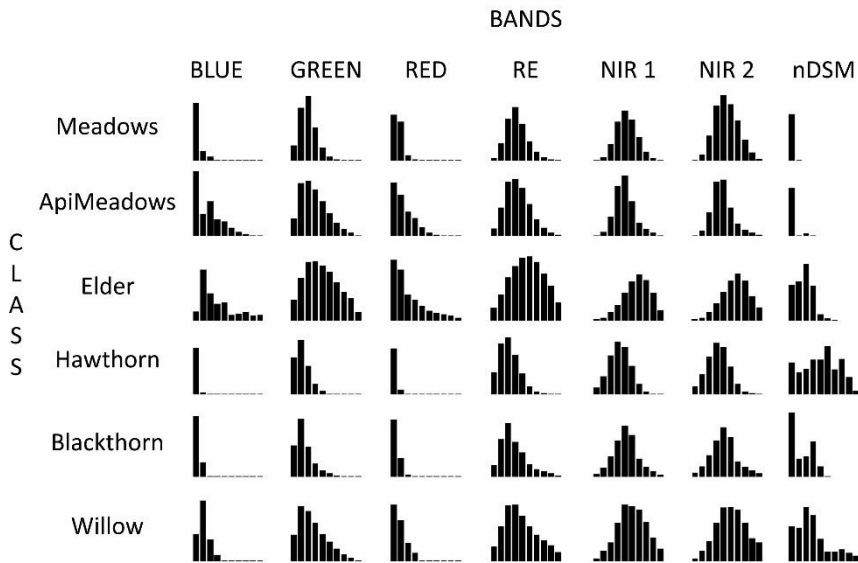


Figure 10. Value distributions in individual classes.

GEOBIA approach is also affected by the precision of the segmentation technique used at the input stage (Alonzo et al., 2014). The Estimation Scale Parameter algorithm - a tool for estimating suitable scales for segmentation based on the local variance - can help with fine-tuning the Scale parameter for a multiresolution segmentation algorithm (Draguț et al., 2014, 2010). No fully automatic approach to the optimizing and quantification of the segmentation algorithm is however available. Another recommended method is testing of individual input parameters followed by a visual inspection (see more

in eCognition user guide). Visual interpretation is one of the widely used references for a quantitative evaluation of the accuracy of various segmentation approaches (Alonzo et al., 2014; Clinton et al., 2010; Draguț et al., 2014). For that reason, we tested the input parameters of the segmentation algorithm for both sites and using the expert knowledge of the study site, we performed a visual inspection over a high resolution orthomosaic and nDSM raster. Our approach ensured that the resulting segments took even the smallest objects in the image (small shrubs with treetop projection of approx. 0.5 m<sup>2</sup> and height approx. 0.5 m) into consideration while, at the same time, larger homogenous areas (ApiMeadows, large willow shrubs) were not unnecessarily fragmented.

## Conclusion

Our study proved that a fusion of multispectral and SfM-derived vertical information significantly improves the accuracies of classification of shrubland vegetation to the level of individual species/genera of shrubs and meadow types. Our findings indicate that it is possible to acquire high quality results of shrubland mapping that can be potentially utilized for ecological research and other applications even without high investments in LiDAR sensor and without the need of several flight missions. However, where the accuracy of the classification based solely on multispectral data was high (approx. 80% producer's accuracy and 90% user's accuracy), supplementing the results with vertical data had little positive effect on the classification accuracies or even worsened the results for some species. Identifying the level of producer's and user's accuracies derived solely from spectral data, after which the fusion with vertical data becomes unnecessary, in various landscape types is an interesting research question for further studies. Our results also demonstrated the high dependency of classification results on the allocation of ground truth data. Although fusion with vertical data reduced that dependency in most cases, we believe that our approach using multiple random allocations and classifications of ground truth data should be a standard approach for similar studies.

## ACKNOWLEDGEMENTS

We acknowledge the anonymous referees for their constructive comments. We would also like to thank Jan Komárek, Ondřej Lagner and Petr Klápště for helping with UAV image acquisition, Kateřina Gdulová for substantial help with ground truth data mapping, Karel Hrach for statistical advice, and Jaroslav Janosek for valuable comments.

## FUNDING

This research was supported by the Internal Grant Agency of the Faculty of Environmental Sciences, Czech University of Life Sciences Prague, under grant No. 42300/1312/3128 and by the Grant Agency of the Czech University of Life Sciences Prague (CIGA No. 20174208).

## Chapter VII – STUDY 4

### Title:

Integration of Hyperspectral and LiDAR Data for Mapping Small Water Bodies

### Authors:

**Jiří Prošek**, Kateřina Gdulová., Vojtěch Barták, Duccio Rocchini, Jiří Vojar, Milič Solský., Vítězslav Moudrý

### Author's contribution: 50%

Conceptualization of methodology, field work, data processing and validation, co-writing of the original draft with respect to technical issues and formulation/interpretation of results.

### Journal:

*Currently submitted and under review in Remote Sensing of Environment, IF (2018) 8.218 – 2 of 30 (D1) rank in WOS Category Remote Sensing; AIS (2018) 1.902 – D1 rank*

### Full citation:

*Currently submitted and under review*

### Cited:

*Currently submitted and under review*

## ABSTRACT

Inland water bodies are globally threatened by environmental degradation and climate change and repeated monitoring is crucial for their successful preservation. Remote sensing, especially multispectral and hyperspectral data, has been widely used for identification of water bodies. However, the use of optical imagery is constrained by accuracy problems related to the difficulty in distinguishing water features from other surfaces with low albedo, such as shadows from buildings and trees. In this study, we evaluated the potential of integrating hyperspectral data with LiDAR-derived variables (hereafter “integrative approach”) to eliminate the effect of shadows. The hyperspectral imagery consisted of 148 bands from 380 to 2450 nm; the spatial resolution was 1.25 m. We used five LiDAR-derived variables at the same resolution: (i) Points density; (ii) Intensity; (iii) Ratio of the number of first returns and of all returns; (iv) Elevation of the normalised digital surface model; (v) Slope of the digital surface model. The study area consisted of several spoil heaps located in North Bohemian brown coal basin, one of the largest mining areas in Europe, that contains heterogeneous water bodies with a high variability of shape and size, located in environments with contrasting vegetation cover. We utilized object-based classification (support vector machine) based solely on hyperspectral or LiDAR data with classification based on integration of both datasets. In addition, we classified hyperspectral data by two traditional pixel-based approaches (K-mean and spectral angle mapper). Our results show a superior classification accuracy of the integrative approach yielding an improved discrimination of open water surface, with the omission error of 2% and commission error of 0.41% compared to individual hyperspectral (omission 7.6% and commission 1.28%) or LiDAR (omission 4.0% and commission 0.41%) variables. Pixel based approaches yielded very high omission errors of 5.2% and 22.4% and commission error of 0.8% and 0.5% for K-mean and Spectral angle mapper, respectively. We also evaluated the success of detecting individual ponds and integrative approach was the only approach that detected the water bodies with both omission and commission error below 10%. Finally, the assessment of misclassification reasons showed a perfect elimination of shadows in the integrative approach. Our finding demonstrate that utilizing LiDAR data successfully eliminated problems with shadows and that integration of hyperspectral and LiDAR data for open surface water classification can greatly improve the identification of small water bodies.

## KEYWORDS

Classification, Fusion, Hyperspectral, LiDAR, Mining, Spoil heap, Water

## Introduction

Water, besides being an essential natural resource, also represents an important environment supporting high biodiversity. Inland water bodies are however globally threatened by agricultural irrigation, ongoing urbanization, environmental degradation and climate change (Vörösmarty et al., 2010) and the spatial and temporal changes of surface water bodies are therefore drawing more and more attention (Pekel et al., 2016). Precise extraction and repeated monitoring of open surface water bodies is needed for better management of water resources as well as for preservation of these threatened ecosystems and preventing biodiversity loss (Harrison et al., 2018).

Mining is one of human activities with strong environmental impacts (Hendrychová and Kabrna, 2016; Svobodova et al., 2012). In particular, surface mining and associated extensive disturbances significantly influence large areas and have negative effects on freshwater biota that persist even after the reclamation of the mining site (Giam et al., 2018; Osenberg, 2018). On the other hand, it has been repeatedly shown that reclaimed areas have a high conservation value (Schulz and Wiegler, 2000; Vanhée and Devigne, 2018; Vymazal and Sklenicka, 2012). This is particularly true about areas left to spontaneous succession as those represent habitats that have been disappearing throughout Europe over past decades (Doležalová et al., 2012). Spoil heaps have been shown to become important biodiversity refuges, especially for aquatic species such as anurans (Vojar et al., 2016) and dragonflies (Harabiš et al., 2013). However, labour intensive and extremely time demanding in situ surveys are often needed to localize habitats of such endangered species. Such a survey was undertaken for example by Doležalová et al. (2012) who identified more than 900 open surface water bodies important for conservation on spoil heaps. Although field surveys provide valuable information for preservation of important habitats and for understanding of various ecological and environmental processes (e.g. Prach and Walker, 2011; Vojar et al., 2016), they are unsuitable for repeated monitoring due to their labour intensiveness. Remote sensing is an efficient and cost effective

alternative for such surveys, although it is only rarely adopted in restoration projects (Cordell et al., 2017).

Remote sensing has been widely used for identification of water bodies and for monitoring their changes. Several processing techniques have been adopted for such purposes (Chen et al., 2004). For example, various spectral water indices are frequently used to extract water bodies due to the ease of use and low computational cost. The Normalized Difference Water Index (NDWI) was developed to distinguish open water bodies from vegetation using green and NIR bands of Landsat satellite images (McFeeters, 1996) and several modifications and improvements on that index have been subsequently introduced (Feyisa et al., 2014; Xu, 2006). Another approach is to extract water features using various classification techniques, of which the support vector machine approach is the most popular (Põssa and Maillard, 2018; Rokni et al., 2015). However, other classification algorithms in combination with various data sources (spectral, LiDAR or radar dataset) have also been used (e.g. neural networks, K-nearest neighbour and random forests) to distinguish water bodies individually (Kaplan and Avdan, 2017; Mahdianpari et al., 2017; Paul et al., 2018) or in the context of several land cover classes (Antonarakis et al., 2008; Brennan and Webster, 2006; Dronova et al., 2015; Luo et al., 2016).

Images from satellite sensors of varying spatial, temporal, and spectral resolution have been extensively used to detect and extract surface water. This includes identification of water bodies using satellite sensors such as Landsat Thematic Mapper or MODIS (Carroll et al., 2009; S. Lu et al., 2011). Data from such sensors are particularly suitable for global scale studies at a relatively coarse resolution. For regional or local scale studies that require detailed information about small water bodies (Šikola et al., 2019; Šimová et al., 2019), airborne hyperspectral data with high spatial and spectral resolution have emerged as an important data source and were utilized for applications such as wetland mapping (Harken and Sugumaran, 2014; Zhang and Xie, 2012), water quality assessment (Giardino et al., 2007; Olmanson et al., 2013) and water bodies identification (Xie et al., 2014).

However, the use of optical imagery is constrained by accuracy problems. In particular, these are related to the difficulty in distinguishing water features from other surfaces with low albedo, such as shadows from clouds and terrain (Verpoorter et al., 2012); where high resolution imagery is used, shadows from buildings and trees may also pose a problem (Liu et al., 2017; Mostafa and Abdelhafiz, 2017). The presence of such surfaces may cause misclassification due to the similarity in reflectance patterns and various approaches have been



proposed to overcome this problem (Mostafa and Abdelhafiz, 2017; Verpoorter et al., 2012).

Combining optical imagery data with digital elevation models (DEM) characterizing e.g. vegetation height or terrain slope is a popular approach, which benefits from the increasing availability of remote sensing data acquired by different sensors for the same area (Pohl and Genderen, 1998). Most often, such information is derived from Light detection and ranging (LiDAR). LiDAR data itself was successfully used for land cover classification (including water; Antonarakis et al., 2008). LiDAR data provide complementary information to optical images and are not affected by shadows. It is increasingly common to have both LiDAR and hyperspectral data available for the same area (Asner et al., 2015, 2007; Hanuš et al., 2016). For example, Degerickx et al. (2019) used airborne LiDAR as an additional data source for spectral unmixing of urban land cover. Gilvear et al. (2004) combined hyperspectral and LiDAR data for mapping estuary and river hydromorphology. Dalponte et al. (2012) and Naidoo et al. (2012) integrated such data for mapping tree species in Alps and African savanna, respectively.

However, the integration of LiDAR-derived variables and hyperspectral data for open surface water classification has not been tested so far, possibly due to the fact that open water absorbs energy on the wavelength commonly used by terrestrial LiDAR (1064 nm). In LiDAR point clouds, water bodies are therefore represented as empty areas without any returns, which makes the use of LiDAR for water feature identification slightly awkward. However, Steuer et al. (2011) utilized this very feature of LiDAR to detect water bodies and Lu et al. (2011) successfully utilized terrain-derived attributes (terrain slope) to improve open surface water classification by eliminating problems with shadows. (S. Lu et al., 2011)

The overall objective of this study is to extract open surface water bodies on spoil heaps from very high resolution data. A crucial step for such task is to eliminate problems caused by shadows from trees and terrain (i.e. false positives). To achieve this goal, we integrated hyperspectral data with LiDAR-derived variables (hereinafter “integrative approach”) and adopted object-based approach, which is capable of providing good results with very high resolution data (Alonzo et al., 2014; Hartfield et al., 2011; Liu et al., 2015). In addition, it is common that LiDAR and hyperspectral data show some level of misalignment (e.g. Parmehr et al., 2014) and it can be assumed that object-based classifications are less prone to such misalignment (Blaschke, 2010). To illustrate the advantages of our integrative

approach, we compared it with object-based classification based solely on hyperspectral or LiDAR data, and with classification of hyperspectral data by two traditional pixel-based approaches. We quantitatively evaluated the accuracy of all above classifications in terms of: (i) overall accuracy per area with stratified random points sampling; (ii) accuracy validated per features classified as water bodies; and (iii) analysed the sources of misclassification.



*Figure 1. Aerial images of representative water bodies. Images were taken in time range from 2011 to 2016.*

# Materials

## STUDY AREA

The present study was conducted on four spoil heaps originating from brown coal mining located in the North Bohemian brown coal basin (Figure 1), which is the largest mining area in the Czech Republic and one of the largest in all of Europe. The overall area of those four spoil heaps is 37.97 km<sup>2</sup> and elevation ranges from 200 m to 410 m above sea level (Figure 2).

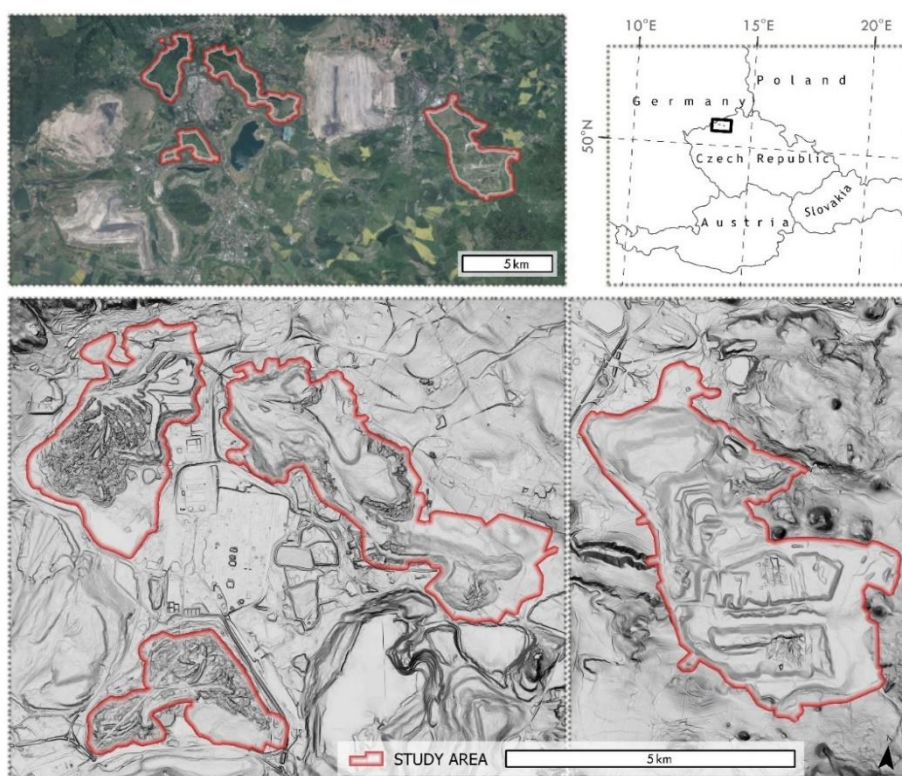


*Figure 2. Study area in a topographical context – represented by a combination of slope and hillshade. The four spoil heaps under study are delineated by red line*

Depending on the age of the spoil heap, adopted reclamation techniques and consequently terrain character, the vegetation consists of forest, steppes (low vegetation with scattered shrubs and trees), grassland, and aquatic vegetation (e.g. [Doležalová et al., 2012](#); [Frouz et al., 2018](#)). Spoil heaps also differ in their character

due to application of different reclamation approaches. Some have been technically reclaimed, which led to formation of a uniform terrain, while others (or their parts) have not and their terrain morphology remained rugged as a result of heaping, forming a typical undulated terrain (Frouz et al., 2018).

The number of surface water bodies in the study area is especially high in areas without technical terrain reclamation, their sizes ranging from several square meters to thousands square meters. Water bodies can occupy up to 10% of the non-reclaimed parts. On technically reclaimed sites, water bodies are also often artificially created, they are however generally larger than those generated spontaneously. Therefore, the study area contains heterogeneous water bodies of high variability of shape and size located in environments with contrasting vegetation cover (e.g. grassland, dense shrubs, and forests; see Doležalová et al., 2012 for more details about the character of the water bodies in study area).

## AIRBORNE DATA COLLECTION and PRE-PROCESSING

The airborne LiDAR and hyperspectral data were acquired simultaneously on 18<sup>th</sup> May 2017 using a remote sensing platform FLIS (The Flying Laboratory of Imaging Spectroscopy; Hanuš et al., 2016). FLIS is operated by the Global Change Research Institute (Czech GLOBE) and equipped with an inertial measurement unit (IMU), global navigation satellite system (GNSS) receiver, two hyperspectral sensors (Visible Near Infrared, VNIR, CASI-1500 and Short Wave Infrared, SWIR, SASI-600), and LiDAR sensor (Riegl LMS Q-780) which are all mounted on an aircraft Cessna 208B Grand Caravan (see Table 1 for sensor parameters and data characteristics). Flights for data collection were conducted at 1030 m above ground with a velocity of 110 knots (ground speed). The data acquisition took three hours (from 14:30 to 17:30 CEST) and consisted of 41 flight lines. Data were provided in the European terrestrial reference system ETRS-89 and Universal transverse Mercator projection (UTM33N).

### Hyperspectral data

The hyperspectral imagery consisted of 48 bands covering the visible near-infrared range from 380 to 1050 nm (CASI-1500) and 100 bands covering the near-infrared and short-wave infrared range from 950 to 2450 nm (SASI-600) with a band width of 15 nm. Pre-processing of the hyperspectral images (i.e., radiometric correction, georeferencing and atmospheric corrections) were all carried out by the provider (Czech GLOBE). Radiometric corrections were performed in the RadCorr software by converting spectral radiances to physical radiance units based

on calibration parameters from the CzechGlobe spectroscopic laboratory (Hanuš et al., 2016). Radiance images were geometrically corrected, orthorectified using a digital terrain model (DTM), and georeferenced. Subsequently, VNIR and SWIR data were merged (VNIR data were resampled to SWIR resolution using pixel aggregate method) and corrected for atmospheric conditions using a radiative model MODTRAN in ATCOR-4 software (Richter and Schläpfer, 2016).

#### LiDAR data

Airborne LiDAR data was acquired with a Riegl LMS Q-780 laser scanner. The scanner has a rotating polygon mirror and scans in parallel lines. The scan field of view is 60° and the wavelength is 1064 nm. The LiDAR data were provided in LAZ format with an average point density of 8 points per square meter. We further processed the LiDAR point cloud using LAStools (LAStools, 2019; <http://lastools.org>). LASnoise and LASground tools of the LAStools software were used to determine ground points. We tested several settings for LASground and visually assessed the resulting DTMs using hill-shaded terrain and the success of the identification of ground points in the most troublesome areas. The best results were acquired using predefined settings for natural environments (Moudrý et al., 2019a, 2019b).

Based on the visual inspection and variables used in prior studies (Antonarakis et al., 2008; S. Lu et al., 2011), we considered the five following variables as suitable for water bodies identification: (i) Points density – number of points per spatial unit; (ii) Intensity - average light intensity of LiDAR returns; (iii) Ratio of the number of first returns and of all returns; (iv) Elevation of the normalised digital surface model based on the triangular network of points identified as non-ground points; (v) Slope of digital surface model – based on triangular network of all first class returns. All LiDAR variables were derived for identical spatial units and sampled to the same raster grid – cells were aligned with the same spatial resolution of 1.25 m in the UTM 33N coordinate system. For subsequent classification steps, we created a composite dataset consisting of a full hyperspectral cube (with all 148 bands) and five LiDAR-derived variables (Figure 3).

Table 1. Hyperspectral sensors and dataset characteristics

Sensor parameters	Sensor	
	VNIR (CASI-1500)	SWIR (SASI-600)
Spectral resolution [nm]	380-1050	950-2450
Bandwidth [nm]	15	15
Max. spectral resolution [nm]	3.2	15
Count of band	48	100
Spatial resolution [m/cell]	0.5	1.25
Angle of view [°]	40	40

Table 2. LiDAR sensor and dataset characteristic

Sensor Parameters	(Riegl LMS Q-780)
Wavelength [nm]	1064
Laser pulse frequency [kHz]	400
Angle of view [°]	60
Beam divergence [mrad]	0.25
Point density [point/m <sup>2</sup> ]	7-8
Field of view [°]	60

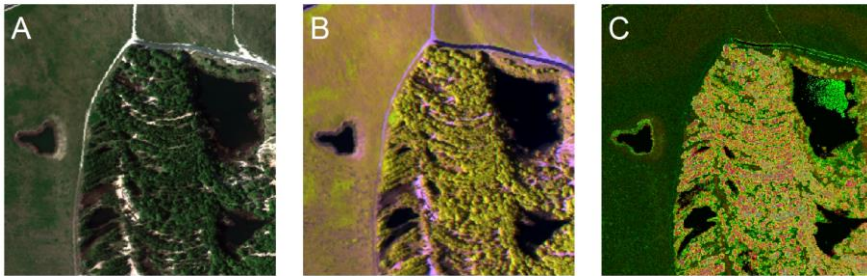


Figure 3. (A) Aerial photo – true colour composite with RGB bands i.e. visible part of the spectrum, (B) false colours composite with Red, NIR, SWIR bands i.e. representation of infrared part of the spectrum and (C) LiDAR variables composite where red band represents nDSM, green band represent light intensity of LiDAR returns, and blue represent points density

# Methods

## OVERVIEW of METHODOLOGY

To classify open surface water, we adopted the Support vector machine (SVM) algorithm as a representative of object-based classification approaches recommended for VHR datasets classification (Blaschke, 2010). SVM algorithms were also successfully used for classification of integrated LiDAR and hyperspectral data by other researchers (Dalponte et al., 2012; Luo et al., 2016; Okiemute and Ruth, 2017). We performed object-based classifications using hyperspectral data and LiDAR variables separately as well as using their combination. In addition, we also used two different pixel-based classification methods based on hyperspectral data, namely, K-mean classification (a representative of unsupervised classification methods) and spectral angle mapper (a recommended and optimal method for hyperspectral datasets). We also tested the suitability of integrated hyperspectral/LiDAR data for pixel based approaches; however, the results were poor and therefore not presented in this study.

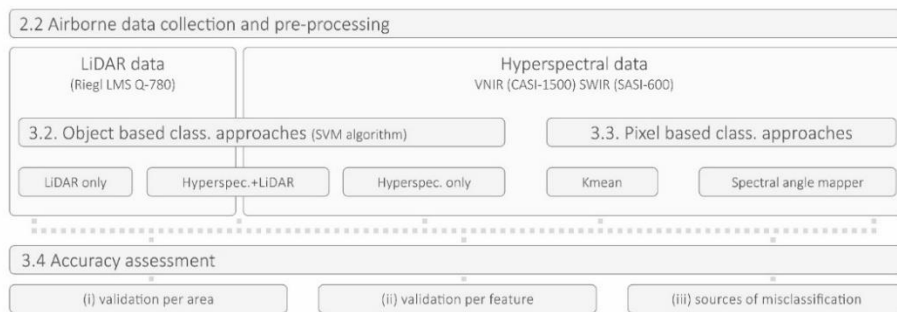


Figure 4. Overview of methodology, classification approaches and accuracy assessment

The accuracy of all classifications was quantitatively assessed in terms of: (i) overall accuracy per area with stratified random points sampling; (ii) accuracy validated per features classified as water bodies (i.e. how successful the individual methods are in detecting particular ponds or lakes); and we assessed (iii) sources of misclassification (e.g. landcover, shadow). The major data processing steps and adopted methods are presented in Figure 4. Data pre-processing and classification were performed in ENVI SW, post-processing and all spatial operations in ArcGIS 10.6 SW (ESRI, Redlands, CA, USA).

## OBJECT-BASED CLASSIFICATION APPROACHES

### Support vector machine

We used the support vector machine (SVM) algorithm as a representative of object-based classification approaches. The process of classification consists of (1) image segmentation and (2) classification of segments. First, based on similar spectral, textural, shape and, in our study, LiDAR variables, the segmentation algorithm divided the image information into basic segments. Segmentation was performed by the Feature Extraction tool with “scale level” and “merge level” being adjustable input parameters. We iteratively tested the scale level in steps of 5 units (ranging from 10 to 100), combined with merge level settings in steps of 5 units (ranging from 10 to 95) on five samples (100x100m). After a visual inspection of tests on those preliminary samples, we used scale level value of 25 and merge level value of 75, or scale level value of 30 and merge level value of 80, depending on the site. Second, we used the supervised classification method based on SVM algorithm independently for (i) full range hyperspectral data; (ii) LiDAR variables; and (iii) combination/composite of hyperspectral data and LiDAR variables. We manually selected 20 representative training samples for each category. The following characteristics per object were used for SVM classification: Basic variables (Mean, Standard Deviation, Min and Max pixel value), Texture variables (Range, Mean, Variance, Entropy), and Spatial variables (Area, Length, Compactness, Convexity, Roundness, Elongation, Numbers of holes, Hole Area/Solid Area).

## PIXEL BASED CLASSIFICATION APPROACHES

### Unsupervised classification approach

K-mean classification is a typical representative of nonparametric, unsupervised classification algorithms (Tou and Gonzalez, 1974). The K-Mean algorithm used in our study (namely ENVI SW implementation) starts with uniform distribution of class means in the space, which are then iteratively clustered into classes based on the minimum distance. After each iteration, class means are recalculated and pixels reclassified according to the new means. The following input parameters were used: number of classes, change threshold, maximum number of iterations. Using an inappropriate number of classes represents a common problem of this approach as it can lead to mixing classes together. A typical example is a combination of water bodies and shadows (Movia et al., 2016). Therefore, we iteratively tested the numbers of classes (a range from 5 to 30) on five samples



(100x100 m) while keeping other parameters unchanged (change threshold: 1%, maximum number of iterations: 50). After each iteration, we performed a visual inspection using high resolution ortho-images as a reference. Based on the results of this preliminary test, 12 classes were used in the final classification, along with the other parameters as mentioned above (change threshold 1%; maximum number of iterations 50).

#### Spectral angle classification approach

Spectral angle mapper (SAM) is a classification approach recommended and optimized for hyperspectral data. The algorithm determines the spectral similarity between two spectral curves by calculating the angle between the spectral bands, treating them as vectors in a space with dimensionality equal to the number of bands (Kruse et al., 1993). Selection of input steps/parameters includes choosing (1) a suitable calibration dataset/spectral library and (2) a threshold maximum angle deviation. We assembled a spectral library based on over 200 samples of water bodies in our study area. We iteratively tested and visually inspected the maximum angle deviation in steps of 0.05 units (ranging from 0.05 to 1.0) on five samples (100x100 m) and used the maximum angle deviation of 0.2 for the final experiment.

## ACCURACY ASSESSMENT

We quantitatively assessed the accuracy of classification methods in the following way: (i) We used a stratified random sampling design according to the good practices for accuracy assessment (Olofsson et al., 2014) with randomly generated 500 points (hereafter validation per area), 250 of which was located in non-water areas and 250 in water; (ii) We compared the classification approaches based on accuracy validated “per features”, i.e. per objects identified as water bodies. We randomly generated altogether 500 points in surfaces classified as water bodies in a way ascertaining that no more than a single point was in each feature. Noise features consisting of less than 4 pixels were omitted. 147 of those points were subsequently manually identified (see below) as non-water and 353 as water surface samples; (iii) We assessed the cause of misclassification (e.g. presence of spectrally similar land cover categories such as shadows or categories with similar LiDAR characteristics such as roads or holes in vegetation structure). Those “misclassification points” were generated for each of the classification approaches separately, until we had 100 points where classification failed for each approach and the reasons of misclassifications were analysed.

For validation per area and validation per feature, we calculated the omission error as the fraction of values that belong to a water category but were misclassified as non-water category and commission error as the fraction of values classified as water but not belonging to that class. All points used for the above validations were assessed over high resolution ortho-images (0.5 m per pixel) and manually assigned to desirable categories by a researcher with expert knowledge of the site. Moreover, water points were subsequently validated in the field.

## Results

### OVERALL ACCURACY

The identification of water bodies was very successful. However, methods differed in the overall accuracy and especially in the identification of particular water bodies and sources of misclassification. The accuracy of open surface water bodies based on validation per area depends on the classification method with omission error ranging from 2% to 22.4% and a generally low difference in commission error – lower than 1.5% (which is however caused predominantly by the fact that the total area of water bodies is smaller than the total remaining area) (Figure 5). The most accurate classification was achieved by the integrative approach (SVM hyperspec.+LiDAR) with omission and commission errors of 2% and 0.4%, respectively. The object-based classification using only hyperspectral data (SVM hyperspec. only) had a relatively high omission (7.6%) as well as commission (1.3%) errors. The object classification based on LiDAR variables (SVM LiDAR only) had a slightly lower omission error than the K-mean classification (4% compared to 5.2% for K-mean), and the commission error was in both approaches lower than 1%. SAM classification approach also had a low commission error (0.5%), but the omission error was the highest of all approaches (22.4%).

### PER FEATURE ACCURACY

Validation per features showed that the integrative approach is more successful in identifying particular water bodies than other methods (Figure 5). It was the only approach that at the same time correctly identified more than 90% of water bodies (omission error 5.3%) as well as more than 90% of non-water surfaces

(commission error 9.6%). In contrast, object classification based on hyperspectral characteristics only have the highest omission error of 19.4% as well as a very high commission error of 30.4%. The remaining methods achieved mutually comparable results with the exception of SAM classification that yielded the highest commission error (Figure 5).

## THE CAUSE of MISCLASSIFICATION

The assessment of misclassification reasons showed that all classifications based solely on hyperspectral data were negatively affected by the presence of shadows and to a certain extent by the presence of artificial surfaces and terrestrial or littoral vegetation (Figure 6). For all three classification methods based solely on hyperspectral data, more than 50% of misclassifications were caused by shadows (due to the similar spectral characteristics, see Figure 7). The method most affected by shadows was the unsupervised K-mean classification where 73 out of 100 misclassification points were shadows misclassified as water areas. In SAM and SVM, 56 and 51 out of 100 misclassified points were shadows. In contrast, LiDAR variables provided additional information (see Figure 8) and classification based on them recorded only 4 out of 100 misclassified points as affected by shadows; this classification was mostly affected by other categories (in particular vegetation and artificial surface – roads). Classification with integrated LiDAR+hyperspectral data also showed minimum errors caused by the presence of shadows (Figure 6). The predominant source of misclassification in this method was littoral vegetation, responsible for 87% of misclassifications.

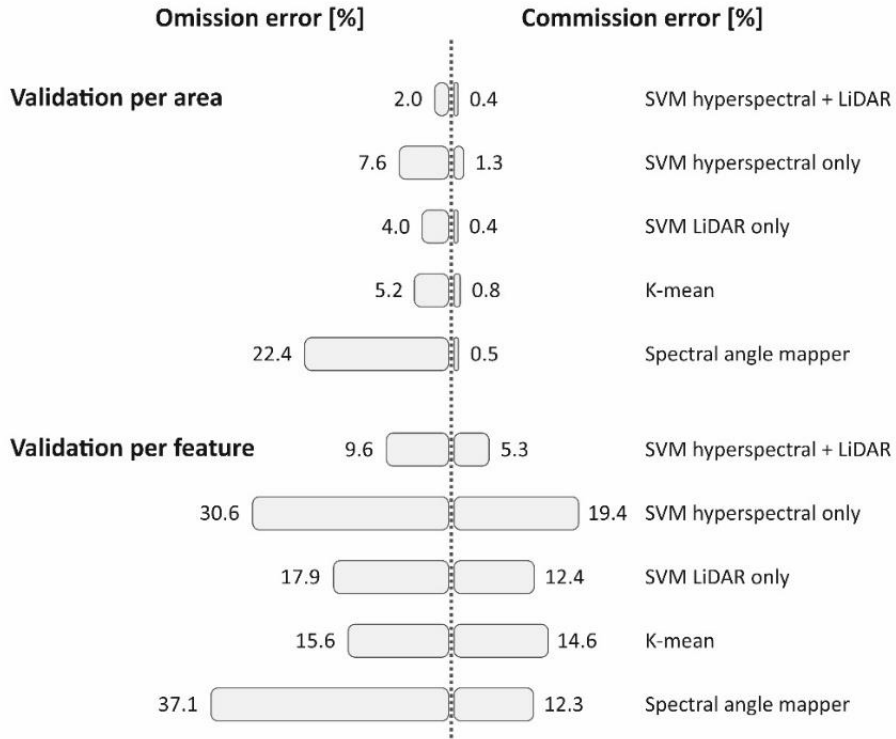


Figure 5. Results of the accuracy assessment for each classification approach 1) Validation per area based on 250 water and 250 non-water randomly generated validation points; 2) Validation per feature based on 353 water and 147 non-water samples

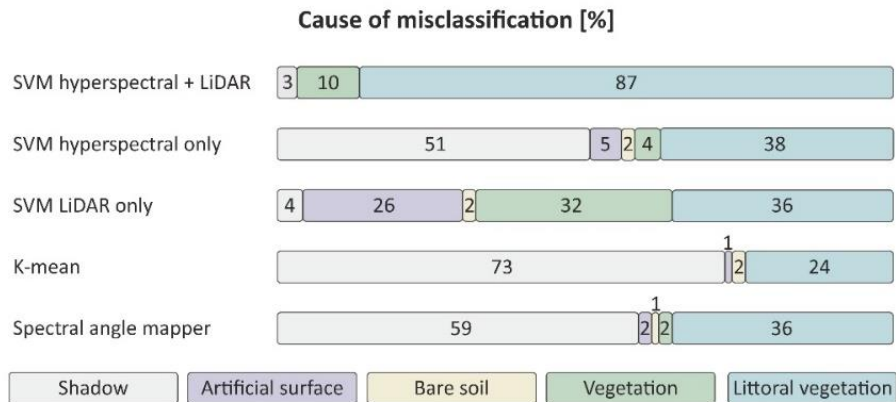


Figure 6. Cause of misclassification for each classification approach based on 100 validation points

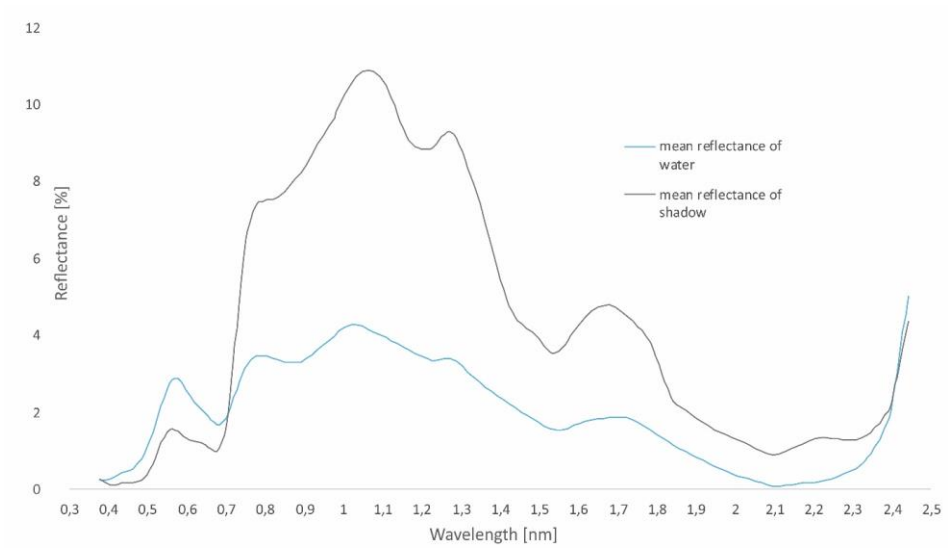


Figure 7. spectral curves of water bodies and shadows on spoil heap areas based on 50 samples of each surface

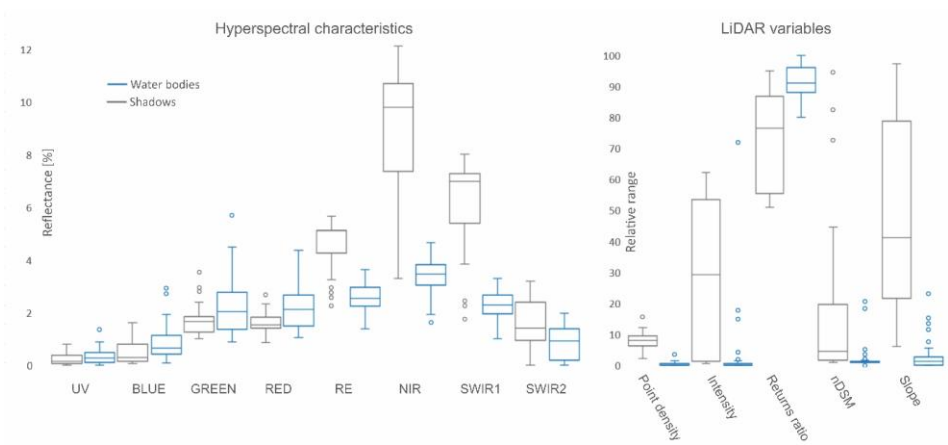


Figure 8. Hyperspectral characteristics (represented by relative surface reflectance) and LiDAR variables (represented by absolute values of parameters resampled to scale in range from 0 to 100) of water bodies and shadows

## Discussion

In this study, we examined the possibility to integrate airborne LiDAR and hyperspectral data to classify open surface water bodies and in particular to mitigate negative effect of shadows caused by their similar spectral signature. We used a range of structural variables derived from LiDAR and spectral, textural and spatial variables derived from hyperspectral data (with 148 bands). We tested both LiDAR variables and hyperspectral data alone and in combination.

Our results show that the integration of LiDAR and hyperspectral data using object-based classification yielded an improved discrimination of open surface water bodies, with the omission error of 2% and commission error of 0.41% compared to individual hyperspectral (omission 7.6% and commission 1.28%) or LiDAR (omission 4.0% and commission 0.41%) variables (Figure 5). These results are comparable to those reported by [Luo et al. \(2016\)](#) who also integrated airborne LiDAR and hyperspectral data to classify land cover (including water surface) with omission error of 3.95% and zero commission error. Their study area however contained few water bodies and only 22 validation points were used to evaluate that category. In contrast, [Okiemute and Ruth \(2017\)](#) classified water surface in context of seven categories of land cover integrating LiDAR and multispectral/hyperspectral data and achieved a low omission error of 0% and relatively high commission error ranging from 19.6% to 4.3%, depending on the classification method. It must be however noted that standard overall accuracy assessment based on validation per area does not accurately reflect the classification accuracy of small water bodies that were our main interest as it is biased due to the presence of large water bodies and due to the fact that the total area of water bodies is smaller than the total remaining area.

We also evaluated the success of detecting individual ponds and investigated the sources of misclassification, which both show a superior classification accuracy of the integrative approach. The accuracy assessment based on random samples per features classified as water shows that the integrative approach is much more successful in detecting particular water bodies than remaining approaches. It was the only approach that detected the water bodies with both omission and commission error below 10% (Figure 5). The assessment of misclassification reasons showed a perfect elimination of shadows in the integrative approach. The predominant source of misclassification in this method was littoral vegetation (i.e. non-submerged aquatic vegetation). As the littoral zone is a part of the water body, this misclassification should nevertheless not be

considered as an error per se (Gairola et al., 2013; Husson et al., 2017). A more detailed classification capable of identification of littoral vegetation is a focus of another ongoing study.

Our results show that the integrative approach (i.e. the fusion of hyperspectral data and LiDAR variables) improves the classification of water bodies derived from remote sensing data, predominantly by eliminating misclassification problems caused by shadows. Shadows are a common problem in the airborne imagery and many studies reported misclassification due to the presence of shadows (Liu et al., 2017; Mostafa and Abdelhafiz, 2017; Verpoorter et al., 2012; Wu et al., 2014). Our results show that all classification approaches based solely on hyperspectral data are strongly negatively affected by shadows, particularly the K-mean classification where 73 out of 100 misclassified points were misclassified due to the presence of shadows (see Figure 7 for spectral waveform of water and shadows in our study area). In contrast, classification approach based only on LiDAR variables is predominantly affected by artificial surfaces and terrestrial or littoral vegetation (Figure 6). It is also noteworthy that our results suggest that the accuracy of the detailed water surface identification based on LiDAR variables alone is comparable as that obtained with hyperspectral data alone (see also Antonarakis et al., 2008).

Although data acquisition during the solar midday is a logical solution for avoiding shadows, it is difficult to accomplish. It is a solution often used with unmanned aerial vehicles (e.g. Cunliffe et al., 2016; Prošek and Šimová, 2019; Weil et al., 2017); however, even when data are acquired during the solar midday, shadows at regions outside the equatorial zone are not eliminated perfectly. Furthermore, with aircraft used over larger areas, it is impossible to acquire data in a short time and in many parts of the world, weather conditions are not always very inviting for a survey. Bad weather conditions also appeared in 2017 at our study area and we had to wait until data acquisition was possible. Wu et al. (2014) suggested an interesting possibility for elimination of the problem with shaded areas based on a difference between images acquired at a different times. This method is however suitable only for satellites or unmanned aerial vehicles, not for aircraft data acquisition as it would incur substantial additional costs.

Our results show that the integration of LiDAR and hyperspectral data is applicable even where surface water bodies are partly covered by vegetation (e.g. littoral zones). We suggest that combining LiDAR and hyperspectral data can improve detection of water bodies even under the vegetation canopy (e.g. high trees). To further test this hypothesis, however, additional field work is required

to accurately detect such water bodies. Theoretically, we could use data from previous studies (Doležalová et al., 2012) that are available to us, however those data were gathered with consumer-grade GNSS receivers and therefore are positionally inaccurate for testing this hypothesis (e.g. Tomašík et al., 2017).

We also tested integration of hyperspectral and LiDAR data with pixel based approaches; however, the results were poor and therefore not presented in this study. We attribute this failure to misalignment between the two datasets. Hyperspectral and LiDAR data integration in pixel-based classification approaches requires reduction of misalignment of image pixels and LiDAR laser spots issues to minimum. This is especially problematic when data originate from different platforms. However, even when the data are acquired from the same aircraft, perfect alignment is not guaranteed. To perfectly align the data, several integration steps are required, from placing the instruments on board of the aircraft to a precise time registration of each measurement and final data fusion (Asner et al., 2012). In contrast, object-based classification is considered less prone to problems with noise and edge mixed pixel (Alonzo et al., 2014; Blaschke et al., 2014).



## Conclusion

In this study, we extracted open surface water bodies on spoil heaps at a very high resolution. We used object-based classification on integrated hyperspectral/LiDAR data. To evaluate advantages of the integrated data approach, we compared it with classifications using LiDAR and hyperspectral data separately and with two pixel based approaches with hyperspectral data alone. Our results show that the integrated approach provides better results than separate use of the datasets and significantly reduces both omission and commission errors. Furthermore, the commission error of integrated approach was predominantly caused by identifying littoral zones of ponds as water surfaces and in principle should not be considered as an error per se while where hyperspectral data alone were used, shadows were the principal misclassification reason. Most importantly, both the LiDAR-only and integrated approach classifications successfully eliminated problems with shadows that have affected all other approaches. We suggest that integration of hyperspectral and LiDAR data for open surface water classification can greatly improve the identification of small water bodies and its repeated monitoring, which is crucial to preserve these important habitats not only in our study area, but worldwide.

## FUNDING

This work was supported by the Czech Science Foundation under Grant No. 17-17156Y.



# Chapter VIII – Discussion and Conclusions

Over the last decades, RS became an irreplaceable source of data for environmental research. The ever increasing number and availability of RS platforms, datasets and processing techniques greatly facilitate environmental mapping. On the other hand, the improving data resolution and ever more sophisticated methods of data acquisition and processing also keep increasing the expectations on the quality and relevance of resulting products. This thesis presents, verifies and successfully applies several types of remotely sensed and ground measured datasets to environmental mapping. Every new phenomena investigated using remote sensing approaches requires a greater or smaller level of individualization of methods. Results and conclusions of the presented case studies show that the following is crucial for successful integration and application of high resolution airborne data in environmental mapping: (a) the choice of a suitable RS platform and sensors, (b) selection of a suitable approach to data processing, its individual steps and parameters, and (c) the choice of a suitable method of accuracy assessment facilitating the process of drawing conclusions from the results. Only a good understanding to all of those principal parts of the process allows to fully utilize the potential of remotely sensed fine resolution data in environmental research.

## Contribution of fusion classification

---

*To fuse or not to fuse, that is the question.*

---

When classifying, it is relatively easy to achieve high accuracy and relevance of the results when distinguishing among generalized classes (e.g. forests, shrubs, meadows or artificial surfaces). With an increasing thematic detail of classification, the accuracy and relevance of classification results however decreases, see results of [STUDY 2](#) or [Ahmed et al. \(2017\)](#). The growing requirements for thematic detail

of the classified layers often exceed the realistic expectations as even in the most detailed spectral datasets, the information may be insufficient for successful distinguishing between classes with similar spectral profiles (e.g. classification of plant species with similar spectral characteristics – [STUDY 2 and 3](#) – or distinguishing between water surfaces and shadows from hyperspectral data – [STUDY 4](#)). Nevertheless, the ever growing number of available RS platforms, sensors and data, integration of multiple remotely sensed datasets is possible. Such integration/fusion approach may add a supplementary information from the other dataset that can make differentiation possible even between classes that cannot be distinguished on the basis of one dataset only (typically, spectral data can be supplemented with vertical structure and variables, LiDAR variables or thermal data). Such approach is therefore instrumental in yielding the full information available from RS platforms.

A potential for improvement of classification results is shown in [STUDY 2, 3, and 4](#). In [STUDY 2 and 3](#), we show that a fusion of UAV spectral data and additional derived datasets significantly improves the accuracies (both user and producer accuracy) of classification of hard-to-distinguish vegetation to the level of individual species/genera. Combination of thermal data and normalized height (nDSM) inputs in [STUDY 2](#) improved classification, even in a very specific environment of an arboretum. The novelty of the approach used in the [STUDY 3](#) for detailed mapping of shrubland vegetation lies in the fusion of spectral and vertical information acquired during a single flight mission from a single multispectral UAV sensor. It indicates that it is possible to acquire high quality results of mapping that can be potentially utilized for ecological research and other applications even without high investments in LiDAR sensor and without the need of several flight missions. In [STUDY 4](#), we extracted open surface water bodies in post mining areas using integration of hyperspectral data and LiDAR variables from manned aircraft. Our results show that the integrated approach provides better results than the separate use of the datasets and significantly increases both user's and producer's accuracy. The novelty of the approach presented in [STUDY 4](#) for water bodies at detailed resolution lies in the integration of hyperspectral data with several LiDAR variables (common approaches use only elevation or slope-derived vertical variables, whereas we used the density of points; intensity of LiDAR pulse; ratio of the number of first returns and of all returns; elevation of the normalised digital surface model; slope of digital surface model). Moreover, to evaluate advantages of the integrated data approach, we compared it with classifications using LiDAR and hyperspectral data separately and with two pixel-based approaches with hyperspectral data alone.

To evaluate the advantages and accuracy improvement of the integrated/fusion data approach, we compared classification results in all classification studies (2-4) with classifications based solely on spectral data. In terms of classification advantages, it is necessary to first consider when classification improvement is actually possible at all and whether it makes any sense. The regression analysis in [STUDY 3](#) revealed a strong negative relationship between the improvement in accuracy caused by adding the height data to the model and the accuracy of the original classification using multispectral data only. It is obvious that in some landscape types, integration of vertical data would likely fail to bring any benefits (e.g. steppes). However, as results of [STUDY 2-4](#) show, there are many classes (e.g. different meadows type, water bodies vs shadows) where the integration of additional information is worthwhile for accurate and relevant results.

Result interpretation is highly affected by the used sampling design ([Congalton and Green, 2002](#); [Olofsson et al., 2014](#)). Hence, we had to adapt the accuracy assessment in each study in a way providing relevant evaluation of the acquired accuracies and enabling the quantification of potential improvement. In [STUDY 4](#), we assessed the classification accuracy in several ways: (i) overall accuracy per area – which allowed to observe how successful the individual methods are in detecting water surface pixels and at the same time allowed us to compare the results with other studies; (ii) accuracy validated per features classified as water bodies – showing how successful the individual methods were in detecting particular ponds or lakes, which represents the most important characteristic from the biotope mapping perspective and which allowed a better mutual comparison of the methods; (iii) sources of misclassification – showing the contributions and weaknesses of individual methods from the point of view of removing errors. In [STUDY 2](#), we had to deal with major differences in the spatial extent of individual categories in the study area. For evaluation of the classification results, we used an accuracy assessment method based on randomly selected spatially independent validation samples. We used a stratified random sampling design for reference polygons to make sure that land cover classes with low spatial extent were not omitted. In [STUDY 3](#), we used another accuracy assessment approach for dealing with the problem of allocation and spatial distribution of calibration and validation samples. We performed a 10-fold random allocation of the ground truth polygons into calibration and validation datasets and a 10-fold repeated classification and validation. A similar validation approach with multiple selections of calibration and validation samples (hereinafter Multiple random selection) was used e.g. by [Weil et al. \(2017\)](#).

In general, many classification approaches are more or less sensitive to allocation and spatial distribution of calibration samples (hereinafter classification sensitivity for sample distribution (Foody and Mathur, 2004). Where pros and cons of a classification approach are assessed, classification sensitivity for sample distribution should be always considered and reported, just like it is common in proving model performance in species distribution modelling. Based on Multiple random selection, we demonstrate in [STUDY 3](#) that the allocation of ground true samples affects the accuracy of the used classification approach. Moreover, we show that where classification integrates vertical information with spectral data, the classification sensitivity to sample distribution is in most cases smaller than when it is built solely on spectral data. In [STUDY 2](#), we use a different approach with 95% confidence intervals, allowing a more general application of results and reducing the dependency on the area of interest.

The accuracy of classification results is also strongly affected by the classification approach. In all studies dealing with classification ([STUDY 2-4](#)), we used object-based classification approach to data integration/fusion. Object-based approach has been shown to provide better results than pixel-based approaches with high resolution data (Alonzo et al., 2014; Blaschke, 2010; Hartfield et al., 2011; Liu et al., 2015). In preliminary testing for [STUDY 2-4](#), we also tried data integration/fusion algorithm with pixel-based classification. The results acquired during testing led us however to disregarding pixel-based classification for data fusion/integration, which applied to all our studies. In [STUDY 2 and 3](#), the poor results of pixel-based approach can be attributed to the high data resolution (the individual distinguished objects consist of hundreds of pixels). Thus, the results showed a high impact of „salt-and-pepper“ problem and the variability of characteristics within an individual class led to a very low accuracy and relevance of the classification. In [STUDY 4](#), two pixel-based approaches with hyperspectral data alone (non-integrative approach) were used as examples of widely used classification approaches and algorithms (namely K-mean and Spectral angle mapper). The failure of the pixel-based integration in [STUDY 4](#) is not due to the high resolution because small water bodies often consisted of relatively small number of pixels. We attribute this failure rather to misalignment between the integrated datasets. For successful hyperspectral and LiDAR data integration in pixel-based classification approaches, it is crucial to minimize misalignment of the image pixels and LiDAR laser spots. Even when the data are acquired from the same platform and at same time, with precise time registration and referencing, perfect alignment can not be guaranteed at the level of pixels. A possible solution for this problem might lie in resampling integrated

data into a coarser grid, which would eliminate the shift in the order of individual neighbouring cells. In [STUDY 4](#), however, such approach was not possible due to the above mentioned efforts to identify small water bodies consisting of a small number of pixels (the smallest water bodies were represented by 4 cells).

## Misclassification reasons and limitations of airborne RS

---

*Is sky the limit?*

*Where are the pitfalls and bottlenecks?*

---

Despite the availability of remotely sensed datasets with uniquely high spatial, spectral and temporal resolution, despite advanced methods of data acquisition and processing of RS datasets using integration/fusion approach, any classification will always bear some level of uncertainties and misclassifications. As a typical example, we can mention misclassification caused by shadows, which represents a problem in many studies ([Liu et al., 2017](#); [Mostafa and Abdelhafiz, 2017](#); [Verpoorter et al., 2012](#); [Wu et al., 2014](#)). The presence of shadows leads to major problems with misclassification due to the similarity in reflectance patterns among groups with normally distinct spectral characteristics such as vegetation or artificial surface and water bodies ([STUDY 4](#)). Various approaches have been proposed to overcome this problem ([Mostafa and Abdelhafiz, 2017](#); [Verpoorter et al., 2012](#)).

Approaches for dealing with the shadows include for example identification of shadows as an individual category as we did in [STUDY 2](#) or as used in other studies ([Movia et al., 2016](#); [Shao et al., 2011](#)), simple thresholding ([Wu and Bauer, 2013](#)) or classification of shadows separately as pre-processing step ([Zhou et al., 2009](#)). However, such classification approaches (mostly based only on spectral characteristics, although that is not the case of [STUDY 2](#)) are still affected by a certain level of error due to similar spectral waveforms (such as the problem

of similar waveforms of water and shadows in [STUDY 4](#)). Besides, if implementing such approach, we still lack information about the real vegetation cover in areas classified as shadows and this class therefore represents areas with unsuccessful classification. Moreover, representation of shadowed areas differs among individual vegetation classes (depending e.g. on the use data, classification approach and the environment itself as shown in [STUDY 4](#)). A situation can therefore occur when a one class more prone to being misclassified as shadows is greatly underrepresented in the resulting thematic layer as much of it is classified as “shadows”. The resulting biotope description then provides information that is not just incomplete but often even misleading. When using thematic maps/layers containing the categories of shadows, we then face the same problems as when using data burdened with positional error, i.e. incorrect characterization of conditions suitable for occurrence of the species in question, which in effect leads to reduction of the model performance e.g. (over/under)estimation of species habitat areas ([Moudrý and Šimová, 2012](#)). Similarly, when analysing land cover changes, the use of thematic maps containing shadows either causes false changes detection ([Shahtahmassebi et al., 2013](#); [Stow et al., 2014](#); [Zhu and Woodcock, 2014b](#)), or, to prevent this, areas that are shadowed in any of the layers must be removed from analysis. Such negative effects are the principal reasons for the search of other methods of their elimination.

An interesting possibility of dealing with this problem lies in the identification of shaded areas based on differences between images acquired at different times ([Wu et al., 2014](#)). However, while this method is suitable for satellites, it is unsuitable for airborne RS acquisition due to additional costs, especially where manned aircraft are concerned. In the case of UAVs, the additional time and image processing costs are lower but still present.

A logical method for minimizing shadows is data acquisition during the solar midday. It is a frequently used option with unmanned aerial vehicles (e.g. [STUDY 2 and 3](#) as well as other studies such as [Cunliffe et al., 2016](#); [Weil et al., 2017](#)). However, even when data are acquired during the solar midday, shadows are not eliminated perfectly in regions outside the equatorial zone (see the presence of shadows in [STUDY 2](#)). Furthermore, where airborne RS is used for a larger area, it is impossible to acquire data in a short time. While satellites can record large areas in a single image (providing that the weather conditions are favourable, i.e. low cloud coverage), airborne surveying takes much longer even for a single flight mission/area of interest. Airborne RS in general, and especially UAVs, is to a great degree limited by the legislation ([Stöcker et al., 2017](#)) and



by weather conditions that may prevent the flight mission (Dandois et al., 2015; Lu and He, 2017). In the case of STUDY 4, we also encountered unfavourable weather conditions in 2017 and we had to wait for a long time until data acquisition was possible. In case of STUDY 3, the extent and number of study sites was also reduced. One reason for that was the necessity for data acquisition around the time of the solar midday, which limited the time available for missions, especially under the strict conditions of a military area where the study was performed. In STUDY 1, the image quality was significantly affected by the wind – gusts of wind caused blurred images.

Light conditions represent the last but not least crucial parameter in the context of short term weather conditions. Good lighting conditions allow the acquisition of sharper images with a better contrast, which subsequently yields better results e.g. during 3D photogrammetry reconstruction (see STUDY 4 or Micheletti et al., 2015). If the images are acquired under different lighting conditions, radiometric corrections/calibration of the images is necessary to obtain relevant surface reflectance values (Lillesand et al., 2015). This is especially true where multitemporal approach is applied, i.e. when the analysed data originate from several time points or where the weather and/or lighting conditions are changing during the image acquisition mission, which is especially typical for airborne RS (Chavez, 1996; Dinguirard and Slater, 1999; D. Lu et al., 2011). As the data in STUDY 3 were subjected to a uni-temporal analysis and the flights were performed under constant weather conditions, no radiometric calibration of the scene was necessary. We however used a mosaic algorithm for correction of colour and brightness of the entire scene. In STUDY 2, however, the changing weather conditions (high clouds and a partial shadowing by low clouds) during data acquisition resulted in a necessity of calibrating the surface reflectance values from the multispectral mosaic. The calibration was performed during SfM photogrammetry procedure using values from onboard irradiance sensor (Sun irradiance and Sun angle) and a calibration target. The imaging mission for acquisition of hyperspectral data for STUDY 4 took the longest (a period from 13:30 to 16:30 pm solar time) and with the highest spectral detail. In effect, major radiometric corrections were needed. The corrections were performed in the RadCorr software by converting spectral radiances to physical radiance units based on calibration parameters from the CzechGlobe spectroscopic laboratory (if interested in details of the method, see more in Hanuš et al., 2016).

When considering a longer time frame, season and phenological stages play a major role for classification and hence, a proper timing is crucial for acquisition of the best possible accuracy (Müllerová et al., 2017; Weil et al., 2017). Timing

of data acquisition in view of the season and phenological stage was crucial for all our case studies. In [STUDY 1](#), the timing in relation to the leaf on/off period was crucial for proper detection of ground in a forest environment. In [STUDY 2 and 3](#), we waited for optimum circumstances in the phenological stage of full vegetation as recommended e.g. by [Sankey et al. \(2017a\)](#) or [Weil et al. \(2017\)](#). The data was acquired in late spring to early summer, which appeared to be the most suitable months for image acquisition under the conditions of the Czech Republic (temperate climate zone, Northern hemisphere). Hyperspectral and LiDAR datasets for [STUDY 4](#) were acquired for use in multiple studies (besides identification of water bodies detailed in [STUDY 4](#), it was also utilized for species distribution modelling). The latter was one of the reasons why the data were acquired in the phenological stage of full vegetation, which turned out to be problematic from the perspective of identification of water bodies (a problem with the littoral vegetation and high shadow-casting vegetation).

## Accuracy of vertical structure from remote sensing imagery

---

*Quantity does not mean quality – and even quality is not always vital.*

---

Image processing using image-matching algorithms (namely SfM and MVS algorithms) are based on combining a high number of images/photos and allow a 3D reconstruction of observed objects even if low (consumer) quality data are used ([Micheletti et al., 2015](#)). The quantity of observed data is however not the only parameter for obtaining reliable results. The quality of processed images plays a crucial role. Images from high quality metering cameras with calibrated lens and high resolution sensor come with lower distortion and higher resolution. As can be expected, they provide better results than low-end consumer grade cameras in the sense of the accuracy of photogrammetry processing and of results of 3D object reconstruction ([Chiabrando et al., 2013](#); [Micheletti et al., 2015](#); [Peipe, 1997](#)). Other crucial factors for obtaining high-quality, accurate and relevant results of 3D terrain reconstruction from airborne imagery include correct settings

of flight parameters and the possibility to customize camera settings suitable for the flight parameters and lighting conditions.

In the [STUDY 1](#), we compared the suitability of two UAV platforms (a commercial eBee system and a home assembled Easystar II motor glider) for mapping of undulated terrain of a post-mining site (spoil heap) during a leaf-off period. Accuracy of the 3D reconstruction (3D point cloud) was evaluated in two types of environment, namely forest and steppes. Easystar achieved better results than eBee in both point density and accuracy, which is most likely due to the use of a better camera and customizable camera/sensor settings. We also tested the impact of quantity/density of images from two mutually perpendicular flights. Combination of more images from mutually perpendicular flights improved the accuracy of the 3D point cloud but the point density remained practically unchanged. In both types of environments (open steppes and forest canopy under leaf-off conditions), both UAV platforms managed to identify the terrain with a better accuracy than that of a nationwide LiDAR-derived DTM. Hence, we can report that photogrammetric methods (namely a combination of fine scale images and SfM approach) can be successfully used both in steppes and deciduous forest stands under leaf-off conditions to generate accurate DTM.

We have to add a few notes to the conclusions of the [STUDY 1](#): (i) in comparison to 2017, the market development led to a significant improvement of the quality of commercially available cameras both from the perspective of the optical quality and from the actual sensor (signal receptor). Nowadays, ready-to-use UAVs with sensors of comparable if not better quality than those that can be mounted on a home-assembled kit are commercially available. The study was however not intended as a criticism of one or the other platform as (ii) the aim was to compare overall performance (i.e. drone + camera) of a commercially available ready-to-use platform with a cheap customizable home-assembled kit. On the other hand, suitability of particular cameras and the automated vs manual setting of parameters was not directly evaluated, although the results suggested that the automatic balancing of the aperture, shutter speed and camera/sensor sensitivity to light (ISO) in the eBee platform (the only option in the camera originally supplied with the eBee UAV) might have been one of the sources of the poorer performance of that platform; (iii) LiDAR-derived DTM from manned aircraft that was used for result comparison in the [STUDY 1](#) was a nationwide model covering the entire area of the Czech Republic, which affected its accuracy. However, this difference is a valuable illustration of the differences in usability of manned and unmanned aircraft in RS (the spatial extent vs detail, accuracy and

resolution) and confirms that on a small scale, UAVs can substitute or even outperform manned aircraft platform.

3D reconstructions using SfM algorithm are generally considered to be less accurate than those based on LiDAR data if both are performed for similar spatial extent and spatial resolution (Dandois and Ellis, 2013; Fonstad et al., 2013; Niethammer et al., 2012; Sankey et al., 2017a). Where the goal is topographic mapping in complicated conditions (such as post-mining areas), choosing the best available solution providing as accurate products as possible is crucial. On the other hand, on the application level (such as classification), even data with relatively lower positional accuracy may play a crucial role and provide a vital information for identification of a particular class (e.g. vertical structure derived from SfM used in STUDY 3 vs. LiDAR vertical information used in Sankey et al., 2017a). The same can be said about data with relatively lower spatial resolution that however contained additional spectral information (e.g. RGB sensor vs multispectral sensor in STUDY 2). This idea was also well documented by Dalponte et al. (2012) who compared the results of classification based on hyperspectral vs multispectral data combined with LiDAR information of low vs high density and demonstrated that data with better spectral resolution provide better classification results. They however noted that from the perspective of the spectral resolution, the information crucial for the classification success was contained in the red-edge band, which was missing in multispectral datasets. We can therefore only speculate about results that would be obtained using a multispectral sensor (i.e. with relatively lower number of bands) that would cover the red edge as the problem may be indeed on the qualitative (suitable wavelengths) than quantitative (number of bands) side. Besides, both low and high density LiDAR point clouds improved the classification performances.

As indicated by results of STUDY 2 and 3, vertical information obtained by SfM can represent a viable alternative to the use of LiDAR-based models for fusion with multispectral data (and thus for improvement of classification of multispectral-based models). The vertical data used in STUDY 2 were obtained using eBee system by SenseFly, i.e. the UAV platform that yielded poorer results in STUDY 1 from the perspective of the 3D terrain structure. In STUDY 3, a single sensor was used for acquisition of multispectral data as well as of the vertical information (namely a multispectral sensor Tetracam Micro-MCA6). The proof that obtaining both information from a single flight with one sensor (i.e. there is no need of multiple flight missions or for dealing with data misalignment as discussed in detail above) is a significant achievement improving practical applicability of the use of multispectral sensors. The used camera

Tetracam Micro-MCA6 is optimized for high spectral resolution (six calibrated, relatively narrow, bands from 380 to 900 nm) but from the perspective of image quality, this camera is far from perfect (for example, the small size of the chip/sensor leads to a relatively high level of noise, which must be prevented by use of slower shutter speed or automatic exposure control).

In a study with a similar number and type of classes as well as with a classification approach similar to that we used in [STUDY 3](#), [Sankey et al. \(2017a\)](#) combined UAV-borne hyperspectral data and LiDAR derived vertical information. A closer comparison of the studies reveals that both producer's and user's accuracies were (as expected) higher when using the hyperspectral than multispectral sensor. After supplementing the spectral information with the vertical, however, the differences in results are much smaller. It is also necessary to point out that so far, a combination of multispectral data and LiDAR has not been tested yet for mapping in detail comparable to [STUDY 2 and 3](#). We therefore can not exclude the possibility that a combination of multispectral data with LiDAR could lead to even better results than our combination of multispectral and SfM data. This, however, should be an object of further studies, along with a practical question if such a possible improvement of vegetation classification is of a degree justifying the substantial difference in costs of obtaining SfM and LiDAR information, especially in the field of ecological research.

## Conclusions

This thesis shows several novel approaches for acquisition, processing and integration of RS products in environmental mapping. We are presenting new possibilities to obtain and describe detailed vertical/horizontal composition and structure of biotopes. We show that photogrammetric methods (namely a combination of UAV-acquired fine scale images and SfM approach) can be used successfully in steppes and deciduous forest stands under leaf-off conditions to generate accurate DTMs. Moreover, based on a comparison of suitability of two UAV platforms, we can conclude that a better point density and vertical accuracy was obtained with the better camera and customizable camera/sensor settings rather than with the use of a seemingly “more professional” carrier without the possibility of customized camera settings. Finally, we show that combining a greater number of images from mutually perpendicular flights increased the accuracy of the 3D point cloud but failed to increase point density.

We have successfully integrated remotely sensed high resolution datasets for classification of vegetation at the level of individual species/genera. Fusion of UAV-acquired spectral data and additional derived vertical information significantly improved both user’s and producer’s accuracies. We newly use the fusion of spectral and vertical information acquired during a single flight mission from a single multispectral UAV sensor, indicating that it is possible to acquire high quality results for shrubland vegetation even without high investments in LiDAR sensor and without the need of several flight missions. We also extracted open surface water bodies in post mining areas using integration of hyperspectral data and LiDAR variables from manned aircraft. Our results show that the integrated approach provides better results than separate use of the datasets and significantly increases both user’s and producer’s accuracies. Furthermore, integration of LiDAR variables successfully eliminated problems with shadows that affected all other approaches based on multispectral data only.

Moreover, results of the presented thesis improve the knowledge about crucial factors for obtaining suitable environmental mapping results in terms of: (i) the date and time of data acquisition; (ii) selection of a suitable sensor; (iii) use of suitable processing methods; (iv) use of a robust and transparent accuracy assessment.

(i) The date and time of data acquisition played a crucial role in obtaining suitable results in all studies. Seasonality (leaf-off period) was the principal prerequisite for being able to identify ground points under the forest canopy. In view of the

phenological stages of classified vegetation categories timing of data acquisition is a crucial step towards obtaining maximum spectral diversity of the classified species. Besides, the effect of shadows was partially eliminated by performing the mission during the solar midday. On the other hand, the acquisition timing could not solve problems with misclassification of water and shadow, which represents a typical example of limitations of airborne RS.

(ii) The sensor quality has a crucial influence on the quality of the resulting RS products (namely on the density and accuracy of 3D point clouds obtained by SfM processing of UAV images). Besides, our results also demonstrate the trade-off between spatial extent and spatial accuracy for DEMs when comparing the use of manned and unmanned aircraft for data acquisition. From the classification point of view, improving resolution is not a sufficient surrogate for spectral information, i.e. an RGB sensor with a better spatial resolution cannot fully substitute additional spectral information acquired using multispectral sensors or thermal data.

(iii) The differences in results obtained through various classification methods demonstrate a strong dependency of the quality of results on the used classification approach. Moreover, preliminary testing clearly showed that pixel-based classification approaches are unsuitable for classification based on integration/fusion of very high resolution data as well as for combining misaligned datasets. For this reason, all studies in this thesis that were focused on fusion classification used object based approach, the use of which facilitated the fusion of datasets and helped overcome the problems associated with misalignment and high resolution.

(iv) From the perspective of accuracy evaluation, all studies adhered to the good practice for accuracy assessment based on a transparent sampling design. To provide data evaluation metrics allowing direct comparison of the classification success with other studies, standard metrics have been used (i.e. overall, user's and producer's accuracy in case of thematic mapping/classification and RMSE in case of DTM, respectively). Moreover, studies investigating vegetation classification represent two possible directions for generalization of the results (namely repeated calibration/validation approach and use of confidence intervals). In addition, besides data evaluation metrics allowing direct comparison of the results with other studies, we showed accuracy validated per features of distinguished classes, which is a crucial parameter from the perspective of biotope mapping allowing a better relative comparison of methods.

## Further research

One of the possible directions of future research is pushing the limits of RS datasets processing. As mentioned in [STUDY 4](#), results of LiDAR and hyperspectral data integration indicated a potential to recognize water surface even where water bodies are partly covered by vegetation, namely in littoral zones. We can therefore assume that such data fusion could improve detection of water bodies even under other types of vegetation canopy (e.g. high trees). [Kükenbrink et al. \(2017\)](#) presented an approach for mapping and quantification of volume inside a forest canopy using airborne laser scanning. A suitably and correctly classified LiDAR point cloud can therefore be instrumental both in characterizing vertical structure of the vegetation and for filtering the vegetation points out. As also mentioned in [STUDY 4](#), open water absorbs energy on the wavelength commonly used by terrestrial LiDAR (1064 nm). In LiDAR point clouds, water bodies are therefore represented as empty areas without any returns or returns with a character of specific “noise”. These properties, combined with specific shape characteristics of water bodies, could be possibly used in object based classification for identification of water bodies under canopy cover. To further test this hypothesis, however, additional field work is required. Theoretically, we could use data from previous studies ([Doležalová et al., 2012](#)) that are available to us, however those data were gathered with consumer-grade GNSS receivers and therefore are not positionally accurate enough for testing this hypothesis (e.g. [Tomašík et al., 2017](#)).

Case studies indicating new options of RS-based environmental mapping are typically performed with a limited spatial extent and thematic detail. Although we may extrapolate from such results, it is not possible to draw conclusions from such studies and apply them universally to all situations that may occur in practice. For example, we report in [STUDY 1](#) that photogrammetric methods can be used successfully in steppes and deciduous forest stands under leaf-off conditions to generate accurate DTMs. Further research is however needed to quantitatively assess the quality of DTM acquired under leaf-off conditions in deciduous forest stands of various types and characteristics (e.g. tree species, structural, and site characteristics). The specific study area used in the [STUDY 2](#) provides a unique opportunity for testing fusion classification approaches on data that can be surveyed during a single UAV mission as it contains multiple cultivars and species in such a small area. However, the unnatural character of the study area can potentially affect the result of classification. It can be therefore assumed that in a more natural environment with a smaller number of species, it is possible to



achieve even better results and accuracies. However, further studies are needed to verify these hypotheses.

In [STUDY 3](#), we identified and described in detail the contribution of adding the vertical information obtained by SfM processing of UAVs images to multispectral data. Comparison of our results with those of studies utilizing significantly more expensive technologies that are also more demanding from the processing perspective (namely a hyperspectral camera and a LiDAR sensor mounted on UAV; [Sankey et al., 2017a](#)), we can see that the classification accuracy based solely on multispectral sensor was poorer than that acquired by hyperspectral sensor. However, after integration of the spectral information with vertical, the accuracy of our significantly cheaper solution is similar/comparable to that reported by [Sankey et al. \(2017a\)](#). It is true that we cannot exclude the possibility that combining our multispectral data with LiDAR instead of SfM data would lead to a further classification improvement. This, however, should be an object of further studies, along with a practical question if such a possible improvement of vegetation classification is of a degree justifying the substantial difference in costs of obtaining SfM and LiDAR information, especially in the field of ecological research.

A repeated calibration/validation approach used in the [STUDY 3](#) allowed us to evaluate of the dependency of classification results on the distribution of the true data samples. This dependency turned out to be quite strong; integration of additional vertical information however reduced that dependency. As classification results are generally more or less dependent on the spatial distribution of true data samples ([Foody and Mathur, 2004](#)), we conclude that the dependency of the classification results on the distribution of true data samples should be always reported in similar studies as an additional measure of robustness of the used approach.



## References

- Addink, E.A., deJong, S.M., Pebesma, E.J., 2007. The importance of scale in object oriented mapping of vegetation parameters with hyperspectral imagery. *Photogramm. Eng. Remote Sensing* 73, 905–912.
- Ahmed, O.S., Shemrock, A., Chabot, D., Dillon, C., Williams, G., Wasson, R., Franklin, S.E., 2017. Hierarchical land cover and vegetation classification using multispectral data acquired from an unmanned aerial vehicle. *Int. J. Remote Sens.* 38, 2037–2052. <https://doi.org/10.1080/01431161.2017.1294781>
- Ali, S.S., Dare, P., Jones, S.D., 2004. Fusion of Remotely Sensed Multispectral Imagery and Lidar Data for Forest Structure Assessment At the Tree Level. *Int. Arch. Photogramm. Remote Sens. Spat. Inf. Sci.* XXXVII, 1089–1094.
- Alonzo, M., Bookhagen, B., Roberts, D.A., 2014. Urban tree species mapping using hyperspectral and lidar data fusion. *Remote Sens. Environ.* 148, 70–83. <https://doi.org/10.1016/j.rse.2014.03.018>
- An, K., Zhang, J., Xiao, Y., 2007. Object-oriented urban dynamic monitoring — A case study of Haidian District of Beijing. *Chinese Geogr. Sci.* 17, 236–242. <https://doi.org/10.1007/s11769-007-0236-1>
- Anderson, K., Gaston, K.J., 2013. Lightweight unmanned aerial vehicles will revolutionize spatial ecology. *Front. Ecol. Environ.* 11, 138–146. <https://doi.org/10.1890/120150>
- Antonarakis, S., Richards, K. S., Brasington, J., 2008. Object-based land cover classification using airborne LiDAR. *Remote Sens. Environ.* 112, 2988–2998. <https://doi.org/http://dx.doi.org/10.1016/j.rse.2008.02.004>
- Asner, G.P., Asner, G.P., Knapp, D.E., Kennedy-Bowdoin, T., Jones, M.O., Martin, R.E., Boardman, J.W., Field, C.B., 2007. Carnegie Airborne Observatory: in-flight fusion of hyperspectral imaging and waveform light detection and ranging for three-dimensional studies of ecosystems. *J. Appl. Remote Sens.* 1, 013536. <https://doi.org/10.1117/1.2794018>
- Asner, G.P., Knapp, D.E., Boardman, J., Green, R.O., Kennedy-bowdoin, T., Eastwood, M., Martin, R.E., Anderson, C., Field, C.B., 2012. Carnegie Airborne Observatory-2 : Increasing science data dimensionality via high- fidelity multi-sensor fusion. *Remote Sens. Environ.* 124, 454–465. <https://doi.org/10.1016/j.rse.2012.06.012>
- Asner, G.P., Martin, R.E., Anderson, C.B., Knapp, D.E., 2015. Remote Sensing of Environment Quantifying forest canopy traits : Imaging spectroscopy versus field survey. *Remote Sens. Environ.* 158, 15–27. <https://doi.org/10.1016/j.rse.2014.11.011>
- Baluja, J., Diago, M.P., Balda, P., Zorer, R., Meggio, F., Morales, F., Tardaguila, J., 2012. Assessment of vineyard water status variability by thermal and multispectral imagery using an unmanned aerial vehicle (UAV). *Irrig. Sci.* 30, 511–522.

- Bazzichetto, M., Malavasi, M., Barták, V., Acosta, A.T.R., Moudrý, V., Carranza, M.L., 2018. Modeling plant invasion on Mediterranean coastal landscapes: An integrative approach using remotely sensed data. *Landsc. Urban Plan.* 171, 98–106.
- Berni, J.A.J., Zarco-Tejada, P.J., Suárez, L., González-Dugo, V., Fereres, E., 2009. Remote sensing of vegetation from UAV platforms using lightweight multispectral and thermal imaging sensors. *Int. Arch. Photogramm. Remote Sens. Spat. Inform. Sci* 38, 6.
- Blanco, P.D., Colditz, R.R., Saldaña, G.L., Hardtke, L.A., Llamas, R.M., Mari, N.A., Fischer, A., Caride, C., Aceñolaza, P.G., del Valle, H.F., 2013. A land cover map of Latin America and the Caribbean in the framework of the SERENA project. *Remote Sens. Environ.* 132, 13–31.
- Blaschke, T., 2010. Object based image analysis for remote sensing. *ISPRS J. Photogramm. Remote Sens.* 65, 2–16. <https://doi.org/10.1016/j.isprsjprs.2009.06.004>
- Blaschke, T., Hay, G.J., 2001. Object-oriented image analysis and scale-space: theory and methods for modeling and evaluating multiscale landscape structure. *Int. Arch. Photogramm. Remote Sens.* 34, 22–29.
- Blaschke, T., Hay, G.J., Kelly, M., Lang, S., Hofmann, P., Addink, E., Queiroz Feitosa, R., van der Meer, F., van der Werff, H., van Coillie, F., Tiede, D., 2014. Geographic Object-Based Image Analysis - Towards a new paradigm. *ISPRS J. Photogramm. Remote Sens.* 87, 180–191. <https://doi.org/10.1016/j.isprsjprs.2013.09.014>
- Blaschke, T., Lang, S., Hay, G., 2008. *Object-Based Image Analysis*. Springer.
- Blistan, P., Kovanič, L., Zelizňaková, V., Palková, J., 2016. Using UAV photogrammetry to document rock outcrops. *Acta Montan. Slovaca* 21.
- Bodlák, L., Křováková, K., Nedbal, V., Pechar, L., 2012. Assessment of landscape functionality changes as one aspect of reclamation quality—the case of Velká podkrušnohorská dump, Czech Republic. *Ecol. Eng.* 43, 19–25.
- Boon, M.A., Drijfhout, A.P., Tesfamichael, S., 2017. Comparison of a Fixed-Wing and Multi-Rotor Uav for Environmental Mapping Applications: A Case Study. *Int. Arch. Photogramm. Remote Sens. Spat. Inf. Sci.* 42, 47.
- Bork, E.W., Su, J.G., 2007. Integrating LIDAR data and multispectral imagery for enhanced classification of rangeland vegetation: A meta analysis. *Remote Sens. Environ.* 111, 11–24. <https://doi.org/10.1016/j.rse.2007.03.011>
- Brazdil, K., 2012. Technical Report DTM5G. Zeměměřický úřad a Vojen. Geogr. a hydrometeorologický úřad.
- Brennan, R., Webster, T.L., 2006. Object-oriented land cover classification of lidar-derived surfaces 32, 162–172.
- Calderón, R., Navas-Cortés, J.A., Lucena, C., Zarco-Tejada, P.J., 2013. High-resolution airborne hyperspectral and thermal imagery for early detection of *Verticillium* wilt of olive using fluorescence, temperature and narrow-band spectral indices. *Remote Sens. Environ.* 139, 231–245.

- Carroll, M.L., Townshend, J.R., Dimiceli, C.M., Noojipady, P., Sohlberg, R.A., Townshend, J.R., Dimiceli, C.M., Noojipady, P., Sohlberg, R.A., 2009. A new global raster water mask at 250 m resolution. <https://doi.org/10.1080/17538940902951401>
- Chavez, P.S., 1996. Image-based atmospheric corrections-revisited and improved. *Photogramm. Eng. Remote Sensing* 62, 1025–1035.
- Chen, Q., Zhang, Y., Ekroos, A., Hallikainen, M., 2004. The role of remote sensing technology in the EU water framework directive ( WFD ) 7, 267–276. <https://doi.org/10.1016/j.envsci.2004.05.002>
- Chiabrando, F., Lingua, A., Piras, M., 2013. Direct photogrammetry using UAV: tests and first results. *Int. Arch. Photogramm. Remote Sens. Spat. Inf. Sci* 1, 81–86.
- Chignell, S.M., Luizza, M.W., Skach, S., Young, N.E., Evangelista, P.H., 2018. An integrative modeling approach to mapping wetlands and riparian areas in a heterogeneous Rocky Mountain watershed. *Remote Sens. Ecol. Conserv.* 4, 150–165.
- Chrétien, L.P., Théau, J., Ménard, P., 2016. Visible and thermal infrared remote sensing for the detection of white-tailed deer using an unmanned aerial system. *Wildl. Soc. Bull.* 40, 181–191. <https://doi.org/10.1002/wsb.629>
- Clapuyt, F., Vanacker, V., Van Oost, K., 2016. Reproducibility of UAV-based earth topography reconstructions based on Structure-from-Motion algorithms. *Geomorphology* 260, 4–15.
- Clinton, N., Holt, A., Scarborough, J., Yan, L., Gong, P., 2010. Accuracy Assessment Measures for Object-based Image Segmentation Goodness. *Photogramm. Eng. Remote Sens.* 76, 289–299. <https://doi.org/10.14358/PERS.76.3.289>
- Cochran, G.W., 1977. *Sampling Techniques*. Wiley.
- Colomina, I., Molina, P., 2014. Unmanned aerial systems for photogrammetry and remote sensing: A review. *ISPRS J. Photogramm. Remote Sens.* 92, 79–97. <https://doi.org/10.1016/j.isprsjprs.2014.02.013>
- Congalton, R., Gu, J., Yadav, K., Thenkabail, P., Ozdogan, M., 2014. Global land cover mapping: A review and uncertainty analysis. *Remote Sens.* 6, 12070–12093.
- Congalton, R.G., Green, K., 2002. *Assessing the accuracy of remotely sensed data: principles and practices*. CRC press.
- Cordell, S., Questad, E.J., Asner, G.P., Kinney, K.M., Thaxton, J.M., Uowolo, A., Brooks, S., Chynoweth, M.W., 2017. Remote sensing for restoration planning : how the big picture can inform stakeholders. *Restor. Ecol.* 25, 147–154. <https://doi.org/10.1111/rec.12448>
- Cunliffe, A.M., Brazier, R.E., Anderson, K., 2016. Ultra-fine grain landscape-scale quantification of dryland vegetation structure with drone-acquired structure-from-motion photogrammetry. *Remote Sens. Environ.* 183, 129–143. <https://doi.org/10.1016/j.rse.2016.05.019>

- Dai, X., Khorram, S., 1998. The effects of image misregistration on the accuracy of remotely sensed change detection. *IEEE Trans. Geosci. Remote Sens.* 36, 1566–1577.
- Dalponte, M., Bruzzone, L., Gianelle, D., 2012. Tree species classification in the Southern Alps based on the fusion of very high geometrical resolution multispectral / hyperspectral images and LiDAR data. *Remote Sens. Environ.* 123, 258–270. <https://doi.org/10.1016/j.rse.2012.03.013>
- Dandois, J., Olano, M., Ellis, E., 2015. Optimal altitude, overlap, and weather conditions for computer vision UAV estimates of forest structure. *Remote Sens.* 7, 13895–13920.
- Dandois, J.P., Ellis, E.C., 2013. High spatial resolution three-dimensional mapping of vegetation spectral dynamics using computer vision. *Remote Sens. Environ.* <https://doi.org/10.1016/j.rse.2013.04.005>
- Degerickx, J., Roberts, D.A., Somers, B., 2019. Enhancing the performance of Multiple Endmember Spectral Mixture Analysis (MESMA) for urban land cover mapping using airborne lidar data and band selection. *Remote Sens. Environ.* 221, 260–273. <https://doi.org/10.1016/j.rse.2018.11.026>
- DeWitt, J.D., Warner, T.A., Chirico, P.G., Bergstresser, S.E., 2017. Creating high-resolution bare-earth digital elevation models (DEMs) from stereo imagery in an area of densely vegetated deciduous forest using combinations of procedures designed for lidar point cloud filtering. *GIScience Remote Sens.* 54, 552–572.
- Díaz-Varela, R.A., Calvo Iglesias, S., Cillero Castro, C., Díaz Varela, E.R., 2018. Sub-metric analysis of vegetation structure in bog-heathland mosaics using very high resolution rpas imagery. *Ecol. Indic.* 89, 861–873. <https://doi.org/10.1016/j.ecolind.2017.11.068>
- Díaz-Varela, R.A., de la Rosa, R., León, L., Zarco-Tejada, P.J., 2015. High-resolution airborne UAV imagery to assess olive tree crown parameters using 3D photo reconstruction: Application in breeding trials. *Remote Sens.* 7, 4213–4232. <https://doi.org/10.3390/rs70404213>
- Díaz-Varela, R.A., Zarco-Tejada, P.J., Angileri, V., Loudjani, P., 2014. Automatic identification of agricultural terraces through object-oriented analysis of very high resolution DSMs and multispectral imagery obtained from an unmanned aerial vehicle. *J. Environ. Manage.* 134, 117–126. <https://doi.org/10.1016/j.jenvman.2014.01.006>
- Dingirard, M., Slater, P.N., 1999. Calibration of space-multispectral imaging sensors: A review. *Remote Sens. Environ.* 68, 194–205.
- Doležalová, J., Vojar, J., Smolová, D., Solský, M., Kopecký, O., 2012. Technical reclamation and spontaneous succession produce different water habitats: A case study from Czech post-mining sites. *Ecol. Eng.* 43, 5–12. <https://doi.org/10.1016/j.ecoleng.2011.11.017>
- Drăguț, L., Csillik, O., Eisank, C., Tiede, D., 2014. Automated parameterisation for multi-scale image segmentation on multiple layers. *ISPRS J. Photogramm. Remote Sens.* 88, 119–127. <https://doi.org/10.1016/j.isprsjprs.2013.11.018>

- Drăguț, L., Tiede, D., Levick, S.R., 2010. ESP: A tool to estimate scale parameter for multiresolution image segmentation of remotely sensed data. *Int. J. Geogr. Inf. Sci.* 24, 859–871. <https://doi.org/10.1080/13658810903174803>
- Dronova, I., Gong, P., Wang, L., Zhong, L., 2015. Mapping dynamic cover types in a large seasonally flooded wetland using extended principal component analysis and object-based classification. *Remote Sens. Environ.* 158, 193–206. <https://doi.org/10.1016/j.rse.2014.10.027>
- Feng, Q., Liu, J., Gong, J., 2015. UAV Remote sensing for urban vegetation mapping using random forest and texture analysis. *Remote Sens.* 7, 1074–1094. <https://doi.org/10.3390/rs70101074>
- Fensholt, R., Anyamba, A., Huber, S., Proud, S.R., Tucker, C.J., Small, J., Pak, E., Rasmussen, M.O., Sandholt, I., Shisanya, C., 2011. Analysing the advantages of high temporal resolution geostationary MSG SEVIRI data compared to Polar Operational Environmental Satellite data for land surface monitoring in Africa. *Int. J. Appl. Earth Obs. Geoinf.* 13, 721–729.
- Feyisa, G.L., Meilby, H., Fensholt, R., Proud, S.R., 2014. Automated Water Extraction Index: A new technique for surface water mapping using Landsat imagery. *Remote Sens. Environ.* 140, 23–35. <https://doi.org/10.1016/j.rse.2013.08.029>
- Fisher, J.R.B., Acosta, E.A., Dennedy-Frank, P.J., Kroeger, T., Boucher, T.M., 2018. Impact of satellite imagery spatial resolution on land use classification accuracy and modeled water quality. *Remote Sens. Ecol. Conserv.* 4, 137–149.
- Fogl, M., Moudrý, V., 2016. Influence of vegetation canopies on solar potential in urban environments. *Appl. Geogr.* 66, 73–80.
- Fonstad, M.A., Dietrich, J.T., Courville, B.C., Jensen, J.L., Carbonneau, P.E., 2013. Topographic structure from motion: A new development in photogrammetric measurement. *Earth Surf. Process. Landforms* 38, 421–430. <https://doi.org/10.1002/esp.3366>
- Foody, G.M., 2009a. Correcting estimates of land cover change and change detection accuracy for error in ground reference data, in: 2009 IEEE International Geoscience and Remote Sensing Symposium. IEEE, p. IV-153.
- Foody, G.M., 2009b. The impact of imperfect ground reference data on the accuracy of land cover change estimation. *Int. J. Remote Sens.* 30, 3275–3281.
- Foody, G.M., 2004. Thematic map comparison. *Photogramm. Eng. Remote Sens.* 70, 627–633.
- Foody, G.M., 2002. Status of land cover classification accuracy assessment. *Remote Sens. Environ.* 80, 185–201.
- Foody, G.M., Boyd, D.S., 2013. Using Volunteered Data in Land Cover Map Validation: Mapping West African Forests. *IEEE J. Sel. Top. Appl. Earth Obs. Remote Sens.* 6, 1305–1312. <https://doi.org/10.1109/JSTARS.2013.2250257>
- Foody, G.M., Mathur, A., 2004. Toward intelligent training of supervised image classifications: directing training data acquisition for SVM classification 93, 107–117. <https://doi.org/10.1016/j.rse.2004.06.017>

- Fraser, C.S., 2013. Automatic camera calibration in close range photogrammetry. *Photogramm. Eng. Remote Sens.* 79, 381–388.
- Frašťia, M., Marčíš, M., Kopecký, M., Liščák, P., Žilka, A., 2014. Complex geodetic and photogrammetric monitoring of the Kral'ovany rock slide. *J. Sustain. Min.* 13, 12–16.
- Freeman, P., Balas, G.J., 2014. Actuation failure modes and effects analysis for a small UAV, in: 2014 American Control Conference. IEEE, pp. 1292–1297.
- Frouz, J., Mudrák, O., Reitschmiedová, E., Walmsley, A., Vachová, P., Šimáčková, H., Albrechtová, J., Moradi, J., Kučera, J., 2018. Rough wave-like heaped overburden promotes establishment of woody vegetation while leveling promotes grasses during unassisted post mining site development. *J. Environ. Manage.* 205, 50–58. <https://doi.org/10.1016/j.jenvman.2017.09.065>
- Gairola, S., Procheş, Ş., Rocchini, D., 2013. High-resolution satellite remote sensing: A new frontier for biodiversity exploration in Indian Himalayan forests. *Int. J. Remote Sens.* 34, 2006–2022. <https://doi.org/10.1080/01431161.2012.730161>
- Gehrke, S., Morin, K., Downey, M., Bohrer, N., Fuchs, T., 2008. Semi-global matching: an alternative to lidar for dsm generation? *Int. Arch. Photogramm. Remote Sens. Spat. Inf. Sci.* XXXVIII-B1, 1–6.
- Geneto, J.A.S., Haerte, V., 1995. Adaptive low-pass fuzzy filter for noise removal. *Photogramm. Eng. Remote Sensing* 61, 1267–1272.
- Ghamisi, P., Member, S., Rasti, B., Yokoya, N., Wang, Q., Bernhard, H., Bruzzone, L., Bovolo, F., Member, S., Chi, M., Member, S., Anders, K., Gloaguen, R., Atkinson, P.M., 2018. Multisource and Multitemporal Data Fusion in Remote Sensing 1–26.
- Giam, X., Olden, J.D., Simberloff, D., 2018. Impact of coal mining on stream biodiversity in the US and its regulatory implications. *Nat. Sustain.* 1, 176–183. <https://doi.org/10.1038/s41893-018-0048-6>
- Giardino, C., Brando, V.E., Dekker, A.G., Strömbeck, N., Candiani, G., 2007. Assessment of water quality in Lake Garda ( Italy ) using Hyperion. *Remote Sens. Environ.* 109, 183–195. <https://doi.org/10.1016/j.rse.2006.12.017>
- Gilvear, D., Tyler, A., Davids, C., 2004. Detection of estuarine and tidal river hydromorphology using hyper-spectral and LiDAR data : Forth estuary , Scotland 61, 379–392. <https://doi.org/10.1016/j.ecss.2004.06.007>
- Gini, R., Passoni, D., Pinto, L., Sona, G., 2014. Use of unmanned aerial systems for multispectral survey and tree classification: A test in a park area of northern Italy. *Eur. J. Remote Sens.* 47, 251–269. <https://doi.org/10.5721/EuJRS20144716>
- Gomasca, M.A., 2009. Basics of geomatics. Springer Science & Business Media.
- Gu, J., Congalton, R.G., Pan, Y., 2015. The Impact of Positional Errors on Soft Classification Accuracy Assessment: A Simulation Analysis. *Remote Sens.* 579–599. <https://doi.org/10.3390/rs70100579>
- Hanuš, J., Fabiáne, T.K., Fajmon, L., 2016. Potential of airborne imaging spectroscopy at czechglobe. *Int. Arch. Photogramm. Remote Sens. Spat. Inf. Sci.* XLI, 15–17. <https://doi.org/10.5194/isprsarchives-XLI-B1-15-2016>



- Harabiš, F., Tichanek, F., Tropek, R., 2013. Dragonflies of freshwater pools in lignite spoil heaps: Restoration management, habitat structure and conservation value. *Ecol. Eng.* 55, 51–61. <https://doi.org/10.1016/j.ecoleng.2013.02.007>
- Harken, J., Sugumaran, R., 2014. Classification of Iowa wetlands using an airborne hyperspectral image : a comparison of the spectral angle mapper classifier and an object-oriented approach. *Can. J. Remote Sens.* 31, 167–174.
- Harrison, I., Abell, R., Darwall, W., Thieme, M.L., Tickner, D., Timboe, I., 2018. The freshwater biodiversity crisis. *Science* (80-. ). 362, 1369.1-1369. <https://doi.org/10.1126/science.aav9242>
- Hartfield, K.A., Landau, K.I., van Leeuwen, W.J.D., 2011. Fusion of high resolution aerial multispectral and lidar data: Land cover in the context of urban mosquito habitat. *Remote Sens.* 3, 2364–2383. <https://doi.org/10.3390/rs3112364>
- Harwin, S., Lucieer, A., Osborn, J., 2015. The impact of the calibration method on the accuracy of point clouds derived using unmanned aerial vehicle multi-view stereopsis. *Remote Sens.* 7, 11933–11953.
- Hawryło, P., Tompalski, P., Wężyk, P., 2017. Area-based estimation of growing stock volume in Scots pine stands using ALS and airborne image-based point clouds. *For. An Int. J. For. Res.* 90, 686–696.
- He, L., Li, J., Plaza, A., Li, Y., 2016. Discriminative low-rank Gabor filtering for spectral-spatial hyperspectral image classification. *IEEE Trans. Geosci. Remote Sens.* 55, 1381–1395.
- He, X., Bai, Y., Pan, D., Huang, N., Dong, X., Chen, J., Chen, C.-T.A., Cui, Q., 2013. Using geostationary satellite ocean color data to map the diurnal dynamics of suspended particulate matter in coastal waters. *Remote Sens. Environ.* 133, 225–239.
- Hendrychová, M., Kabrna, M., 2016. An analysis of 200-year-long changes in a landscape affected by large-scale surface coal mining: History, present and future. *Appl. Geogr.* 74, 151–159. <https://doi.org/10.1016/j.apgeog.2016.07.009>
- Hodgson, M.E., Jensen, J., Raber, G., Tullis, J., Davis, B.A., Thompson, G., Schuckman, K., 2005. An evaluation of lidar-derived elevation and terrain slope in leaf-off conditions. *Photogramm. Eng. Remote Sens.* 71, 817–823.
- Holmgren, J., Persson, Å., Söderman, U., 2008. Species identification of individual trees by combining high resolution LiDAR data with multi-spectral images. *Int. J. Remote Sens.* 29, 1537–1552. <https://doi.org/10.1080/01431160701736471>
- Huang, X., Lu, Q., 2014. A novel relearning approach for remote sensing image classification post-processing, in: 2014 IEEE Geoscience and Remote Sensing Symposium. IEEE, pp. 3554–3557.
- Hubacek, M., Kovarik, V., Kratochvíl, V., 2016. Analysis of influence of terrain relief roughness on dem accuracy generated from lidar in the czech republic territory. *Int. Arch. Photogramm. Remote Sens. Spat. Inf. Sci.* 41.

- Husson, E., Reese, H., Ecke, F., 2017. Combining Spectral Data and a DSM from UAS-Images for Improved Classification of Non-Submerged Aquatic Vegetation. *Remote Sens.* 9, 247. <https://doi.org/10.3390/rs9030247>
- James, M.R., Robson, S., 2014. Mitigating systematic error in topographic models derived from UAV and ground-based image networks. *Earth Surf. Process. Landforms* 39, 1413–1420. <https://doi.org/10.1002/esp.3609>
- James, M.R., Robson, S., d'Oleire-Oltmanns, S., Niethammer, U., 2017. Optimising UAV topographic surveys processed with structure-from-motion: Ground control quality, quantity and bundle adjustment. *Geomorphology* 280, 51–66.
- Jensen, J., Mathews, A., 2016. Assessment of image-based point cloud products to generate a bare earth surface and estimate canopy heights in a woodland ecosystem. *Remote Sens.* 8, 50.
- Kalacska, M., Chmura, G.L., Lucanus, O., Bérubé, D., Arroyo-Mora, J.P., 2017. Structure from motion will revolutionize analyses of tidal wetland landscapes. *Remote Sens. Environ.* 199, 14–24. <https://doi.org/10.1016/j.rse.2017.06.023>
- Kaplan, G., Avdan, U., 2017. Object-based water body extraction model using Sentinel-2 satellite imagery. *Eur. J. Remote Sens.* 50. <https://doi.org/10.1080/22797254.2017.1297540>
- Klouček, T., Lagner, O., Šimová, P., 2015. How does data accuracy influence the reliability of digital viewshed models? A case study with wind turbines. *Appl. Geogr.* 64, 46–54. <https://doi.org/10.1016/J.APGEOG.2015.09.005>
- Koch, K.-R., 1999. Parameter estimation and hypothesis testing in linear models. Springer Science & Business Media.
- Komárek, J., Klouček, T., Prošek, J., 2018. The potential of Unmanned Aerial Systems: A tool towards precision classification of hard-to-distinguish vegetation types? *Int. J. Appl. Earth Obs. Geoinf.* 71, 9–19. <https://doi.org/10.1016/j.jag.2018.05.003>
- Koska, B., Jirka, V., Urban, R., Křemen, T., Hesslerová, P., Jon, J., Pospíšil, J., Fogl, M., 2017. Suitability, characteristics, and comparison of an airship UAV with lidar for middle size area mapping. *Int. J. Remote Sens.* 38, 2973–2990.
- Kršák, B., Blišťan, P., Pauliková, A., Puškárová, P., Kovanič, L., Palková, J., Zelizňaková, V., 2016. Use of low-cost UAV photogrammetry to analyze the accuracy of a digital elevation model in a case study. *Measurement* 91, 276–287.
- Kruse, F.A., Lefkoff, A.B., Boardman, J.B., Heidebrecht, K.B., Shapiro, A.T., Barloon, P.J., Goetz, A.F.H., 1993. The Spectral Image Processing System (SIPS) - Interactive Visualization and Analysis of Imaging spectrometer Data. *Remote Sens. Environ.* 44, 145–163.
- Kükenbrink, D., Schneider, F.D., Leiterer, R., Schaepman, M.E., Morsdorf, F., 2017. Quantification of hidden canopy volume of airborne laser scanning data using a voxel traversal algorithm. *Remote Sens. Environ.* 194, 424–436. <https://doi.org/10.1016/j.rse.2016.10.023>
- Kumhálová, J., Moudrý, V., 2014. Topographical characteristics for precision agriculture in conditions of the Czech Republic. *Appl. Geogr.* 50, 90–98.

- Kuria, D.N., Menz, G., Misana, S., Mwita, E., Thamm, H.-P., Alvarez, M., Mogha, N., Becker, M., Oyieke, H., 2014. Seasonal Vegetation Changes in the Malinda Wetland Using Bi-Temporal , Multi-Sensor , Very High Resolution Remote Sensing Data Sets. *Adv. Remote Sens.* 3, 33–48.  
<https://doi.org/10.4236/ars.2014.31004>
- Laba, M., Tsai, F., Ogurcak, D., Smith, S., Richmond, M.E., 2005. Field determination of optimal dates for the discrimination of invasive wetland plant species using derivative spectral analysis. *Photogramm. Eng. Remote Sensing* 71, 603–611.  
<https://doi.org/10.14358/PERS.71.5.603>
- Laberte, A.S., Goforth, M.A., Steele, C.M., Rango, A., 2011. Multispectral remote sensing from unmanned aircraft: Image processing workflows and applications for rangeland environments. *Remote Sens.* 3, 2529–2551.  
<https://doi.org/10.3390/rs3112529>
- Lillesand, T., Kiefer, R.W., Chipman, J., 2015. *Remote Sensing and Image Interpretation*. Wiley.
- Lisein, J., Michez, A., Claessens, H., Lejeune, P., 2015. Discrimination of deciduous tree species from time series of unmanned aerial system imagery. *PLoS One* 10, 1–20.  
<https://doi.org/10.1371/journal.pone.0141006>
- Liu, J., Li, P., Wang, X., 2015. A new segmentation method for very high resolution imagery using spectral and morphological information. *ISPRS J. Photogramm. Remote Sens.* 101, 145–162. <https://doi.org/10.1016/j.isprsjprs.2014.11.009>
- Liu, X., Hou, Z., Shi, Z., Bo, Y., Cheng, J., 2017. A shadow identification method using vegetation indices derived from hyperspectral data. *Int. J. Remote Sens.* 38, 5357–5373. <https://doi.org/10.1080/01431161.2017.1338785>
- Lu, B., He, Y., 2017. Species classification using Unmanned Aerial Vehicle (UAV)-acquired high spatial resolution imagery in a heterogeneous grassland.  
<https://doi.org/10.1016/j.isprsjprs.2017.03.011>
- Lu, D., Moran, E., Hetrick, S., 2011. Detection of impervious surface change with multitemporal Landsat images in an urban–rural frontier. *ISPRS J. Photogramm. Remote Sens.* 66, 298–306.
- Lu, D., Weng, Q., 2007. A survey of image classification methods and techniques for improving classification performance. *Int. J. Remote Sens.*  
<https://doi.org/10.1080/01431160600746456>
- Lu, S., Wu, B., Yan, N., Wang, H., 2011. Water body mapping method with HJ-1A/B satellite imagery. *Int. J. Appl. Earth Obs. Geoinf.* 13, 428–434.  
<https://doi.org/10.1016/j.jag.2010.09.006>
- Lucieer, A., Turner, D., King, D.H., Robinson, S.A., 2014. Using an Unmanned Aerial Vehicle (UAV) to capture micro-topography of Antarctic moss beds. *Int. J. Appl. Earth Obs. Geoinf.* 27, 53–62.
- Lunetta, R.S., Johnson, D.M., Lyon, J.G., Crotwell, J., 2004. Impacts of imagery temporal frequency on land-cover change detection monitoring 89, 444–454.  
<https://doi.org/10.1016/j.rse.2003.10.022>

- Lunetta, R.S., Knight, J.F., Ediriwickrema, J., Lyon, J.G., Worthy, L.D., 2006. Land-cover change detection using multi-temporal MODIS NDVI data 105, 142–154. <https://doi.org/10.1016/j.rse.2006.06.018>
- Luo, S., Wang, C., Xi, X., Zeng, H., Li, D., Xia, S., Wang, P., 2016. Fusion of Airborne Discrete-Return LiDAR and Hyperspectral Data for Land Cover Classification. *Remote Sens.* 8, 19. <https://doi.org/10.3390/rs8010003>
- Mahdianpari, M., Salehi, B., Mohammadimanesh, F., Motagh, M., 2017. Random forest wetland classification using ALOS-2 L-band , RADARSAT-2 C-band , and TerraSAR-X imagery. *ISPRS J. Photogramm. Remote Sens.* 130, 13–31. <https://doi.org/10.1016/j.isprsjprs.2017.05.010>
- Mairota, P., Cafarelli, B., Labadessa, R., Lovergine, F., Tarantino, C., Lucas, R.M., Nagendra, H., Didham, R.K., 2015. Very high resolution Earth observation features for monitoring plant and animal community structure across multiple spatial scales in protected areas. *Int. J. Appl. Earth Obs. Geoinf.* 37, 100–105. <https://doi.org/10.1016/j.jag.2014.09.015>
- Mancini, F., Dubbini, M., Gattelli, M., Stecchi, F., Fabbri, S., Gabbianelli, G., 2013. Using unmanned aerial vehicles (UAV) for high-resolution reconstruction of topography: The structure from motion approach on coastal environments. *Remote Sens.* 5, 6880–6898. <https://doi.org/10.3390/rs5126880>
- Manfreda, S., McCabe, M.F., Miller, P.E., Lucas, R., Madrigal, V.P., Mallinis, G., Dor, E. Ben, Helman, D., Estes, L., Ciraolo, G., Müllerová, J., Tauro, F., de Lima, M.I., de Lima, J.L.M.P., Maltese, A., Frances, F., Caylor, K., Kohv, M., Perks, M., Ruiz-Pérez, G., Su, Z., Vico, G., Toth, B., 2018. On the use of unmanned aerial systems for environmental monitoring. *Remote Sens.* 10. <https://doi.org/10.3390/rs10040641>
- Marris, E., 2013. Drones in science: Fly, and bring me data. *Nat. News* 498, 156.
- Matese, A., Toscano, P., Di Gennaro, S.F., Genesio, L., Vaccari, F.P., Primicerio, J., Belli, C., Zaldei, A., Bianconi, R., Gioli, B., 2015. Intercomparison of UAV, Aircraft and Satellite Remote Sensing Platforms for Precision Viticulture. *Remote Sens.* 2971–2990. <https://doi.org/10.3390/rs70302971>
- McFeeters, S.K., 1996. The use of the Normalized Difference Water Index (NDWI) in the delineation of open water features. *Int. J. Remote Sens.* 17, 1425–1432. <https://doi.org/10.1080/01431169608948714>
- McGlone, C., 2013. *Manual of photogrammetry*, 5th ed. American Society of Photogrammetry and Remote Sensing.
- Meng, X., Currit, N., Zhao, K., 2010. Ground filtering algorithms for airborne LiDAR data: A review of critical issues. *Remote Sens.* 2, 833–860.
- Micheletti, N., Chandler, J.H., Lane, S.N., 2015. Structure from motion (SFM) photogrammetry.
- Michez, A., Piégay, H., Lisein, J., Claessens, H., Lejeune, P., 2016. Classification of riparian forest species and health condition using multi-temporal and hyperspatial imagery from unmanned aerial system. *Environ. Monit. Assess.* 188, 1–19. <https://doi.org/10.1007/s10661-015-4996-2>

- Míkita, T., Klimánek, M., Cibulka, M., 2013. Evaluation of airborne laser scanning data for tree parameters and terrain modelling in forest environment. *Acta Univ. Agric. Silvic. Mendelianae Brun.* 61, 1339–1347.
- Milas, A.S., Arend, K., Mayer, C., Simonson, M.A., Mackey, S., 2017. Different colours of shadows: classification of UAV images. *Int. J. Remote Sens.* 38, 3084–3100.
- Moravec, D., Komárek, J., Kumhálová, J., Kroulík, M., Prošek, J., Klápště, P., 2017. Digital elevation models as predictors of yield: Comparison of an UAV and other elevation data sources. *Agron. Res.* 15, 249–255.
- Mostafa, Y., Abdelhafiz, A., 2017. Shadow Identification in High Resolution Satellite Images in the Presence of Water Regions 87–94. <https://doi.org/10.14358/PERS.83.2.87>
- Moudrý, V., Gdulová, K., Fogl, M., Klápště, P., Urban, R., Komárek, J., Moudrá, L., Štroner, M., Barták, V., Solský, M., 2019a. Comparison of leaf-off and leaf-on combined UAV imagery and airborne LiDAR for assessment of a post-mining site terrain and vegetation structure: Prospects for monitoring hazards and restoration success. *Appl. Geogr.* 104, 32–41. <https://doi.org/10.1016/j.apgeog.2019.02.002>
- Moudrý, V., Šímová, P., 2012. Influence of positional accuracy, sample size and scale on modelling species distributions: a review. *Int. J. Geogr. Inf. Sci.* 26, 2083–2095. <https://doi.org/10.1080/13658816.2012.721553>
- Moudrý, V., Urban, R., Štroner, M., Komárek, J., Brouček, J., Prošek, J., 2019b. Comparison of a commercial and home-assembled fixed-wing UAV for terrain mapping of a post-mining site under leaf-off conditions. *Int. J. Remote Sens.* 40, 555–572. <https://doi.org/10.1080/01431161.2018.1516311>
- Movia, A., Beinat, A., Crosilla, F., 2016. Shadow detection and removal in RGB VHR images for land use unsupervised classification. *ISPRS J. Photogramm. Remote Sens.* 119, 485–495. <https://doi.org/10.1016/j.isprsjprs.2016.05.004>
- Mueller, P.W., Hoffer, R.N., 1989. Low-pass spatial filtering of satellite radar data. *Photogramm. Eng. Remote Sensing* 55, 887–895.
- Müllerová, J., Brůna, J., Bartaloš, T., Dvořák, P., Vítková, M., Pyšek, P., 2017. Timing Is Important: Unmanned Aircraft vs. Satellite Imagery in Plant Invasion Monitoring. *Front. Plant Sci.* 8, 887. <https://doi.org/10.3389/fpls.2017.00887>
- Naidoo, L., Cho, M.A., Mathieu, R., Asner, G., 2012. Classification of savanna tree species, in the Greater Kruger National Park region, by integrating hyperspectral and LiDAR data in a Random Forest data mining environment. *ISPRS J. Photogramm. Remote Sens.* 69, 167–179. <https://doi.org/10.1016/j.isprsjprs.2012.03.005>
- Näsi, R., Honkavaara, E., Lyytikäinen-Saarenmaa, P., Blomqvist, M., Litkey, P., Hakala, T., Viljanen, N., Kantola, T., Tanhuanpää, T., Holopainen, M., 2015. Using UAV-Based Photogrammetry and Hyperspectral Imaging for Mapping Bark Beetle Damage at Tree-Level. *Remote Sens.* 7, 15467–15493. <https://doi.org/10.3390/rs71115467>

- Neininger, B.G., Hacker, J.M., 2012. Manned or unmanned - does this really matter? Manned or unmanned – does this really matter? *Int. Arch. Photogramm. Remote Sens. Spat. Inf. Sci.* <https://doi.org/10.5194/isprsarchives-XXXVIII-1-C22-223-2011>
- Nevalainen, O., Honkavaara, E., Tuominen, S., Viljanen, N., Hakala, T., Yu, X., Hyypä, J., Saari, H., Pölonen, I., Imai, N.N., Tommaselli, A.M.G., 2017. Individual tree detection and classification with UAV-Based photogrammetric point clouds and hyperspectral imaging. *Remote Sens.* 9. <https://doi.org/10.3390/rs9030185>
- Nex, F., Remondino, F., 2014. UAV for 3D mapping applications: a review. *Appl. Geomatics* 6, 1–15. <https://doi.org/10.1007/s12518-013-0120-x>
- Ni, W., Sun, G., Ranson, K.J., Pang, Y., Zhang, Z., Yao, W., 2015. Extraction of ground surface elevation from ZY-3 winter stereo imagery over deciduous forested areas. *Remote Sens. Environ.* 159, 194–202.
- Niethammer, U., James, M.R., Rothmund, S., Travelletti, J., Joswig, M., 2012. UAV-based remote sensing of the Super-Sauze landslide: Evaluation and results. *Eng. Geol.* 128, 2–11. <https://doi.org/10.1016/j.enggeo.2011.03.012>
- Nishar, A., Richards, S., Breen, D., Robertson, J., Breen, B., 2016. Thermal infrared imaging of geothermal environments and by an unmanned aerial vehicle (UAV): A case study of the Wairakei–Tauhara geothermal field, Taupo, New Zealand. *Renew. Energy* 86, 1256–1264.
- Okiemute, A., Ruth, A., 2017. Object-based habitat mapping using very high spatial resolution multispectral and hyperspectral imagery with LiDAR data. *Int. J. Appl. Earth Obs. Geoinf.* 59, 79–91. <https://doi.org/10.1016/j.jag.2017.03.007>
- Olmanson, L.G., Brezonik, P.L., Bauer, M.E., 2013. Airborne hyperspectral remote sensing to assess spatial distribution of water quality characteristics in large rivers: The Mississippi River and its tributaries in Minnesota. *Remote Sens. Environ.* 130, 254–265. <https://doi.org/10.1016/j.rse.2012.11.023>
- Olofsson, P., Foody, G.M., Herold, M., Stehman, S. V., Woodcock, C.E., Wulder, M.A., 2014. Good practices for estimating area and assessing accuracy of land change. *Remote Sens. Environ.* 148, 42–57. <https://doi.org/10.1016/J.RSE.2014.02.015>
- Oort, P.A.J. Van, 2007. Improving land cover change estimates by accounting for classification errors 1161. <https://doi.org/10.1080/01431160500057848>
- Osenberg, C.W., 2018. No clean coal for stream animals. *Nat. Sustain.* 1, 160–161. <https://doi.org/10.1038/s41893-018-0049-5>
- Pajares, G., 2015. Overview and current status of remote sensing applications based on unmanned aerial vehicles (UAVs). *Photogramm. Eng. Remote Sens.* 81, 281–330.
- Panchal, S., Thakker, R.A., 2017. Improved image pansharpener technique using nonsubsampling contourlet transform with sparse representation. *J. Indian Soc. Remote Sens.* 45, 385–394.
- Parmehr, E.G., Fraser, C.S., Zhang, C., Leach, J., 2014. Automatic registration of optical imagery with 3D LiDAR data using statistical similarity. *ISPRS J. Photogramm. Remote Sens.* 88, 28–40. <https://doi.org/10.1016/j.isprsjprs.2013.11.015>

- Paul, A., Tripathi, D., Dutta, D., 2018. Application and comparison of advanced supervised classifiers in extraction of water bodies from remote sensing images. *Sustain. Water Resour. Manag.* 4, 905–919. <https://doi.org/10.1007/s40899-017-0184-6>
- Peipe, J., 1997. High-resolution CCD area array sensors in digital close range photogrammetry, in: *Videometrics V. International Society for Optics and Photonics*, pp. 153–156.
- Pekel, J.F., Cottam, A., Gorelick, N., Belward, A.S., 2016. High-resolution mapping of global surface water and its long-term changes. *Nature* 540, 418.
- Peña, J.M., Torres-Sánchez, J., Isabel De Castro, A., Kelly, M., López-Granados, F., 2013. Weed Mapping in Early-Season Maize Fields Using Object-Based Analysis of Unmanned Aerial Vehicle (UAV) Images. *PLoS One* 8. <https://doi.org/10.1371/journal.pone.0077151>
- Pérez-Ortiz, M., Peña, J.M., Gutiérrez, P.A., Torres-Sánchez, J., Hervás-Martínez, C., López-Granados, F., 2015. A semi-supervised system for weed mapping in sunflower crops using unmanned aerial vehicles and a crop row detection method. *Appl. Soft Comput.* 37, 533–544. <https://doi.org/10.1016/j.ASOC.2015.08.027>
- Pohl, C., Genderen, J.L. Van, 1998. Review article Multisensor image fusion in remote sensing : Concepts , methods and applications 19, 823±854 Review. <https://doi.org/10.1080/014311698215748>
- Pohl, C., J. L. Van Genderen, 2016. *Remote Sensing Image Fusion: A Practical Guide.* Taylor & Francis.
- Pohl, C., van Genderen, J., 2014. Remote sensing image fusion: An update in the context of Digital Earth. *Int. J. Digit. Earth* 7, 158–172. <https://doi.org/10.1080/17538947.2013.869266>
- Pôssa, É.M., Maillard, P., 2018. Precise Delineation of Small Water Bodies from Sentinel-1 Data using Support Vector Machine Classification Precise Delineation of Small Water Bodies from Sentinel-1 Data using. *Can. J. Remote Sens.* 44, 179–190. <https://doi.org/10.1080/07038992.2018.1478723>
- Prach, K., Walker, L.R., 2011. Four opportunities for studies of ecological succession. *Trends Ecol. Evol.* 26, 119–123. <https://doi.org/10.1016/j.tree.2010.12.007>
- Pošek, J., Šimová, P., 2019. UAV for mapping shrubland vegetation: Does fusion of spectral and vertical information derived from a single sensor increase the classification accuracy? *Int. J. Appl. Earth Obs. Geoinf.* 75, 151–162. <https://doi.org/10.1016/j.jag.2018.10.009>
- Pukanska, K., Bartos, K., Sabova, J., 2014. Comparison of Survey Results of the Surface Quarry Spišské Tomášovce by the Use of Photogrammetry and Terrestrial Laser Scanning. *Inžynieria Miner.* 15.
- Rampi, L.P., Knight, J.F., Pelletier, K.C., 2014. Wetland Mapping in the Upper Midwest United States. *Photogramm. Eng. Remote Sens.* 80, 439–448. <https://doi.org/10.14358/PERS.80.5.439>

- Rapinel, S., Hubert-Moy, L., Clément, B., 2015. Combined use of LiDAR data and multispectral earth observation imagery for wetland habitat mapping. *Int. J. Appl. earth Obs. Geoinf.* 37, 56–64.
- Reese, H., Nordkvist, K., Nyström, M., Bohlin, J., Olsson, H., 2015. Combining point clouds from image matching with SPOT 5 multispectral data for mountain vegetation classification. *Int. J. Remote Sens.* 36, 403–416.  
<https://doi.org/10.1080/2150704X.2014.999382>
- Richter, R., Schläpfer, D., 2016. ATCOR-4 User Guide. Ger. Aerosp. Center, Ger. 7.0.3, 565-01.
- Rokni, K., Ahmad, A., Solaimani, K., Hazini, S., 2015. A new approach for surface water change detection : Integration of pixel level image fusion and image classification techniques. *Int. J. Appl. Earth Obs. Geoinf.* 34, 226–234.  
<https://doi.org/10.1016/j.jag.2014.08.014>
- Sabins, F.F., 1978. Remote sensing: Principles and interpretation (Series of books in the earth sciences). W. H. Freeman.
- Sankey, T., Donager, J., McVay, J., Sankey, J.B., 2017a. UAV lidar and hyperspectral fusion for forest monitoring in the southwestern USA. *Remote Sens. Environ.* 195, 30–43. <https://doi.org/10.1016/j.rse.2017.04.007>
- Sankey, T., McVay, J., Swetnam, T.L., McClaran, M.P., Heilman, P., Nichols, M., 2017b. UAV hyperspectral and lidar data and their fusion for arid and semi-arid land vegetation monitoring. *Remote Sens. Ecol. Conserv.* 1–14.  
<https://doi.org/10.1002/rse2.44>
- Sapiano, M.R.P., Arkin, P.A., 2009. An intercomparison and validation of high-resolution satellite precipitation estimates with 3-hourly gauge data. *J. Hydrometeorol.* 10, 149–166.
- Schmidt, J., Fassnacht, F.E., Neff, C., Lausch, A., Kleinschmit, B., Förster, M., Schmidlein, S., 2017. Adapting a Natura 2000 field guideline for a remote sensing-based assessment of heathland conservation status. *Int. J. Appl. earth Obs. Geoinf.* 60, 61–71.
- Schulz, F., Wiegand, G., 2000. Development options of natural habitats in a post-mining landscape. *L. Degrad. Dev.* 110, 99–110.
- Shahtahmassebi, A., Yang, N., Wang, K., Moore, N., Shen, Z., 2013. Review of shadow detection and de-shadowing methods in remote sensing. *Chinese Geogr. Sci.* 23, 403–420.
- Shao, Y., Taff, G.N., Walsh, S.J., 2011. Shadow detection and building-height estimation using IKONOS data. *Int. J. Remote Sens.* 32, 6929–6944.  
<https://doi.org/10.1080/01431161.2010.517226>
- Shortis, M.R., Bellman, C.J., Robson, S., Johnston, G.J., Johnson, G.W., 2006. Stability of zoom and fixed lenses used with digital SLR cameras. *Int. Arch. Photogramm. Remote Sens.* 36.



- Šíkola, M., Chajma, P., Anděl, P., Solský, M., Vojar, J., 2019. Finding water: Reliability of remote-sensing methods in searching for water bodies within diverse landscapes. *Ecohydrol. Hydrobiol.* 1–10. <https://doi.org/10.1016/j.ecohyd.2019.01.001>
- Šilhavý, J., Čada, V., 2015. New Automatic Accuracy Evaluation of Altimetry Data: DTM 5G Compared with ZABAGED® Altimetry, in: *Surface Models for Geosciences*. Springer, pp. 225–236.
- Šimová, P., Moudrý, V., Komárek, J., Hrach, K., Fortin, M.-J., 2019. Fine scale waterbody data improve prediction of waterbird occurrence despite coarse species data. *Ecography (Cop.)*. 42, 511–520. <https://doi.org/10.1111/ecog.03724>
- Stehman, S. V., 2013. Estimating area from an accuracy assessment error matrix. *Remote Sens. Environ.* 132, 202–211. <https://doi.org/10.1016/j.rse.2013.01.016>
- Steuer, H., Schäffler, U., Gross, A., 2011. Detection of standing water bodies in Lidar-data 49. GIS group · Technische Universität München.
- Stöcker, C., Bennett, R., Nex, F., Gerke, M., Zevenbergen, J., 2017. Review of the current state of UAV regulations. *Remote Sens.* 9, 33–35. <https://doi.org/10.3390/rs9050459>
- Stow, D.A., Shih, H.-C., Coulter, L.L., 2014. Discrete classification approach to land cover and land use change identification based on Landsat image time sequences. *Remote Sens. Lett.* 5, 922–931.
- Strahler, A.H., Woodcock, C.E., Smith, J.A., 1986. On the nature of models in remote sensing. *Remote Sens. Environ.* 20, 121–139.
- Streets, D.G., Canty, T., Carmichael, G.R., de Foy, B., Dickerson, R.R., Duncan, B.N., Edwards, D.P., Haynes, J.A., Henze, D.K., Houyoux, M.R., 2013. Emissions estimation from satellite retrievals: A review of current capability. *Atmos. Environ.* 77, 1011–1042.
- Štroner, M., Urban, R., Královič, J., 2013. Testing of the relative precision in local network with use of the Trimble Geo XR GNSS receivers. *Reports Geod. Geoinformatics* 94, 27–36.
- Su, T.-C., 2016. A filter-based post-processing technique for improving homogeneity of pixel-wise classification data. *Eur. J. Remote Sens.* 49, 531–552.
- Svobodova, K., Sklenicka, P., Molnarova, K., Salek, M., 2012. Visual preferences for physical attributes of mining and post-mining landscapes with respect to the sociodemographic characteristics of respondents. *Ecol. Eng.* 43, 34–44. <https://doi.org/10.1016/j.ecoleng.2011.08.007>
- Szostak, M., Wezyk, P., Tompalski, P., 2014. Aerial orthophoto and airborne laser scanning as monitoring tools for land cover dynamics: A case study from the Miłicz Forest District (Poland). *Pure Appl. Geophys.* 171, 857–866.
- Teo, T.-A., Huang, C.-H., 2016. Object-Based Land Cover Classification Using Airborne Lidar and Different Spectral Images. *Terr. Atmos. Ocean. Sci.* 27, 491. [https://doi.org/10.3319/TAO.2016.01.29.01\(ISRS\)](https://doi.org/10.3319/TAO.2016.01.29.01(ISRS))

- Toheni, K., Giacomini, A., Murtagh, R., Kniest, E., 2014. A comparison of multi-view 3D reconstruction of a rock wall using several cameras and a laser scanner. *Int. Arch. Photogramm. Remote Sens. Spat. Inf. Sci.* 40, 573.
- Tomaščík, J.J., Sr., T.J., Saloň, Š., Piroh, R., 2017. Horizontal accuracy and applicability of smartphone GNSS positioning in forests. *Forestry* 187–198. <https://doi.org/10.1093/forestry/cpw031>
- Tong, X., Liu, X., Chen, P., Liu, S., Luan, K., Li, L., Liu, S., Liu, X., Xie, H., Jin, Y., 2015. Integration of UAV-based photogrammetry and terrestrial laser scanning for the three-dimensional mapping and monitoring of open-pit mine areas. *Remote Sens.* 7, 6635–6662.
- Torresan, C., Berton, A., Carotenuto, F., Di Gennaro, S.F., Gioli, B., Matese, A., Miglietta, F., Vagnoli, C., Zaldei, A., Wallace, L., 2017. Forestry applications of UAVs in Europe: A review. *Int. J. Remote Sens.* 38, 2427–2447.
- Toth, C., Józków, G., 2016. Remote sensing platforms and sensors: A survey. *ISPRS J. Photogramm. Remote Sens.* 115, 22–36. <https://doi.org/10.1016/j.isprsjprs.2015.10.004>
- Tou, J.T., Gonzalez, R.C., 1974. *Pattern Recognition Principles*. Addison- Wesley Publ. Co.
- Turner, D., Lucieer, A., Watson, C., 2012. An Automated Technique for Generating Georectified Mosaics from Ultra-High Resolution Unmanned Aerial Vehicle (UAV) Imagery, Based on Structure from Motion (SfM) Point Clouds. *Remote Sens.* 4, 1392–1410. <https://doi.org/10.3390/rs4051392>
- Van Blyenburgh, P., 2013. 2013–2014 RPAS Yearbook: Remotely Piloted Aircraft Systems: The Global Perspective 2013/2014. UVS Int. Paris, Fr.
- Van Genderen, J.L., Pohl, C., 1994. Image fusion: Issues, techniques and applications. *Proc. EARSeL Work.* 18–26.
- Vanhée, B., Devigne, C., 2018. Differences in collembola species assemblages (Arthropoda) between spoil tips and surrounding environments are dependent on vegetation development. *Sci. Rep.* 8, 18067. <https://doi.org/10.1038/s41598-018-36315-1>
- Verpoorter, C., Kutser, T., Tranvik, L., 2012. Oceanography : Methods automated mapping of water bodies using Landsat multispectral data 1037–1050. <https://doi.org/10.4319/lom.2012.10.1037>
- Vojar, J., Doležalová, J., Milič, S., Smolová, D., Kopecký, O., Kadlec, T., Knapp, M., 2016. Spontaneous succession on spoil banks supports amphibian diversity and abundance rich Kopecky. *Ecol. Eng.* 90, 278–284. <https://doi.org/10.1016/j.ecoleng.2016.01.028>
- Vörösmarty, C.J., McIntyre, P.B., Gessner, M.O., Dudgeon, D., Prusevich, A., Green, P., ..., Davies, P.M., 2010. Rivers in crisis: Global water insecurity for humans and biodiversity. *Nature* 467, 555–561.
- Vosselman, G., Maas, H.-G., 2010. *Airborne and terrestrial laser scanning*. CRC press.

- Vymazal, J., Sklenicka, P., 2012. Restoration of areas affected by mining. *Ecol. Eng.* 43, 1–4. <https://doi.org/https://doi.org/10.1016/j.ecoleng.2012.02.008>
- Wallace, L., Lucieer, A., Malenovsky, Z., Turner, D., Vopěnka, P., 2016. Assessment of forest structure using two UAV techniques: A comparison of airborne laser scanning and structure from motion (SfM) point clouds. *Forests* 7, 1–16. <https://doi.org/10.3390/f7030062>
- Wang, R., Gamon, J.A., Cavender- Bares, J., Townsend, P.A., Zyguelbaum, A.I., 2018. The spatial sensitivity of the spectral diversity–biodiversity relationship: an experimental test in a prairie grassland. *Ecol. Appl.* 28, 541–556.
- Wehr, A., Lohr, U., 1999. Airborne laser scanning—an introduction and overview. *J. Photogramm. Remote Sens.* 54, 68–82.
- Weil, G., Lensky, I., Resheff, Y., Levin, N., 2017. Optimizing the Timing of Unmanned Aerial Vehicle Image Acquisition for Applied Mapping of Woody Vegetation Species Using Feature Selection. *Remote Sens.* 9, 1130. <https://doi.org/10.3390/rs9111130>
- Wenbo, W., Yao, J., Kang, T., 2008. Study of remote sensing image fusion and its application in image classification. *Int. Arch. Photogramm. Remote Sens. Spat. Inf. Sci.* 37, 1141–1146.
- Westoby, M.J., Brasington, J., Glasser, N.F., Hambrey, M.J., Reynolds, J.M., 2012. “Structure-from-Motion” photogrammetry: A low-cost, effective tool for geoscience applications. *Geomorphology* 179, 300–314. <https://doi.org/10.1016/j.geomorph.2012.08.021>
- Weżyk, P., Szostak, M., Krzaklewski, W., Pająk, M., Pierzchalski, M., Szwed, P., Hawryło, P., Ratajczak, M., 2015. Landscape monitoring of post-industrial areas using LiDAR and GIS technology. *Geod. Cartogr.* 64, 125–137.
- Woodhouse, I.H., 2017. *Introduction to Microwave Remote Sensing*, 1st ed. Taylor & Francis. <https://doi.org/doi.org/10.1201/9781315272573>
- Wu, J., Bauer, M.E., 2013. Evaluating the effects of shadow detection on quickbird image classification and spectroradiometric restoration. *Remote Sens.* 5, 4450–4469. <https://doi.org/10.3390/rs5094450>
- Wu, S.T., Hsieh, Y.T., Chen, C.T., Chen, J.C., 2014. A comparison of 4 shadow compensation techniques for land cover classification of shaded areas from high radiometric resolution aerial images. *Can. J. Remote Sens.* 40, 315–326. <https://doi.org/10.1080/07038992.2014.979488>
- Xie, H., Luo, X., Xu, X., Tong, X., Jin, Y., Pan, H., Zhou, B., 2014. New hyperspectral difference water index for the extraction of urban water bodies by the use of airborne hyperspectral images. *J. Appl. Remote Sens.* 8, 15.
- Xu, H., 2006. Modification of normalised difference water index NDWI to enhance open water features in remotely sensed imagery. *Int. J. Remote Sens.* 27, 9.

- Yu, Q., Gong, P., Clinton, N., Biging, G., Kelly, M., Schirokauer, D., 2006. Object-based Detailed Vegetation Classification with Airborne High Spatial Resolution Remote Sensing Imagery. *Photogramm. Eng. Remote Sens.* 72, 799–811. <https://doi.org/10.14358/PERS.72.7.799>
- Zarco-Tejada, P.J., González-Dugo, V., Berni, J.A.J., 2012. Fluorescence, temperature and narrow-band indices acquired from a UAV platform for water stress detection using a micro-hyperspectral imager and a thermal camera. *Remote Sens. Environ.* 117, 322–337.
- Zhang, C., Xie, Z., 2012. Combining object-based texture measures with a neural network for vegetation mapping in the Everglades from hyperspectral imagery. *Remote Sens. Environ.* 124, 310–320. <https://doi.org/10.1016/j.rse.2012.05.015>
- Zhen, Z., Quackenbush, L.J., Stehman, S. V., Zhang, L., 2013. Impact of training and validation sample selection on classification accuracy and accuracy assessment when using reference polygons in object-based classification. *Int. J. Remote Sens.* 34, 6914–6930. <https://doi.org/10.1080/01431161.2013.810822>
- Zhou, W., Huang, G., Troy, A., Cadenasso, M.L., 2009. Object-based land cover classification of shaded areas in high spatial resolution imagery of urban areas: A comparison study. *Remote Sens. Environ.* 113, 1769–1777. <https://doi.org/10.1016/j.rse.2009.04.007>
- Zhou, Y., Qiu, F., 2015. Fusion of high spatial resolution WorldView-2 imagery and LiDAR pseudo-waveform for object-based image analysis. *ISPRS J. Photogramm. Remote Sens.* 101, 221–232. <https://doi.org/10.1016/j.isprsjprs.2014.12.013>
- Zhu, Z., Woodcock, C.E., 2014a. Continuous change detection and classification of land cover using all available Landsat data. *Remote Sens. Environ.* 144, 152–171. <https://doi.org/10.1016/j.rse.2014.01.011>
- Zhu, Z., Woodcock, C.E., 2014b. Automated cloud, cloud shadow, and snow detection in multitemporal Landsat data: An algorithm designed specifically for monitoring land cover change. *Remote Sens. Environ.* 152, 217–234.
- Zuiev, O. V., Demydko, V.G., Musyenko, A.O., Gerasymenko, T.S., 2015. Analysis of control processes influence on UAV equipment classification veracity, in: 2015 IEEE International Conference Actual Problems of Unmanned Aerial Vehicles Developments (APUAVD). IEEE, pp. 102–105.

# Curriculum vitae

## Personal:

Jiří Prošek, born 1990 in the Czech Republic

## Affiliations:

Since 2015 Department of Applied Geoinformatics and Spatial Planning at the Faculty of Environmental Sciences, Czech University of Life Sciences Prague

Since 2017 Department of GIS and Remote Sensing at the Institute of Botany, Czech Academy of Sciences

Since 2017 Spatial Science in Environment and Ecology Research Group at the Faculty of Environmental Sciences, Czech University of Life Sciences Prague

## Education:

Czech University of Life Sciences Prague, Faculty of Environmental Sciences

2013 – Present PhD degree – Applied and Landscape Ecology; thesis topic: Integration of Airborne High Resolution Spectral and Vertical Structure Information for Environmental Mapping.

2013 – 2015 Master's degree – Landscape Planning; thesis topic: Possibilities of use of GIS analyses for paths network design

2010 – 2013 Bachelor's degree – Spatial Planning; thesis topic: Analysis of traffic accessibility changes (network analysis).

## Teaching experience:

Since 2015 Lecturer of GIS, Remote Sensing, Remote Sensing using UAVs

Since 2015 Supervisor and reviewer of Bachelor and Master Thesis (applications in Remote Sensing, GIS application)

## Participation in research projects:

(2019-2022) Technology Agency of the Czech Republic (“TACR”), „Identification of nationally important wintering grounds of aquatic bird species“, *RS data processing for species distribution modelling*

(2018-2019) Grant Agency of the Czech Republic (“GAČR”), „Fusion of LiDAR and UAV borne multispectral data to assess physiographic diversity of post-mining sites“, *RS data processing and analysis (integration of LiDAR and Hyperspectral data)*

(2018-2019) Grant Agency of the Czech Republic (“GAČR”), „The impact of urbanization on bird species diversity“, *GIS data processing and noise pollution modelling*

(2017-2019) European Regional Development Fund; Cross-border cooperation project – „landscape memory“; *RS data processing and analysis (Object based image analysis)*

(2015-2016) EEA Grants and Norway Grants; Fragmentation of biotopes, *GIS data processing and publication*

(2016-2019) Co-investigator of three Internal Grant Agency at Faculty of Environmental Sciences and Czech University of Life Sciences Prague with RS application topic.

## Other:

Authorized operator of UAVs, member of the Academic Senate.

## Impact publications (J<sub>imp</sub>)

**Prošek, J., & Šimová, P.** (2019). UAV for mapping shrubland vegetation: Does fusion of spectral and vertical information derived from a single sensor increase the classification accuracy? *International Journal of Applied Earth Observation and Geoinformation*, 75, 151-162.

Moudrý, V., Urban, R., Štroner, M., Komárek, J., Brouček, J., & **Prošek, J.** (2019). Comparison of a commercial and home-assembled fixed-wing UAV for terrain mapping of a post-mining site under leaf-off conditions. *International Journal of Remote Sensing*, 40(2), 555-572.

Komárek, J., Klouček, T., & **Prošek, J.** (2018). The potential of Unmanned Aerial Systems: A tool towards precision classification of hard-to-distinguish vegetation types? *International Journal of Applied Earth Observation and Geoinformation*, 71, 9-19.

## Scopus publications (J<sub>sc</sub>)

Moravec, D., Komárek, J., Kumhálová, J., Kroulík, M., **Prošek, J.,** & Klápště, P. (2017). Digital elevation models as predictors of yield: Comparison of an UAV and other elevation data sources. *Agronomy Research*, 15(1), 249-255.